

Transformers Learn Faster with Semantic Focus

Parikshit Ram[†], Kenneth L. Clarkson[†], Tim Klinger[†],
Shashanka Ubaru[†], Alexander G. Gray[‡].

[†]IBM Research, [‡]Centaur AI Institute.

Email: parikshit.ram@ibm.com

Abstract

Various forms of sparse attention have been explored to mitigate the quadratic computational and memory cost of the attention mechanism in transformers. We study sparse transformers not through a lens of efficiency but rather in terms of learnability and generalization. Empirically studying a range of attention mechanisms, we find that input-dependent sparse attention models appear to converge faster and generalize better than standard attention models, while input-agnostic sparse attention models show no such benefits – a phenomenon that is robust across architectural and optimization hyperparameter choices. This can be interpreted as demonstrating that concentrating a model’s “semantic focus” with respect to the tokens currently being considered (in the form of input-dependent sparse attention) accelerates learning. We develop a theoretical characterization of the conditions that explain this behavior. We establish a connection between the stability of the standard softmax and the loss function’s Lipschitz properties, then show how sparsity affects the stability of the softmax and the subsequent convergence and generalization guarantees resulting from the attention mechanism. This allows us to theoretically establish that input-agnostic sparse attention does not provide any benefits. We also characterize conditions when semantic focus (input-dependent sparse attention) can provide improved guarantees, and we validate that these conditions are in fact met in our empirical evaluations.

1 Introduction

Transformers [Vaswani et al., 2017] are expressive set encoders, which when paired with positional encodings, can serve as sequence encoders. The attention mechanism in a *transformer block* allows us to model the long and short term dependencies in a sequence in an input-dependent manner instead of relying on handcrafted dependency modeling as in recurrent (uni-directional and bi-directional) and convolutional models. The single hidden layer multi-layered perceptron (or MLP) in the transformer block introduces non-linearities enabling further expressivity. Transformers have been extremely successful in modeling natural language, and are the core blocks of various large language models or LLMs. They have also been successful in vision, tabular data, and time series among various other applications.

The expressivity of attention-based transformers [Yun et al., 2020a] comes with a computational overhead where the attention mechanism requires time and memory quadratic in the sequence length. To address this, various efficient transformers have been developed [Tay et al., 2022], utilizing various techniques such as fixed sparse attention patterns, low rank approximations of the attention matrix, and input-dependent sparse attention patterns. In this work, we focus on sparse attention mechanisms, both input-dependent and input-agnostic. Existing literature has studied sparse attention as a way to speed up the forward pass (inference), which in turn can speed up each training step [Tay et al., 2021]. However, sparse attention has always been viewed as an approximation of the gold standard full attention.

Contributions. One can view sparse attention as a form of *sensory gating*, and this is considered an essential component of biological cognitive systems, allowing rapid learning [Jones et al., 2016, Fritzsche, 2020], and the absence of it is often considered a marker for schizophrenia [Judd et al., 1992]. The gating is often achieved via inhibitory signals. Related observations made by Bengio [2019] suggest some motivations. He makes a connection between a form of input-dependent sparse attention and the global workspace theory of consciousness in cognitive science, as well as the properties of natural language sentences and symbolic AI representations used in planning and reasoning [nss, 2024], “*stipulating that elements of a conscious thought are selected through an attention mechanism (such as the content-based attention mechanism we introduced in Bahdanau et al. [2016]) and then broadcast to the rest of the brain, strongly influencing downstream perception and action as well as the content of the next conscious thought*”. As the “elements” or weight vectors being attended to are often discussed as semantic concepts, one can refer to the same phenomenon as “semantic focus” and explore its possible benefit to learning efficacy. Motivated by this, we consider the following question in this paper: “Can sparse attention in transformers be beneficial in terms of learning convergence and generalization, in comparison to full attention?”. To this end, we share the following findings:

- (§4) Focusing on benchmarks of structured languages designed to evaluate capabilities of transformers [Tay et al., 2021, Deletang et al., 2023], and controlling for all involved hyperparameters, we make two empirical observations:
 - Sparse attention with input-agnostic sparsity patterns empirically struggles with expressivity (as implied by Yun et al. [2020a,b]), and does not show benefits in terms of learning convergence and generalization even when equipped with enough expressivity (via *global tokens* [Ainslie et al., 2020, Zaheer et al., 2020]).
 - Sparse attention with a specific form of input-dependent sparsity pattern that limits the attention to the top attention scores – the *heavy-hitters* (such as top- k attention [Gupta et al., 2021, Zeng et al., 2025]) – are empirically as expressive as the standard full attention, and can converge significantly faster during training, while generalizing as well as, and at times better than, the full attention model. These improvements hold across various hyperparameters, both related to the architecture (such as the number of heads per transformer block, the number of transformer blocks, the MLP activation function), and the optimizer (such as the initial learning rate, and the learning rate decay).
- (§5) We then try to theoretically understand why this might be happening, and characterize conditions under which sparse attention can provide better learning convergence and generalization guarantees. Our analysis is based on two critical insights:
 - For any λ -Lipschitz learning objective (with respect to the learnable parameters), the convergence rate and algorithmic stability [Bousquet and Elisseeff, 2000] of (stochastic) gradient-descent based algorithms are dependent on Lipschitz constant λ , with smaller values implying better convergence and stability guarantees; better stability implies better generalization [Hardt et al., 2016]. We show that the Lipschitz constant of a transformer-based model is tied to the input-stability of the softmax in the attention mechanism – better input-stability implies better Lipschitz constant. Thus, we establish how the input-stability of softmax directly affects the learning convergence and generalization.
 - The sparsity pattern of the sparse attention affects the overall learning convergence and generalization through its effect on the input-stability of the softmax. The input-stability of the (sparse) softmax is closely tied to the range or the *semantic dispersion* of the values (the query-key dot-products) over which the softmax is applied (formally discussed in definition 2) – larger dispersion implies worse input-stability. While input-agnostic sparsity patterns do not necessarily improve the dispersion over the full-attention model, input-dependent sparsity that only focuses on the *heavy-hitters* can significantly improve this dispersion, thus implying improved input-stability. This effectively translates to an improved Lipschitz constant, thus convergence and generalization guarantees. We also empirically validate that the dispersion and the *estimated* Lipschitz constant of input-dependent sparse attention show improvements over full attention.

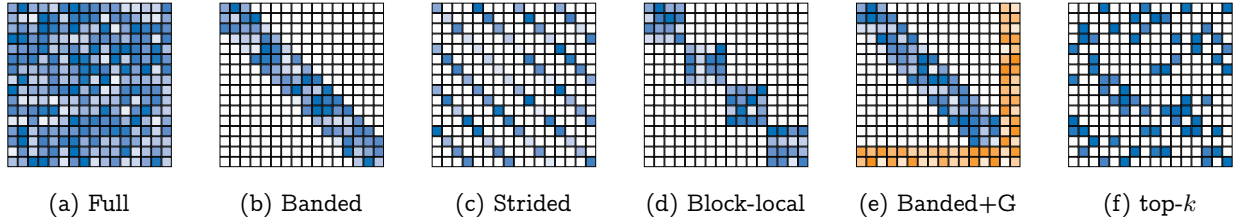


Figure 1: Visualizations of dot-product based attention scores matrices, which along with the value matrix $\mathbf{V}\mathbf{X}$, gives us the attention-based token updates $\mathbf{A}(\mathbf{X})$ (see equation (1) in section 3). The horizontal axis denotes keys and the vertical axis queries. The color intensities denote the value of the attention scores (higher intensities denote higher scores), and the white entries in the matrices corresponds to masked entries. Figure 1a depicts standard full attention score matrix; figure 1b, figure 1c and figure 1d depict various input-agnostic sparse attention score matrices. Figure 1e shows the use of global tokens (attention scores are shown in orange) in conjunction with banded attention (scores are shown in blue), with the last two tokens being the global tokens – all tokens attend to and are attended by these global tokens. Note that the per-query semantic dispersion (see definition 2, figure 9) of the unmasked attention scores in the input-agnostic masks would be similar *in general* to that of standard attention. Input-dependent masked attention such as top- k attention (shown in figure 1f) can have a much smaller attention semantic dispersion compared to standard attention.

Outline. We begin by discussing relevant literature on transformers and their analyses (both empirical and theoretical) in section 2. We present the precise problem setup including the data, the model and the training loss in section 3. Following that, in section 4, we present our empirical observations regarding the effect of sparse attention on the learning convergence and generalization on 8 tasks. In section 5, we try to theoretically understand the observed behavior, and try to characterize when and how sparse attention can provide benefits over the standard full attention. We conclude in section 6, summarizing our contributions, and discussing future work.

2 Related Work

In this section, we cover literature on efficient transformers, and the theoretical and empirical investigations on the capabilities and limitations of transformers. Finally, we will also briefly discuss the existing research on optimization with transformers.

Efficient transformers with sparse attention. The transformer architecture [Vaswani et al., 2017] has had tremendous impact in various fields such as language modeling, vision and tabular data, and spurred new research into the development of architectural variants or X-formers [Tay et al., 2022, Phuong and Hutter, 2022, Lin et al., 2022]. Many of these have been developed to address the quadratic computational complexity of the attention mechanism in a transformer block with respect to the context length (the number of tokens in the context), with the goal of increasing the context length. One common technique is to sparsify the attention mechanism. Usually each (query) token in the context attends to all other (key) tokens as in figure 1a, leading to the quadratic cost. Instead, we can limit the set of key tokens attended to by any particular query token. Input-agnostic sparsification strategies include attending (i) within a window as in figure 1b [Parmar et al., 2018] or a block as in figure 1d [Qiu et al., 2020], (ii) in a strided manner as in figure 1c [Beltagy et al., 2020, Child et al., 2019], (iii) to random tokens Zaheer et al. [2020], or (iv) to only a small number of *global tokens* and these global tokens attend to all other tokens [Ainslie et al., 2020, Zaheer et al., 2020]; this is often used in conjunction with other forms of sparse attention as shown in figure 1e. Input-dependent sparsification strategies include (i) using a scoring mechanism and attending only to the highest scoring tokens as in figure 1f [Tay et al., 2020, Gupta et al., 2021], or (ii) clustering [Roy et al., 2021]

or hashing [Kitaev et al., 2020] tokens into buckets and attending only to in-bucket tokens. Surveys such as Tay et al. [2022] and Lin et al. [2022] cover various other forms. These input-dependent sparse attention mechanisms focus the attention on the keys corresponding to the highest dot-product scores – the *heavy hitters* – while explicitly ignoring the remaining keys. Sparse attention is considered in all these cases as a way to speed up the attention mechanism in the transformer block during the forward pass without significantly deteriorating the downstream performance, with the standard full attention being the gold-standard. The *Long-range Arena* or LRA [Tay et al., 2021] serves as one such benchmark comparing different efficient transformers to the standard transformer.

In contrast to above, we theoretically study the effect of sparse attention based transformers on the *learning or empirical risk minimization (ERM) convergence* of the whole model (containing multiple transformer blocks), and the *in-distribution* generalization of the model obtained via ERM. We attempt to characterize conditions under which sparse attention might show improvements over full attention.

Empirical evaluations of transformer capabilities. While benchmarks such as the LRA [Tay et al., 2021] focus on the efficiency and in-distribution generalization, transformers have also been thoroughly evaluated on benchmarks studying specific forms of *out-of-distribution generalization* such as compositional generalization and length generalization. Compositional generalization benchmarks such as COGS [Kim and Linzen, 2020] and SCAN [Lake and Baroni, 2018] consider sequence-to-sequence translation problems, and they have been used to highlight the inability of transformers to systematically generalize [Sikarwar et al., 2022]. However, subsequent work such as Csordás et al. [2021], Ontanon et al. [2022] have demonstrated ways in which transformers can systematically generalize. The Neural Networks and Chomsky Hierarchy or NNCH benchmark [Deletang et al., 2023] considers language transduction tasks from different formal language classes such as regular, deterministic context-free and context-sensitive languages. This benchmark studies the ability of various models (including transformers) to length generalize – that is, generalize to longer input sequences when being trained in a length limited manner. There has also been a lot of research on improving the performance of transformer based models on these out-of-distribution generalization benchmarks leveraging auxiliary tasks [Jiang and Bansal, 2021] and chain-of-thought prompting [Drozdo et al., 2023].

In our work, we focus on the theoretical analysis of the ERM convergence and the in-distribution generalization of models based on multiple transformer blocks, and empirically validate our theoretical insights utilizing these above benchmarks. We consider one multiclass classification task from the LRA benchmark [Tay et al., 2021] and a subset of the tasks from the NNCH benchmark [Deletang et al., 2023] that can be posed as supervised classification problems.

Theoretical treatment of transformer capabilities. Given the widespread success of transformers, there have been various theoretical studies on the capabilities and limitations of transformers. One line of research focuses on the ability of transformers to express (and thus recognize) formal languages [Strobl et al., 2024]. Some of these works study transformers with hard attention [Bhattamishra et al., 2020, Hahn, 2020, Hao et al., 2022, Merrill et al., 2022], while others consider the more commonly used softmax attention [Chiang and Cholak, 2022, Chiang et al., 2023]. Another line of research has focused on understanding the capabilities of transformers as algorithms [Li et al., 2023], demonstrating how transformers can, under specific parameter settings, perform *in-context* gradient descent for linear regression [Von Oswald et al., 2023] or in-context clustering [Geshkovski et al., 2023], and how easily can such parameters can be found [Li et al., 2023, Ahn et al., 2023, Zhang et al., 2024]. Yun et al. [2020b] focus on universal approximation of sparse attention transformer for sequence-to-sequence problems, and establish conditions on the sparsity pattern that ensure desired expressivity given enough number of transformer layers.

Viewing hard-attention as a form of input-dependent sparse attention, these existing expressivity results [Strobl et al., 2024] are complementary to our focus on learning convergence and in-distribution generalization for models using multiple sparse attention based transformer blocks – existing hard-attention expressivity results discuss whether sparse attention transformers are expressive enough for the task at hand.

Our study here focuses on how quickly and sample efficiently can such transformers learn the task, and how the attention sparsity pattern plays a role.

Optimization with transformers. There has been a lot of work on understanding the optimization of transformers in terms of the benefit of adaptive methods such as Adam over non-adaptive SGD [Zhang et al., 2020, Pan and Li, 2022, Jiang et al., 2023, Kunstner et al., 2023, Ahn et al., 2024]. However, the focus there is to understand why optimizers such as Adam converge significantly faster than SGD with transformer models; no such consistent difference has been established for previous architectures such as convolutional or residual. Li et al. [2025] recently present an analysis of the training dynamics with SignGD for a single transformer block model for a specific noisy binary classification problem, working in the “feature learning framework”, and empirically demonstrating that the dynamics of SignGD and Adam are quite similar, thus making SignGD a useful proxy for analyzing Adam.

Our study is complementary to this line of work where we study the effect of sparsity in attention to non-adaptive SGD convergence and generalization. We also consider a more general sequence learning problem with multiple transformer blocks.

3 Problem Setup

In this section, we detail the problem setup, introducing the notation, and presenting the transformer based model, the training data and the learning loss.

Notation. We denote the index set as $\llbracket n \rrbracket \triangleq \{1, \dots, n\}$ for any natural number $n \in \mathbb{N}$. We use X for input sequences of token indices $v \in \llbracket D \rrbracket$ in a vocabulary \mathcal{V} of size D , and y for labels or targets. We use $\mathbf{x} \in \mathbb{R}^d$ for a token embedding vector and $\mathbf{X} \in \mathbb{R}^{d \times L}$ for the sequence (matrix) of L token embeddings. For any vector \mathbf{v} , we use v_i to denote its i -th entry, and $\|\mathbf{v}\|$ to denote its Euclidean norm. For a matrix \mathbf{W} , we denote its (i, j) -th entry as W_{ij} , i -th column as $\mathbf{W}_{:i}$ and i -th row as $\mathbf{W}_{i\cdot}$. We use $\|\mathbf{W}\|$ and $\|\mathbf{W}\|_{2,1}$ to denote the spectral and $\ell_{2,1}$ norms of \mathbf{W} , where $\ell_{2,1}$ norm is the sum of the Euclidean norms of the columns $\mathbf{W}_{:i}$ of the matrix \mathbf{W} . For a tuple $\theta = (\mathbf{W}^{(1)}, \dots, \mathbf{W}^{(n)})$ of n matrices, we let $\|\theta\| = \max_{i \in \llbracket n \rrbracket} \|\mathbf{W}^{(i)}\|$. We consider a learning problem with input sequences $X = [v_1, \dots, v_L] \in \llbracket D \rrbracket^L$ of length exactly L with its i -th entry v_i denoting the v_i -th token in a vocabulary \mathcal{V} , with outputs $y \in \mathcal{Y}$.¹ For a learnable function $f : \mathcal{X} \rightarrow \mathcal{Y}$ with learnable parameters θ , we explicitly write the function as $f_\theta(X)$ with $X \in \mathcal{X}$.

Transformer block. Consider a L length sequence of token embeddings $\mathbf{X} \in \mathbb{R}^{d \times L}$ with the i -th token embedding denoted as $\mathbf{X}_{:i} \in \mathbb{R}^d$. Let $\text{TF} : \mathbb{R}^{d \times L} \rightarrow \mathbb{R}^{d \times L}$ denote a transformer block with learnable parameters $\theta = (\mathbf{W}, \mathbf{V}, \mathbf{P}, \mathbf{R})$ with $\mathbf{W}, \mathbf{V} \in \mathbb{R}^{d \times d}$, $\mathbf{P}, \mathbf{R} \in \mathbb{R}^{d_{\text{MLP}} \times d}$. The transformer block output is then defined as:

$$\text{TF}_\theta(\mathbf{X}) = \text{LN}(\underbrace{\tilde{\mathbf{X}} + \mathbf{R}^\top \sigma(\mathbf{P}\tilde{\mathbf{X}})}_{\text{MLP}_{\mathbf{P}, \mathbf{R}}(\tilde{\mathbf{X}})}), \quad \text{and} \quad \tilde{\mathbf{X}} = \text{LN}(\mathbf{X} + \underbrace{\mathbf{V}\mathbf{X} \text{softmax}(\mathbf{X}^\top \mathbf{W}\mathbf{X})}_{\text{A}_{\mathbf{W}, \mathbf{V}}(\mathbf{X})}), \quad (1)$$

where $\text{LN} : \mathbb{R}^d \rightarrow \mathbb{R}^d$ is the token-wise (columnwise) layer normalization (or LayerNorm [Ba et al., 2016]; one can also use RMSNorm [Zhang and Sennrich, 2019]), and the $\mathbf{R}^\top \sigma(\mathbf{P}\tilde{\mathbf{X}})$ denotes the token-wise single hidden layer MLP : $\mathbb{R}^d \rightarrow \mathbb{R}^d$. One simplification here is that we are not considering learnable parameters in the LayerNorm. The learnable parameters of the LayerNorm can be incorporated in our analysis much like that of the MLP block but with additional notation. The columnwise $\text{softmax}(\cdot)$ of the dot-products $\mathbf{X}^\top \mathbf{W}\mathbf{X}$ between the query and key matrices,² combined with the value matrix $\mathbf{V}\mathbf{X}$ denotes the dot-product

¹In our experiments, we consider supervised learning with \mathcal{Y} as a set of labels, but our analysis applies to any \mathcal{Y} where we have a scalar loss $\ell : \mathcal{Y} \times \hat{\mathcal{Y}} \rightarrow \mathbb{R}$, where $\hat{\mathcal{Y}}$ is the model output space: $\hat{\mathcal{Y}} \subset \mathbb{R}^{|\mathcal{Y}|}$ for multi-class classification with cross-entropy loss, and $\mathcal{Y} = \hat{\mathcal{Y}} \subset \mathbb{R}^m$ for m -output regression with mean-squared loss.

²With queries $\mathbf{Q}\mathbf{X}$, $\mathbf{Q} \in \mathbb{R}^{d_{\text{KQ}} \times d}$ and keys $\mathbf{K}\mathbf{X}$, $\mathbf{K} \in \mathbb{R}^{d_{\text{KQ}} \times d}$, the attention scores $(\mathbf{Q}\mathbf{X})^\top (\mathbf{K}\mathbf{X}) = \mathbf{X}^\top (\mathbf{Q}^\top \mathbf{K})\mathbf{X}$; we use $\mathbf{W} = \mathbf{Q}\mathbf{K}^\top$ for simplicity.

self-attention $A : \mathbb{R}^{d \times L} \rightarrow \mathbb{R}^{d \times L}$. Here d is the transformer “ d_{model} ”. We consider single head attention here for the ease of exposition, but our analysis can be easily extended to multi-headed attention; please see appendix D.4. While Vaswani et al. [2017] utilized ReLU as the activation function σ in the MLP, subsequent works [Devlin et al., 2019] have used other activation functions such as the GELU [Hendrycks and Gimpel, 2016] and the ELU [Clevert et al., 2015]. Furthermore, many different variations of the transformer block has also been utilized in literature. ³

Masked softmax. The columnwise softmax $: \mathbb{R}^L \rightarrow S_L$ independently transforms each column of its $(L \times L)$ input to a L -dimensional simplex $S_L \triangleq \{\mathbf{s} \in \mathbb{R}^L, s_j \geq 0 \forall j \in \llbracket L \rrbracket, \sum_{j=1}^L s_j = 1\}$; that is the i -th column softmax $(\mathbf{D})_{:,i} \in S_L$ for a pre-activation dot-product matrix $\mathbf{D} \in \mathbb{R}^{L \times L}$. A common modification of this transformer block is the replacement of the softmax with a sparse *masked* softmax which has an associated masking function $m : \mathbb{R}^{L \times L} \rightarrow \{0, 1\}^{L \times L}$. For standard self-attention, with a pre-activation dot-product matrix $\mathbf{D} = \mathbf{X}^\top \mathbf{W} \mathbf{X} \in \mathbb{R}^{L \times L}$, the attention mask matrix $\mathbf{M} = m(\mathbf{D})$ is trivially given with $M_{ji} = 1$ for all $j, i \in \llbracket L \rrbracket$. For causal attention, the (j, i) -th mask matrix entry is $M_{ji} = \mathbb{I}(j < i)$. For banded attention with a window width of $w \in \mathbb{N}$, the (j, i) -th mask matrix entry is $M_{ji} = \mathbb{I}(i - w \leq j \leq i + w)$. The (j, i) -th entry A_{ji} of the post-activation attention matrix $\mathbf{A} = \text{softmax}(\mathbf{D})$ for standard and masked attention is given as follows:

$$A_{ji} = \frac{\exp(D_{ji})}{\sum_{j'=1}^L \exp(D_{j'i})}, \quad A_{ji} = \frac{\exp(D_{ji}) \cdot M_{ji}}{\sum_{j'=1}^L \exp(D_{j'i}) \cdot M_{j'i}}. \quad (2)$$

For the simplicity of notation we will denote the masked softmax based sparse self-attention as $A : \mathbb{R}^{d \times L} \rightarrow \mathbb{R}^{d \times L}$ with the implicit understanding that standard softmax attention is a special case of sparse attention with a trivial mask.

Complete model. The model is defined as $f_\Theta : \llbracket D \rrbracket^L \rightarrow \hat{\mathcal{Y}}$ with token and position embeddings $\mathbf{T} \in \mathbb{R}^{d \times D}$ and $\mathbf{E} \in \mathbb{R}^{d \times L}$ respectively, τ transformer blocks each with parameters $\theta^{(t)} = (\mathbf{W}^{(t)}, \mathbf{V}^{(t)}, \mathbf{P}^{(t)}, \mathbf{R}^{(t)})$, $t \in \llbracket \tau \rrbracket$, and a readout linear layer with weights $\Phi \in \mathbb{R}^{Y \times d}$ using token projection vector $\omega \in \mathbb{R}^L$, where Y is the dimensionality of the output $\hat{\mathcal{Y}}$ (for example, the number of classes in output domain \mathcal{Y}). The i -th token $v_i \in \llbracket D \rrbracket$ in the input X is initially embedded as $\mathbf{T}_{:,v_i} + \mathbf{E}_{:,i}$ using the token and position embeddings:

$$f_\Theta(X) = \Phi(\mathbf{X}^{(\tau)} \omega), \quad \mathbf{X}^{(t)} = \text{TF}_{\theta^{(t)}}(\mathbf{X}^{(t-1)}), \forall t \in \llbracket \tau \rrbracket, \quad \mathbf{X}^{(0)} = [\mathbf{T}_{:,v_1} + \mathbf{E}_{:,1}, \dots, \mathbf{T}_{:,v_L} + \mathbf{E}_{:,L}]. \quad (3)$$

Here $\omega \in \mathbb{R}^L$ is the (*fixed*) token projection vector – we can set the $\omega = [0, 0, \dots, 0, 1]^\top$ to select the last token to make the final prediction, and $\omega = (1/L)\mathbf{1}_L$ uses the average of the L tokens (along the sequence length dimension), where $\mathbf{1}_L$ is the all-one L dimensional vector. The Θ in $f_\Theta(\cdot)$ denotes the tuple of all the (learnable) model parameters, that is $\Theta \triangleq (\mathbf{T}, \theta^{(1)}, \dots, \theta^{(\tau)}, \Phi)$. Here we are assuming that the position encodings are not learned, but that can also be incorporated in our study.

Training. Given a set S of n sequence-output pairs (X, y) , $X \in \llbracket D \rrbracket^L$, $y \in \mathcal{Y}$ for training, and a per-sample loss function $\ell : \mathcal{Y} \times \hat{\mathcal{Y}} \rightarrow \mathbb{R}$, the learning involves solving the following empirical risk minimization or ERM problem:

$$\min_{\Theta \triangleq (\mathbf{T}, \theta^{(1)}, \dots, \theta^{(\tau)}, \Phi)} \mathcal{L}(\Theta) \triangleq \frac{1}{n} \sum_{(X, y) \in S} \ell(y, f_\Theta(X)) \quad (f_\Theta(\cdot) \text{ defined in equation (3)}). \quad (4)$$

In the sequel, we will study, first empirically and then theoretically, (i) the convergence rate of stochastic gradient descent for this learning problem, and (ii) the generalization of the learned model.

³For example, instead of the transformer block described in equation (1), there are versions that modify the location where the LayerNorm is applied: $\text{TF}_\theta(\mathbf{X}) = \tilde{\mathbf{X}} + \text{MLP}_{\mathbf{P}, \mathbf{R}}(\text{LN}(\tilde{\mathbf{X}}))$ and $\tilde{\mathbf{X}} = \mathbf{X} + \text{A}_{\mathbf{W}, \mathbf{V}}(\text{LN}(\mathbf{X}))$.

4 Empirical Observations

In this section, we focus on empirically ablating the effect of the different forms of sparse attention on the ERM convergence and generalization. For this purpose, we ensure that all hyperparameters (architectural and optimization) are the same between the standard full attention, and the various sparse attention. We will first discuss the tasks and sparse attention choices; the hyperparameter (architectural and optimization) selection procedure and our compute resources are discussed in appendix B. Then, we will present the comparison between the standard full attention and various sparse attention. Subsequently, focusing on full attention and heavy-hitter style input-dependent sparse attention, we will study the effect of hyperparameters (or the lack thereof) on their relative behaviors.

Tasks. We consider the List Operations or ListOps task [Nangia and Bowman, 2018] from the LRA benchmark [Tay et al., 2021] with sequence lengths between 500 and 600 both for training and testing because we are evaluating in-distribution learning and generalization. This is a 10-class classification problem. We select this task over the other tasks in the LRA benchmark because (i) this is a task where transformers have better than random performance (around 30-40% compared to a random 10% performance), but there is still a significant room for improvement, and (ii) we can control the length of the input sequences and still have a meaningful problem, which is not as straightforward with the other document or image processing tasks in LRA. From the NNCH benchmark [Deletang et al., 2023], we consider 3 tasks that can be solved as a binary classification problem – Parity, Even Pairs, and Missing Duplicates, and 4 tasks that can be solved as a multi-class classification problem – Cycle Navigation, Stack Manipulation, Modular Arithmetic with Brackets and Solve Equation. Parity, Even Pairs and Cycle Navigation are regular languages. Stack Manipulation, Modular Arithmetic and Solve Equation are deterministic context-free languages, while Missing Duplicates is a context-sensitive language. For the NNCH tasks, we consider input sequences of length 40 both for training and testing; Deletang et al. [2023] train on the same length but test on longer to evaluate out-of-distribution length generalization. For all the tasks, we utilize a training / holdout sets of sizes 5000 / 2000.

Sparse attention. While there are various sparse attention mechanisms (as we discussed in section 2), we will consider a representative subset for our empirical evaluations. For input-agnostic sparse attention, we choose banded attention (figure 1b [Parmar et al., 2018]) and block-local attention (figure 1d [Qiu et al., 2020]), with varying band and block sizes respectively. For input-dependent heavy-hitter sparse attention, we choose top- k attention (figure 1f [Gupta et al., 2021]). The main motivation for selecting top- k over LSH based [Kitaev et al., 2020] or clustering based [Roy et al., 2021] input-dependent sparse attention is that we can then easily ensure that the input-dependent sparse attention attends to exactly the same number of tokens as in the input-agnostic ones – that is, the number of nonzeros in each column of the attention score matrix is exactly the same across all sparse attention patterns we consider. We also consider versions of these input-agnostic sparse attention with varying number of global tokens (figure 1e). Note that, as we have highlighted before, **the number of learnable parameters is exactly the same between the model using standard full attention and the one using sparse attention.** A *minor difference* is with global tokens where we also learn their initial global token embeddings. For this reason, we use *exactly the same hyperparameters* for the full and sparse attention versions of the same model to ablate the effect of the sparse attention.

4.1 Overall Learning Convergence and Generalization

We present our first set of experimental results in figure 2 and figure 3, comparing the overall learning convergence and generalization of full attention based models to those using sparse attention. For these experiments, we use the ReLU activation for the MLP component of the transformer block as in the original configuration [Vaswani et al., 2017]. These results are aggregated over 10 repetitions, and we present the median performance and its inter-quartile range. Note that, for the 8 tasks we consider, the full attention

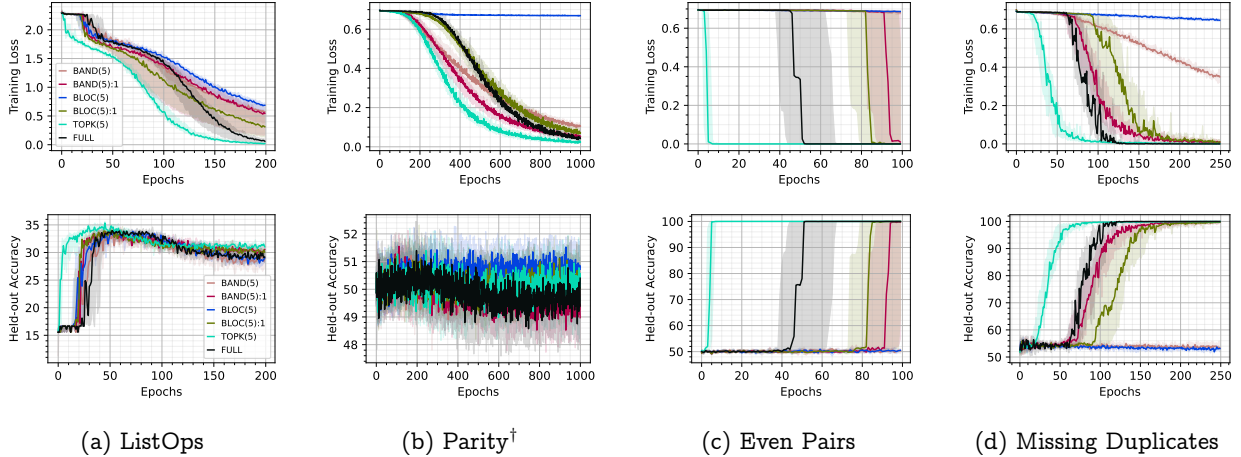


Figure 2: Learning convergence and generalization curves for full attention and various sparse attention based models. Each column corresponds to a task; we present 4 tasks here and 4 more in figure 3. *The legend is the same across all datasets* – BAND(5) denotes banded attention (figure 1b) with a band size of 5; BAND(5):1 denotes the same with a single global token (figure 1e). BLOC(5) denotes block local attention (figure 1d) with a block size of 5; BLOC(5):1 denotes the same with single global token. TOPK(5) is top- k attention with $k = 5$. **Top row:** Training cross-entropy loss trajectories – lower is better. **Bottom row:** Generalization performance on held-out set as training progresses – higher is better. Further results with different mask sizes and different number of global tokens is presented in figure 11 (training cross-entropy), figure 12 (training accuracy), table 2 (generalization) and table 3 (convergence). [†] For the Parity task, all forms of attention have poor generalization, with a held-out accuracy as low as random guessing (50% for binary classification).

model is expressive enough to achieve 100% training accuracy in all tasks, but generalizes non-trivially for only 4 of these 8 tasks – ListOps, Even Pairs, Missing Duplicates and Stack Manipulation. For the remaining 4 tasks – Parity, Modular Arithmetic, Solve Equation and Cycle Navigation – the full attention model has generalization performance close to random guessing. While we only present results for a single sparsity level (mask size) here, we present more detailed results and different sparsity levels in appendix C.1.

Observation 1. *Input-dependent heavy-hitter sparse attention significantly speeds up ERM convergence while input-agnostic sparse attention do not show any consistent improvement over full attention.*

The results in the top row of figure 2 and figure 3 show that the input-agnostic sparse attention often converges slower than full attention. They also often struggle with expressivity in the absence of the global tokens, as seen for block-local attention with Parity and Cycle Navigation, and both block local and banded attention with Even Pairs and Missing Duplicates. This is expected as per the expressivity results of Yun et al. [2020b]. The inclusion of the global token addresses this issue. In contrast, the training loss of top- k attention converges significantly faster than full attention all cases except Stack Manipulation, where all forms of attention converge extremely rapidly. Top- k attention shows improvements (in terms of achieving 95% training accuracy) over full attention ranging between $1.37\times$ (121 epochs vs 167 epochs) with ListOps to $8.83\times$ (6 epochs vs 53 epochs) with Even Pairs (see table 3 in appendix C.1 for further results on this). In all these cases, top- k attention is able to be as expressive as full attention without the need for any global tokens. This consistent faster training of top- k attention in terms of the number of optimization steps needed to converge is not something discussed in existing literature to the best of our knowledge.

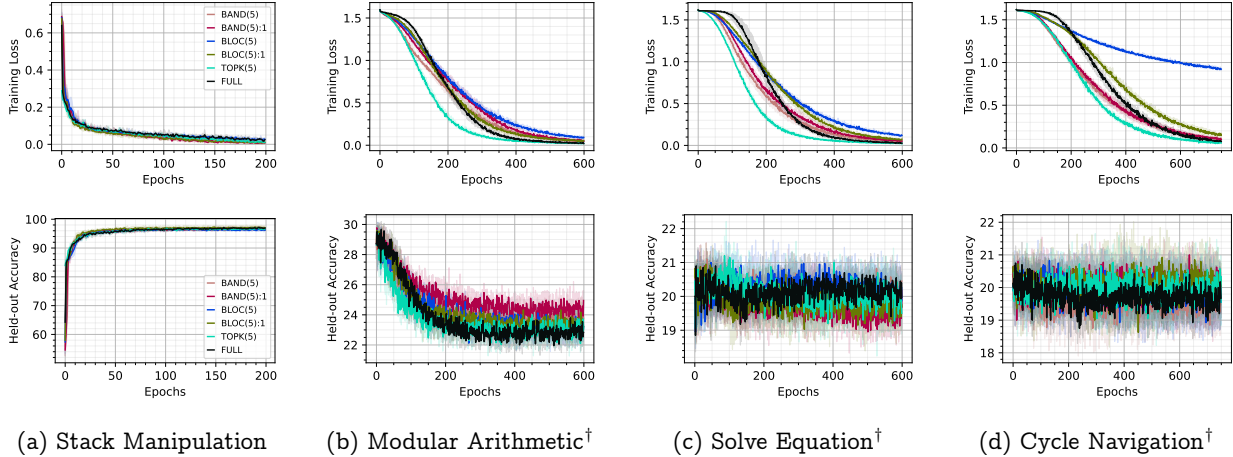


Figure 3: Same as figure 2 with 4 more NNCH tasks. Further results with different mask sizes and different number of global tokens is presented in figure 13 (training cross-entropy) and figure 14 (training accuracy). [†] For the Modular Arithmetic, Solve Equation and Cycle Navigation tasks, all forms of attention have poor generalization, with a held-out accuracy as low as random guessing (20% for each of these 5-class classification tasks).

Observation 2. *Input-dependent heavy-hitter sparse attention generalizes faster during the training process.*

The results in the bottom row of figure 2 and figure 3 show that, in all cases of non-trivial generalization, the input-dependent sparse attention achieves similar (Even Pairs and Missing Duplicates) or better (ListOps) holdout accuracy when compared to the full attention. Furthermore, it attains this generalization level much earlier during the training process. This does not hold for the other 5 tasks, where either (i) the full attention models generalizes poorly, and so do all other attention forms (Parity, Modular Arithmetic, Solve Equation, Cycle Navigation), or (ii) all attention forms generalize equally well (Stack Manipulation). Note that input-dependent heavy-hitter top- k achieves better empirical generalization performance both in terms of the highest holdout accuracy during the training trajectory, and the final holdout accuracy. The latter highlights that the faster ERM convergence of input-dependent sparse attention does not lead to overfitting. In fact, with the ListOps task, the final holdout accuracy with full attention drops from around $35.1 \pm 0.6\%$ to $28.9 \pm 1.4\%$, while the drop with top- k attention is only from $36.3 \pm 0.3\%$ to $31.3 \pm 0.9\%$. In general, the top- k attention based transformers also have comparatively lower variations in their performance as evidenced by the fairly tight inter-quartile ranges of the trajectories of the training loss and holdout accuracy.

4.2 Effect of Hyperparameters

Here we study the effect of the different hyperparameter choices on the relative performances of the full and different sparse attention models. First we study the effect of changing the activation function in the MLP component of a transformer block to evaluate whether the differences in empirical performance are due to the attention component or the MLP component of the block. Then, we study the effect of varying the number of blocks and the number of heads in the model. Finally, we study the effect of varying various optimizer hyperparameters such as the learning rate and its scheduling. In these sets of experiments, we mainly focus on the 3 tasks where the full attention model demonstrates nontrivial generalization (thus excluding Parity, Modular Arithmetic, Solve Equation and Cycle Navigation), and there is a difference between the full and the different sparse attention models (thus excluding Stack Manipulation). Details results on additional tasks and different levels of sparsity are presented in appendix C.2.

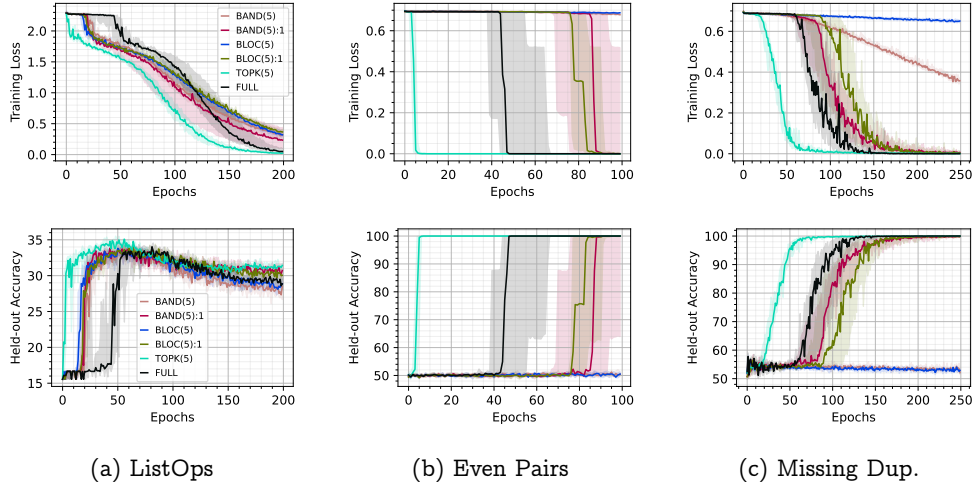


Figure 4: Same as figure 2 for 3 of the tasks with GELU activation. See results for additional tasks and configurations in appendix C.2.

Observation 3. *The improvement of input-dependent heavy-hitter sparse attention over full attention in terms of learning convergence and generalization is not affected by the choice of the activation function σ in the MLP block of a transformer block.*

We present the performances of the different attention mechanisms (full and sparse) with the GELU activation [Hendrycks and Gimpel, 2016] in figure 4 and with the Mish activation [Misra, 2019] in figure 5 for 3/8 tasks. For these experiments, we have kept all other hyperparameters (number of heads and blocks, learning rate and its scheduling, batch size) exactly the same as in figure 2 and figure 3 to ablate the effect of the change in the MLP activation. Comparing these results to figure 2, we see that there is not a lot of qualitative differences in the performances both in terms of learning convergence and generalization.

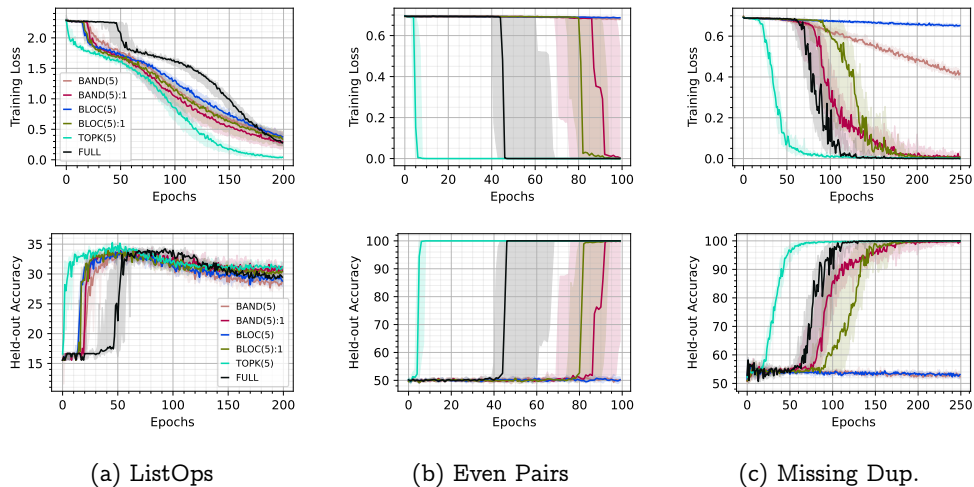


Figure 5: Same as figure 2 for 3 of the tasks with Mish activation. See additional results in appendix C.2.

The input-agnostic sparse attention models continue to converge comparably to full attention with ListOps and Missing Duplicates while falling behind in Even Pairs. One marked difference here is that, with ListOps, the full attention model initially converges slower than the other sparse attention models (compare figure 2a with figure 4a and figure 5a). This is more marked with the Mish activation. However, finally

the full attention model convergence catches up to the input-agnostic sparse attention models. This initial slowdown in the convergence is also reflected in the initial lower generalization accuracy. In contrast, the input-dependent heavy-hitter top- k attention continues to consistently converge faster than full attention in terms of the training loss for both these MLP activations, with very little differences from the results with ReLU activation. This form of sparse attention also achieves better generalization performance earlier in the training process. This indicates that the difference in performance is probably due to the differences in the attention mechanism and not an artifact of the MLP block configuration.

Observation 4. *The improvement of the input-dependent heavy-hitter sparse attention over full attention is agnostic to the transformer architecture in terms of the number of blocks utilized in the model, and appears to increase with the number of heads in each block.*

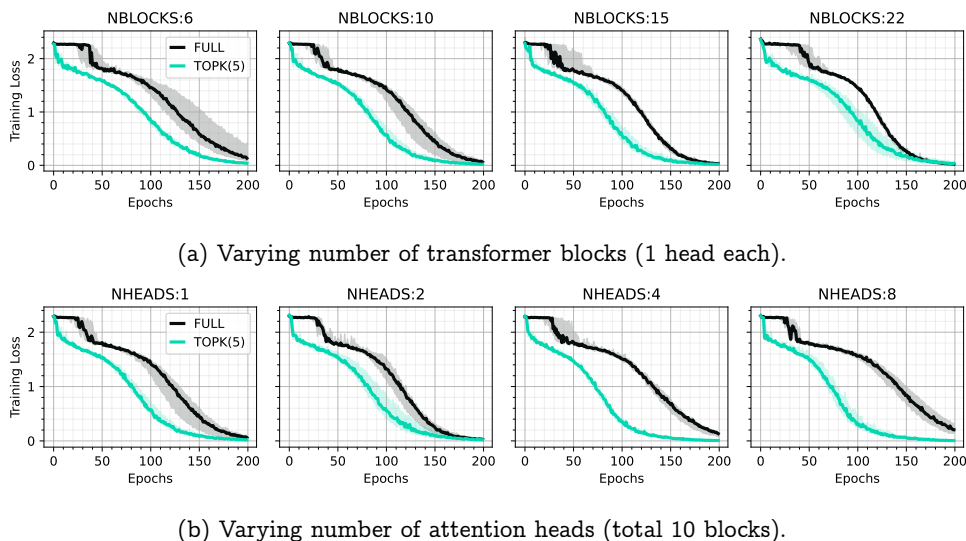
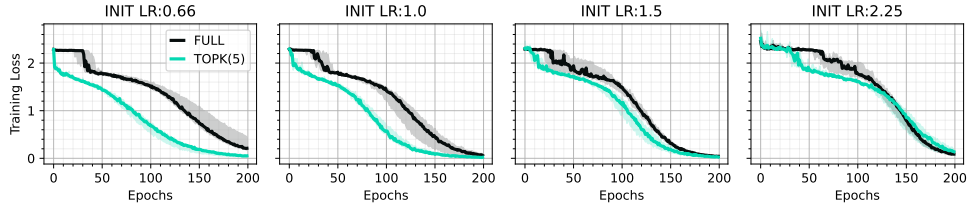


Figure 6: Comparison of full attention and top- k attention in terms of the training loss trajectory for varying model architectures with the ListOps task.

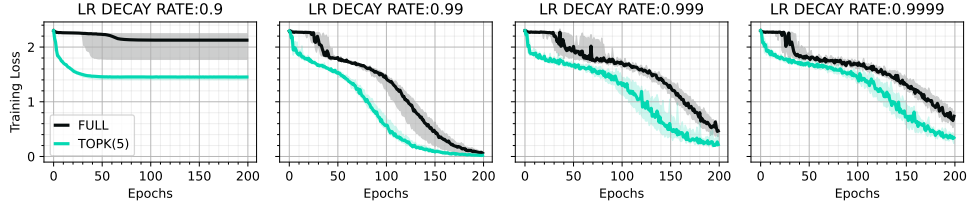
In figure 6, we study the effect of varying the model architecture in terms of the number of transformer blocks or the number of attention heads per transformer block. We have again fixed all other hyperparameters as in figure 2 to solely ablate the effect of the considered architectural changes. Here we only present results for full attention and top- k attention (with $k = 5$) for the ListOps task. The effect of the number of transformer blocks is shown in figure 6a, and the results indicate that top- k attention continues to converge faster than full attention across all number of blocks τ tried ($\tau \in \{6, 10, 15, 22\}$). The relative performance difference does not seem to be affected by the number of blocks. The effect of the number of heads is presented in figure 6b. These results indicate again that top- k sparse attention based models continue to converge faster than their full attention variants. Furthermore, as the number of heads increase from 1 to 4 and 8, the convergence of the full attention model appears to slow down while the convergence of the top- k sparse attention stays almost the same, and thus, the relative improvement increases with the increase in the number of heads.

Observation 5. *The improvement of the input-dependent heavy-hitter sparse attention over full attention holds across varying optimizer hyperparameters, especially for hyperparameters that have the most promising convergence.*

In figure 7, we present the effect of varying the learning rate and its decay rate in the SGD optimization for full and top- k attention with the ListOps task. In figure 7a, we fix the decay rate to 0.99 (as in figure 2)



(a) Varying initial learning rate (decay rate is 0.99).



(b) Varying learning rate decay (initial learning rate is 1.0).

Figure 7: Comparison of full attention and top- k attention in terms of the training loss trajectory for varying optimization hyperparameters with the ListOps task.

and vary the initial learning rate from 0.66 (column 1), 1.0 (column 2; used in previous experiments with ListOps), 1.5 (column 3) and 2.25 (column 4). We see that for the smaller values of the learning rate (0.66 and 1), both full attention and top- k attention have the best convergence, with top- k converging faster than full attention. For the larger initial learning rate (1.5 and 2.25), convergence slows down for both, and the difference between full and top- k attention is less pronounced, though top- k appears to be slightly better, especially in the initial part of the training. In figure 7b, we fix the initial learning rate to 1.0, and vary the decay rate to be 0.9 (column 1), 0.99 (column 2; used in previous experiments with ListOps), 0.999 (column 3) and 0.9999 (column 4). For slower decay rates (0.9999 and 0.999), the overall convergence for both methods slow down though top- k continues to converge faster than full attention. For faster decay rate of 0.9, top- k initially appears to outperform full attention with a big margin. However, very quickly both method stall prematurely as the learning rate becomes too small.

Observation 6. *The improvement of the input-dependent heavy-hitter sparse attention over full attention also holds for the Adam optimizer with varying learning rates, especially for hyperparameters that have the most promising convergence.*

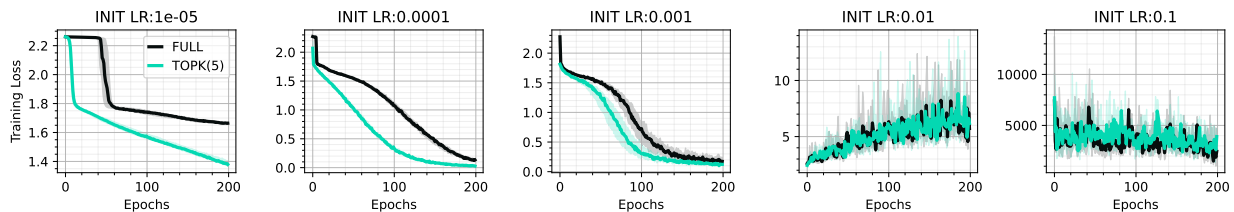


Figure 8: Varying learning rates for Adam optimizer.

While all our previous empirical observations were utilizing the SGD optimizer, in figure 8, we also evaluate whether some of the relative performances translate to the more widely utilized Adam optimizer [Kingma and Ba, 2015] on the ListOps task. We evaluate various learning rates, and see that the learning rate that provided convergence for SGD (initial learning rate of around 0.1-1.0) lead to divergence with Adam. Hence,

we tried smaller learning rates and see that the improved convergence of the input-dependent heavy-hitter sparse attention is also present when using the Adam optimizer for learning, with significant differences in some cases.

5 Theoretical Understanding

The empirical observations we made in the previous section demonstrate that input-agnostic sparse attention can struggle with expressivity, and does not show any consistent benefit over full attention. In contrast, input-dependent heavy-hitter top- k attention show significant speedup in training convergence and achieving strong generalization. In this section, we want to theoretically understand why this might be happening. We begin by considering the factors that affect the convergence and generalization of SGD based training.

First considering convergence, standard analysis of SGD show that, for a α -Lipschitz and β -smooth finite-sum (non-convex) objective, with learning rates η_i at the i -th step, converge to a ϵ -stationary point in T steps where $\epsilon \sim O(\beta\alpha^2(\sum_{i=0}^{T-1} \eta_i^2)/(\sum_{i=0}^{T-1} \eta_i))$. Different choices of $\eta_i, i \in \llbracket T \rrbracket$ (such as η/i or η/\sqrt{i} for some constant η with $\eta_0 = \eta$) provide different convergence rates (such as $O(1/\log(T))$ or $O(1/\sqrt{T})$). As we control for the the learning rate and its scheduling for all forms of attention in our empirical evaluations, and we ensure that all models start learning from the same initial set of parameters, the main distinction between the different forms of attention could be the Lipschitz constant α and the smoothness constant β . Note that, with non-smooth activation function like ReLU, we are using stochastic sub-gradient descent, where the guarantees are much weaker but still depend on the Lipschitz constant.

Generalization error of a model is defined as the difference between empirical risk (computed on the training samples) and the true risk (computed over the population). A low training error combined with a low generalization error implies strong performance on unseen data. Utilizing the seminal work [Bousquet and Elisseeff, 2000] on algorithmic stability, Hardt et al. [2016, Theorem 2.2] show that learning with ϵ -stable randomized algorithm guarantees an expected generalization error (with expectation over the randomness in the algorithm and the training data sampling) of at most ϵ . Furthermore, they show that, for α -Lipschitz and β -smooth finite-sum nonconvex objective, the T step SGD algorithm with per-step learning rate $\eta_i \leq \eta/i$ is ϵ -uniformly stable with $\epsilon \sim O((\eta\alpha^2)^{1/1+\beta\eta}(1+1/\beta\eta)T^{\beta\eta/1+\beta\eta})$ [Hardt et al., 2016, Theorem 3.12]. As we have again controlled for the learning rates and its schedule, the only distinguishing factor between the different forms of attention (full or sparse) are the Lipschitz and smoothness constants.

Based on this intuition, we will focus on the Lipschitz constant. First, we will try to characterize how the behavior of the softmax – specifically the input stability of the softmax function – in the attention mechanism of the transformer block affects the Lipschitz constant of the overall learning objective. Then, we will characterize how the different forms of sparse attention affect the input-stability of the softmax function and the attention mechanism.

5.1 From Softmax Input-stability to Loss Lipschitz Constant

This learning is performed with SGD, and we are interested in understanding the effect of the masked softmax operation on both this optimization for learning the model, and the subsequent generalization of this model. Note that, fixing all other hyperparameters (such as the embedding dimension d , the MLP hidden layer size d_{MLP} , the number of transformer blocks τ), there is no difference in the number of learnable parameters between a model that uses the standard softmax and the one using masked softmax (assuming that the masking does not introduce additional learnable parameters). We explicitly study the effect of this masked softmax operation in terms of the stability or Lipschitz property of the (masked) softmax.

Definition 1. A masked softmax is ξ -input-stable if $\forall \mathbf{z}, \bar{\mathbf{z}} \in \mathbb{R}^d$,

$$\|\text{softmax}(\mathbf{z}) - \text{softmax}(\bar{\mathbf{z}})\|_1 \leq \xi \|\mathbf{z} - \bar{\mathbf{z}}\|_1. \quad (5)$$

The self-attention operation $A : \mathbb{R}^{d \times L} \rightarrow \mathbb{R}^{d \times L}$ with learnable parameters $\mathbf{W}, \mathbf{V} \in \mathbb{R}^{d \times d}$ is stable with respect to its input and parameters if $\forall \mathbf{X}, \bar{\mathbf{X}} \in \mathbb{R}^{d \times L}, \mathbf{W}, \bar{\mathbf{W}}, \mathbf{V}, \bar{\mathbf{V}} \in \mathbb{R}^{d \times d}$:

$$\|A_{\mathbf{W}, \mathbf{V}}(\mathbf{X}) - A_{\mathbf{W}, \mathbf{V}}(\bar{\mathbf{X}})\|_{2,1} \leq \lambda_X(\xi) \|\mathbf{X} - \bar{\mathbf{X}}\|_{2,1}, \quad (6)$$

$$\|A_{\mathbf{W}, \mathbf{V}}(\mathbf{X}) - A_{\bar{\mathbf{W}}, \mathbf{V}}(\mathbf{X})\|_{2,1} \leq \lambda_W(\xi) \|\mathbf{W} - \bar{\mathbf{W}}\|, \quad (7)$$

$$\|A_{\mathbf{W}, \mathbf{V}}(\mathbf{X}) - A_{\mathbf{W}, \bar{\mathbf{V}}}(\mathbf{X})\|_{2,1} \leq \lambda_V \|\mathbf{V} - \bar{\mathbf{V}}\|, \quad (8)$$

where $\lambda_X(\xi), \lambda_W(\xi)$ are constants that depend on ξ .

We will precisely characterize the values of the constants in the above definition ($\xi, \lambda_X(\xi), \lambda_W(\xi), \lambda_V$) for the different (masked) softmax operations and corresponding (masked) self-attention operations in the sequel. However, we define them here to highlight how the stability of the softmax operation affects the stability of the self-attention operator A , and how this affects the Lipschitz-ness of the learning objective in equation (4) with respect to the model parameters $\Theta = (\mathbf{T}, \theta^{(1)}, \dots, \theta^{(\tau)}, \Phi)$. For completeness, we first need to establish the stability properties of the MLP component of a TF block (see proof in appendix D.1):

Lemma 1. Assuming that the MLP activation σ is λ_σ -Lipschitz with $\sigma(0) = 0$, and the MLP parameters have norms bounded by $B > 0$, that is $\|\mathbf{P}\| \leq B$ and $\|\mathbf{R}\| \leq B$, the token-wise MLP and LN operations are stable with respect to their input and model parameters as follows $\forall \mathbf{x}, \mathbf{x}' \in \mathbb{R}^d, \|\mathbf{x}\|, \|\bar{\mathbf{x}}\| \leq \Xi, \mathbf{P}, \bar{\mathbf{P}} \in \mathbb{R}^{d_{\text{MLP}} \times d}, \mathbf{R}, \bar{\mathbf{R}} \in \mathbb{R}^{d_{\text{MLP}} \times d}$:

$$\|\text{MLP}_{\mathbf{P}, \mathbf{R}}(\mathbf{x}) - \text{MLP}_{\mathbf{P}, \mathbf{R}}(\bar{\mathbf{x}})\| \leq \eta_X \|\mathbf{x} - \bar{\mathbf{x}}\|, \quad (9)$$

$$\|\text{MLP}_{\mathbf{P}, \mathbf{R}}(\mathbf{x}) - \text{MLP}_{\bar{\mathbf{P}}, \mathbf{R}}(\mathbf{x})\| \leq \eta_P \|\mathbf{P} - \bar{\mathbf{P}}\|, \quad (10)$$

$$\|\text{MLP}_{\mathbf{P}, \mathbf{R}}(\mathbf{x}) - \text{MLP}_{\mathbf{P}, \bar{\mathbf{R}}}(\mathbf{x})\| \leq \eta_R \|\mathbf{R} - \bar{\mathbf{R}}\|, \quad (11)$$

$$\|\text{LN}(\mathbf{x}) - \text{LN}(\bar{\mathbf{x}})\| \leq \zeta_{\text{LN}} \|\mathbf{x} - \bar{\mathbf{x}}\|, \quad (12)$$

where $\eta_X = B^2 \lambda_\sigma$, $\eta_P = \eta_R = \lambda_\sigma B \Xi$.

The Lipschitz property of the LayerNorm (and the corresponding value of ζ_{LN}) has been previously established in Kim et al. [2021]. Given this, we can establish the following results for a transformer block (see proof in appendix D.2):

Theorem 1. Given definition 1 and lemma 1, a transformer block TF with learnable parameters $\theta = (\mathbf{W}, \mathbf{V}, \mathbf{P}, \mathbf{R})$ is $\lambda_\theta(\xi)$ -stable with respect to its learnable parameters θ with

$$\lambda_\theta(\xi) = \zeta_{\text{LN}} (\zeta_{\text{LN}} (1 + \eta_X) (\lambda_W(\xi) + \lambda_V) + L(\eta_P + \eta_R)), \quad (13)$$

and TF is $\lambda_X(\xi)$ -stable with respect to its input \mathbf{X} with

$$\lambda_X(\xi) = \zeta_{\text{LN}}^2 (1 + \eta_X) (1 + \lambda_X(\xi)), \quad (14)$$

where we explicitly note the dependence of the stability constant with respect to learnable parameters $\lambda_\theta(\xi)$, and input $\lambda_X(\xi)$ to the Lipschitz constant ξ of the (masked) softmax operation. Thus, for any parameter tuples $\theta, \bar{\theta}$ and input $\mathbf{X}, \bar{\mathbf{X}}$, we have

$$\|\text{TF}_\theta(\mathbf{X}) - \text{TF}_{\bar{\theta}}(\mathbf{X})\|_{2,1} \leq \lambda_\theta(\xi) \|\theta - \bar{\theta}\|, \quad \text{and} \quad \|\text{TF}_\theta(\mathbf{X}) - \text{TF}_\theta(\bar{\mathbf{X}})\|_{2,1} \leq \lambda_X(\xi) \|\mathbf{X} - \bar{\mathbf{X}}\|. \quad (15)$$

This allows us to establish the following result for the aforementioned model with τ transformer blocks (see proof in appendix D.3):

Theorem 2. Assuming that the sample wise loss ℓ in equation (4) is α -Lipschitz and $\|\Phi\| \leq 1$ with $\omega = (1/L)\mathbf{1}_L$, under the conditions of definition 1 and theorem 1, the learning objective \mathcal{L} in equation (4) is $\lambda_{\mathcal{L}}(\xi)$ -Lipschitz with respect to the learnable parameters $\Theta = (\mathbf{T}, \theta^{(1)}, \dots, \theta^{(\tau)}, \Phi)$, where

$$\lambda_{\mathcal{L}}(\xi) = \alpha \left(\Xi + \lambda_{\mathbf{X}}(\xi)^\tau \left(1 + \frac{\lambda_{\theta}(\xi)}{L(\lambda_{\mathbf{X}}(\xi) - 1)} \right) \right), \quad \text{and} \quad |\mathcal{L}(\Theta) - \mathcal{L}(\bar{\Theta})| \leq \lambda_{\mathcal{L}}(\xi) \|\Theta - \bar{\Theta}\|, \quad (16)$$

for any set of model parameters $\Theta, \bar{\Theta}$.

This characterizes how the Lipschitz constant of the learning loss, and thus the convergence rate of the SGD based ERM, is tied to the input-stability constant ξ of the (masked) softmax. Thus, based on theorem 1, the larger the values of $\lambda_W(\xi)$, $\lambda_X(\xi)$ and λ_V in definition 1, the larger the Lipschitz constant of the training loss. We will characterize these quantities in the sequel.

5.2 Role of Sparse Softmax

To understand the effect of sparsity on the stability of the softmax function, we begin with understanding the stability of the standard full softmax and the subsequent full attention operation. Li et al. [2023] establish the following stability of the standard softmax (see lemma S2 in appendix E.1):

Lemma 2 (adapted from Li et al. [2023] Lemma B.1). For any $\mathbf{z}, \bar{\mathbf{z}} \in \mathbb{R}^L$ with

$$\max_{i,j \in \llbracket L \rrbracket} z_i - z_j \leq \delta, \quad \text{and} \quad \max_{i,j \in \llbracket L \rrbracket} \bar{z}_i - \bar{z}_j \leq \delta, \quad (17)$$

for a positive constant $\delta > 0$, we have the following:

$$\|\text{softmax}(\mathbf{z})\|_\infty \leq \frac{e^\delta}{L}, \quad \|\text{softmax}(\mathbf{z}) - \text{softmax}(\bar{\mathbf{z}})\|_1 \leq \frac{e^\delta}{L} \|\mathbf{z} - \bar{\mathbf{z}}\|_1. \quad (18)$$

A critical factor in the softmax stability is this quantity δ that is the upper bound on the difference between the largest and smallest values over which the softmax is applied. In the context of dot-product self-attention, it corresponds to the difference between the largest and smallest query-key dot-products for any query. We call this term the *semantic dispersion*, and define it precisely as follows:

Definition 2. For a (sparse) attention transformer block with L length input sequences $\mathbf{X} \in \mathbb{R}^{d \times L}$, and a mask $\mathbf{M} \in \{0, 1\}^{L \times L}$ (input dependent or input agnostic), we define the per-query semantic dispersion as a scalar $\delta > 0$ such that, for any query token $\mathbf{X}_{:i}, i \in \llbracket L \rrbracket$ the maximum difference between the largest and smallest unmasked query-key dot-products is bounded from above by δ . That is, for any input sequence of token representations $\mathbf{X} \in \mathbb{R}^{d \times L}$, mask $\mathbf{M} \in \{0, 1\}^{L \times L}$ and attention parameters $\mathbf{W} \in \mathbb{R}^{d \times d}$, for all query tokens $i \in \llbracket L \rrbracket$, we have

$$\delta \geq \max_{j,j' \in \llbracket L \rrbracket: M_{ji}=M_{j'i}=1} (\mathbf{X}_{:i}^\top \mathbf{W} \mathbf{X}_{:j} - \mathbf{X}_{:i}^\top \mathbf{W} \mathbf{X}_{:j'}). \quad (19)$$

We discuss this definition with examples in figure 9. Based on this definition, we can establish the stability of the softmax and the attention operation A in terms of the $\xi, \lambda_X(\xi), \lambda_W(\xi)$ in definition 1 as follows (see theorem S3 in appendix E.1 for details):

Theorem 3 (partially adapted from [Li et al., 2023] Lemma B.2). Assuming that the per-token Euclidean norms are bounded as $\|\mathbf{X}_{:i}\| \leq \Xi \forall i \in \llbracket L \rrbracket$, and the parameter norms are bounded at $\|\mathbf{W}\| \leq \Gamma$ and $\|\mathbf{V}\| \leq \Upsilon$, and the per-query semantic dispersion (definition 2) is bounded by $\delta_s > 0$. Then the standard softmax is ξ_s -stable with $\xi_s = e^{\delta_s}/L$, and the standard attention is stable as in

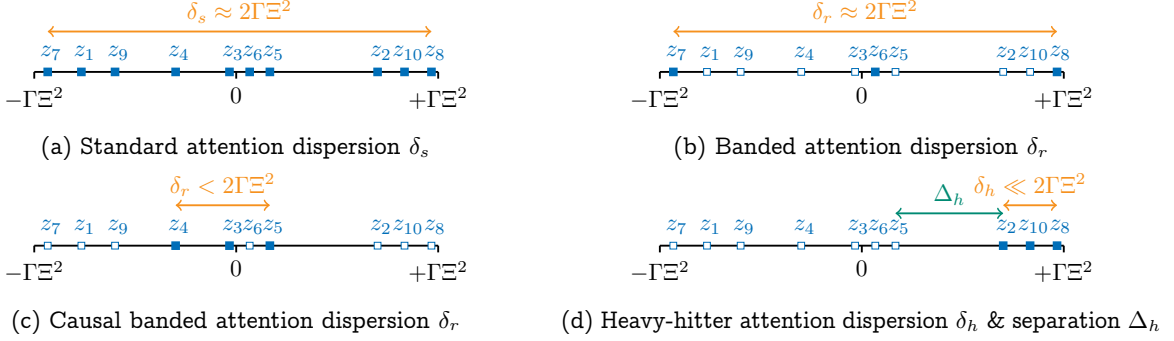


Figure 9: Examples of per-query semantic dispersion δ (definition 2) and heavy-hitter semantic separation Δ (definition 3): Consider a sequence of length $L = 10$, and we will demonstrate the concepts for query token $\mathbf{X}_{:6}$. Let $z_j = \mathbf{X}_{:6}^\top \mathbf{W} \mathbf{X}_{:j}$, $j \in \llbracket L \rrbracket$ denote the j -th query-key dot-product. (a) Figure 9a shows that in standard full attention (no masking), the z_j s (denoted by the \blacksquare) can range between $-\Gamma\Xi^2$ and $+\Gamma\Xi^2$ under the conditions of theorem 1 (namely $\|\mathbf{W}\| \leq \Gamma$, $\|\mathbf{X}_{:i}\| \leq \Xi \forall i \in \llbracket L \rrbracket$), thereby giving us a semantic dispersion $\delta_s \approx 2\Gamma\Xi^2$ in this example. In general, with full attention, we cannot expect a tighter bound on δ_s than $2\Gamma\Xi^2$. (b) Figure 9b shows the same example with an input-agnostic banded masked attention with the same dot-product values, where the query token $\mathbf{X}_{:6}$ only attends to succeeding key tokens $\mathbf{X}_{:6}, \mathbf{X}_{:7}, \mathbf{X}_{:8}$ (the \blacksquare), while the remaining dot-products are masked (the \square). In this example, the semantic dispersion $\delta_r \approx \delta_s \approx 2\Gamma\Xi^2$, no better than with full-attention. (c) Figure 9c shows the example with an input-agnostic causal banded attention mask where token $\mathbf{X}_{:6}$ only attends to the preceding key tokens $\mathbf{X}_{:5}, \mathbf{X}_{:4}, \mathbf{X}_{:3}$, masking out the rest. In this case, this input-agnostic masked attention has a small dispersion $\delta_r < 2\Gamma\Xi^2$ better than that of full-attention $\delta_s \approx 2\Gamma\Xi^2$. However, there is usually no way to ensure that a condition where $\delta_r \ll \delta_s$ will exist. (d) Figure 9d shows the example with an input-dependent heavy-hitter attention, where only the high values are unmasked, and there is a significant semantic separation Δ_h between the masked and unmasked dot-products. With this form of input-dependent masking, we can potentially have a significantly smaller semantic dispersion $\delta_h \ll 2\Gamma\Xi^2$ implying $\delta_h \ll \delta_s$.

definition 1 with

$$\lambda_X(\xi_s) = \xi_s \Upsilon L(2\Gamma\Xi^2 + 1) = e^{\delta_s} \Upsilon(2\Gamma\Xi^2 + 1), \quad \lambda_W(\xi_s) = \xi_s \Upsilon L^2 \Xi^3 = e^{\delta_s} \Upsilon L \Xi^3, \quad \lambda_V = L\Xi. \quad (20)$$

Note that the semantic dispersion δ_s plays a significant role in $\lambda_X(\xi_s)$ and $\lambda_W(\xi_s)$. Thus, larger the value of δ_s , the higher the values of these constants, and thus higher per-transformer-block stability constants $\lambda_\theta(\xi_s)$ and $\lambda_X(\xi_s)$ in theorem 1. We discuss the semantic dispersion for full attention in figure 9a. In general, we cannot expect this dispersion δ_s to be significantly smaller than $2\Gamma\Xi^2$.

Next we study the stability of input-agnostic *regular* k -sparse attention transformers, where *each query token attends to exactly k key tokens, and each key token is attended to by exactly k query tokens.*⁴ This form includes the aforementioned banded attention (figure 1b), block-local attention (figure 1d) and strided attention (figure 1c); random attention satisfies this only in expectation. It seems intuitive that sparse attention would increase the stability because it reduces the number of pairwise token interactions, and thus, the propagation of any input perturbation, with more sparsity leading to more stability. However, we show that the effect of this form of sparse attention is more nuanced (see theorem S4 in appendix E.2):

Theorem 4. Consider the self-attention operation $\mathbf{A} : \mathbb{R}^{d \times L} \rightarrow \mathbb{R}^{d \times L}$ with input \mathbf{X} of L token representations and parameters $\mathbf{W}, \mathbf{V} \in \mathbb{R}^{d \times d}$ utilizing a k -regular input-agnostic masking function $m : \mathbb{R}^{L \times L} \rightarrow \{0, 1\}^{L \times L}$ where $m(\mathbf{D}) = \mathbf{M} \forall \mathbf{D} \in \mathbb{R}^{L \times L}$. Assuming that the per-token Euclidean

⁴This naming is inspired from *regular graphs* in which each node has the same number of (incoming and outgoing) edges, and thus each row and each column in the adjacency matrix have the same number of nonzeros.

norms are bounded as $\|\mathbf{X}_{:i}\| \leq \Xi \forall i \in \llbracket L \rrbracket$, and the parameter norms are bounded at $\|\mathbf{W}\| \leq \Gamma$ and $\|\mathbf{V}\| \leq \Upsilon$, and the per-query semantic dispersion (definition 2) is bounded by $\delta_r > 0$. Then the masked softmax is ξ_r -stable with $\xi_r = e^{\delta_r}/k$, and the regular k -sparse attention is stable as in definition 1 with

$$\lambda_X(\xi_r) = \xi_r \Upsilon k (2\Gamma \Xi^2 + 1) = e^{\delta_r} \Upsilon (2\Gamma \Xi^2 + 1), \quad \lambda_W(\xi_r) = \xi_r \Upsilon L k \Xi^3 = e^{\delta_r} \Upsilon L \Xi^3, \quad \lambda_V = L \Xi. \quad (21)$$

This result shows that input-agnostic k -regular sparse attention provides guarantees very similar to those of full attention except for the e^{δ_r} term involving the per-query semantic dispersion. This implies that this sparse attention would have significant improvement in stability **only** if the per-query semantic dispersion δ_r is sufficiently small relative to the full attention semantic dispersion δ_s ; one such situation is visualized in figure 9c. With regular sparse attention such as banded, block-local or strided, the dispersion δ_r would be small only if the per-query dot-products somehow align with the sparsity patterns – with temporal locality based patterns such as banded and block-local, the dot-products for nearby keys (in terms of sequence position) would require to have a small range; with strided patterns, the dot-products for keys matching the stride regularity should span a small range. These conditions are too restrictive, and thus, δ_r will generally not be sufficiently smaller than the semantic dispersion of standard full-attention $\delta_s \approx 2\Gamma \Xi^2$ (as shown in the example of figure 9b). An important aspect of this above result in theorem 4 is that, if $k \rightarrow L$ (that is, we are considering full attention), then $\delta_r \rightarrow \delta_s$, and the results reduce to exactly those of theorem 3.

An input-dependent sparse attention is the “heavy-hitter attention”, where, for any query token $i \in \llbracket L \rrbracket$, we mask all but the highest values $\mathbf{X}_{:i}^\top \mathbf{W} \mathbf{X}$ in column i of the attention dot-product matrix $\mathbf{X}^\top \mathbf{W} \mathbf{X}$, and there is a significant gap between the unmasked dot-product $\mathbf{X}_{:i}^\top \mathbf{W} \mathbf{X}_{:j}$ for the unmasked keys j with $M_{ji} = 1$, and the masked dot-product $\mathbf{X}_{:i}^\top \mathbf{W} \mathbf{X}_{:j'}$ for the masked keys j' , $M_{j'i} = 0$. LSH based attention [Kitaev et al., 2020], top- k attention [Gupta et al., 2021], cluster attention [Roy et al., 2021], and thresholded attention [Zhao et al., 2019] fit this form of sparse attention. Unlike the regular k -sparse attention, here each token can attend to a small number of tokens (figure 1f), but each token can be attended to by anything between 0 and L tokens, making the stability analysis of input-agnostic regular sparse attention (theorem 4) inapplicable. To study these heavy-hitter sparse attention forms, we need to formalize a notion of *semantic separation* between the masked and unmasked query-key dot-products:

Definition 3. For a sparse attention transformer block with L length input sequences $\mathbf{X} \in \mathbb{R}^{d \times L}$, and an input-dependent heavy-hitter mask $\mathbf{M} \in \{0, 1\}^{L \times L}$, we define the per-query semantic separation as a scalar $\Delta > 0$ such that, for any query token $\mathbf{X}_{:i}$, $i \in \llbracket L \rrbracket$ the minimum difference between the a pair of masked and unmasked query-key dot-products is bounded from below by Δ . That is, for all query tokens $i \in \llbracket L \rrbracket$, with unmasked key j and masked key j' , we have

$$\Delta \leq \min_{\forall j, j' \in \llbracket L \rrbracket: M_{ji}=1, M_{j'i}=0} (\mathbf{X}_{:i}^\top \mathbf{W} \mathbf{X}_{:j} - \mathbf{X}_{:i}^\top \mathbf{W} \mathbf{X}_{:j'}). \quad (22)$$

The notion of separation is visualized in figure 9d. Given this definition, we present the stability of the heavy-hitter attention in the following (see theorem S5 in appendix E.3):

Theorem 5. Consider the self-attention operation $A : \mathbb{R}^{d \times L} \rightarrow \mathbb{R}^{d \times L}$ with input \mathbf{X} of L token representations and parameters $\mathbf{W}, \mathbf{V} \in \mathbb{R}^{d \times d}$ utilizing a k -heavy-hitter input-dependent masking function $m : \mathbb{R}^L \rightarrow \{0, 1\}^L$, applied columnwise to the dot-product matrix to get a mask matrix $\mathbf{M} \in \{0, 1\}^{L \times L}$. Assuming the following: (i) For any query-key pairs $\mathbf{X}, \bar{\mathbf{X}} \in \mathbb{R}^{d \times L}$, the k -heavy-hitter mask $\mathbf{M} = m(\bar{\mathbf{X}}^\top \mathbf{W} \mathbf{X})$ (applied columnwise) has a minimum per-query semantic separation (definition 3) of $\Delta_h > 0$, (ii) A maximum of $\beta k, \beta > 1$ query tokens attend to a single key token, that is, $\|\mathbf{M}_{:i}\|_1 \leq \beta k$ for any $i \in \llbracket L \rrbracket$, (iii) The per-token Euclidean norms are bounded as $\|\mathbf{X}_{:i}\| \leq \Xi \forall i \in \llbracket L \rrbracket$, and the parameter norms are bounded at $\|\mathbf{W}\| \leq \Gamma$ and $\|\mathbf{V}\| \leq \Upsilon$, and (iv) The per-query semantic dispersion (definition 2) is bounded by $\delta_h > 0$. Then the masked

Table 1: Bounds for ξ , $\lambda_X(\xi)$, $\lambda_W(\xi)$, λ_V from definition 1 for different forms of attention. Note that $\lambda_V = L\Xi$ for all forms of attention, and thus elided from this table.

Attention	ξ	$\lambda_X(\xi)$	$\lambda_W(\xi)$
Full (theorem 3)	$\frac{e^{\delta_s}}{L}$	$e^{\delta_s} \Upsilon(2\Gamma\Xi^2 + 1)$	$e^{\delta_s} \Upsilon L\Xi^3$
k -regular (theorem 4)	$\frac{e^{\delta_r}}{k}$	$e^{\delta_r} \Upsilon(2\Gamma\Xi^2 + 1)$	$e^{\delta_r} \Upsilon L\Xi^3$
k -heavy-hitter (theorem 5)	$\frac{e^{\delta_h}}{k}(1 + 1/\Delta_h)$	$e^{\delta_h} \Upsilon(\beta + 2\Gamma\Xi^2(\beta + 1)(1 + 1/\Delta_h))$	$2e^{\delta_h} \Upsilon L\Xi^3(1 + 1/\Delta_h)$

softmax is ξ_h -stable with $\xi_h = (e^{\delta_h/k})(1 + 1/\Delta_h)$, and the k -heavy-hitter sparse attention is stable as in definition 1 with

$$\begin{aligned} \lambda_X(\xi_h) &= \xi_h \Upsilon k \left(2\Gamma\Xi^2(\beta + 1) + \frac{\beta}{1 + 1/\Delta_h} \right) = e^{\delta_h} \Upsilon(\beta + 2\Gamma\Xi^2(\beta + 1)(1 + 1/\Delta_h)), \\ \lambda_W(\xi_h) &= 2\xi_h \Upsilon L k \Xi^3 = 2e^{\delta_h} \Upsilon L \Xi^3(1 + 1/\Delta_h), \quad \lambda_V = L\Xi. \end{aligned} \quad (23)$$

First, note that, with the heavy-hitter attention, we would expect the per-query semantic separation δ_h – the gap between the highest and lowest unmasked dot-products – to be significantly smaller than δ_s especially for small k .

To compare the stability constants for all different forms of attention, we have put them together in table 1. To characterize the conditions when the stability constants for the heavy-hitter sparse attention provides improved guarantees over full attention, we have the following result:

Corollary 1. *Consider the definitions and conditions of theorem 3 and theorem 5. Further assume that (i) the maximum per-query semantic dispersion for standard attention is $\delta_s \leq 2\Gamma\Xi^2$, while that of heavy-hitter attention is $\delta_h = c_1\delta_s$, and (ii) the heavy-hitter minimum per-query semantic separation is $\Delta_h = c_2\delta_s$ for some positive constants c_1, c_2 . Then $\lambda_W(\xi_h) < \lambda_W(\xi_s)$ when*

$$c_1 + \frac{1}{\delta_s} \log 2 \left(1 + \frac{1}{c_2\delta_s} \right) < 1, \quad (24)$$

and $\lambda_X(\xi_h) < \lambda_X(\xi_s)$ when

$$c_1 + \frac{1}{\delta_s} \log \left(2\Gamma\Xi^2(1 + \beta) \left(1 + \frac{1}{c_2\delta_s} \right) + \beta \right) - \frac{1}{\delta_s} \log(2\Gamma\Xi^2 + 1) < 1. \quad (25)$$

This result shows that moderate reduction in the dispersion (δ_h vs δ_s) allow for significant improvements in λ_W even for small separation Δ_h , while improvements in λ_X are more moderate. We discuss this in detail in appendix E.4.

To see how these stability constants affect the loss landscapes, we also visualize them in figure 10 (top and middle rows) utilizing the techniques proposed in Li et al. [2018] (see appendix E.5). We see that the contours on the loss surfaces of full attention model are somewhat asymmetric – see for example, around the center in figure 10b, figure 10c, and moderately in figure 10a. In contrast, the loss surfaces of the heavy-hitter top- k attention model are quite symmetric, especially around the center. We also utilize the loss surface to approximately estimate the Lipschitz constant across the loss landscape (see details in appendix E.5). We plot the distribution of these estimates in the bottom row of figure 10 for varying distance from the optimum – we plot the 50-th, 75-th, 95-th and 99-th percentile values of these estimates of the full attention model and the heavy-hitter top- k attention model. We see that near the optimum (the final trained model), the distributions of these estimates are close for both the models. However, as we move farther away from the trained model, the distributions change significantly, and top- k attention provides a smaller Lipschitz constant estimate compared to full attention all percentiles of the distribution. This indicates that, empirically, the

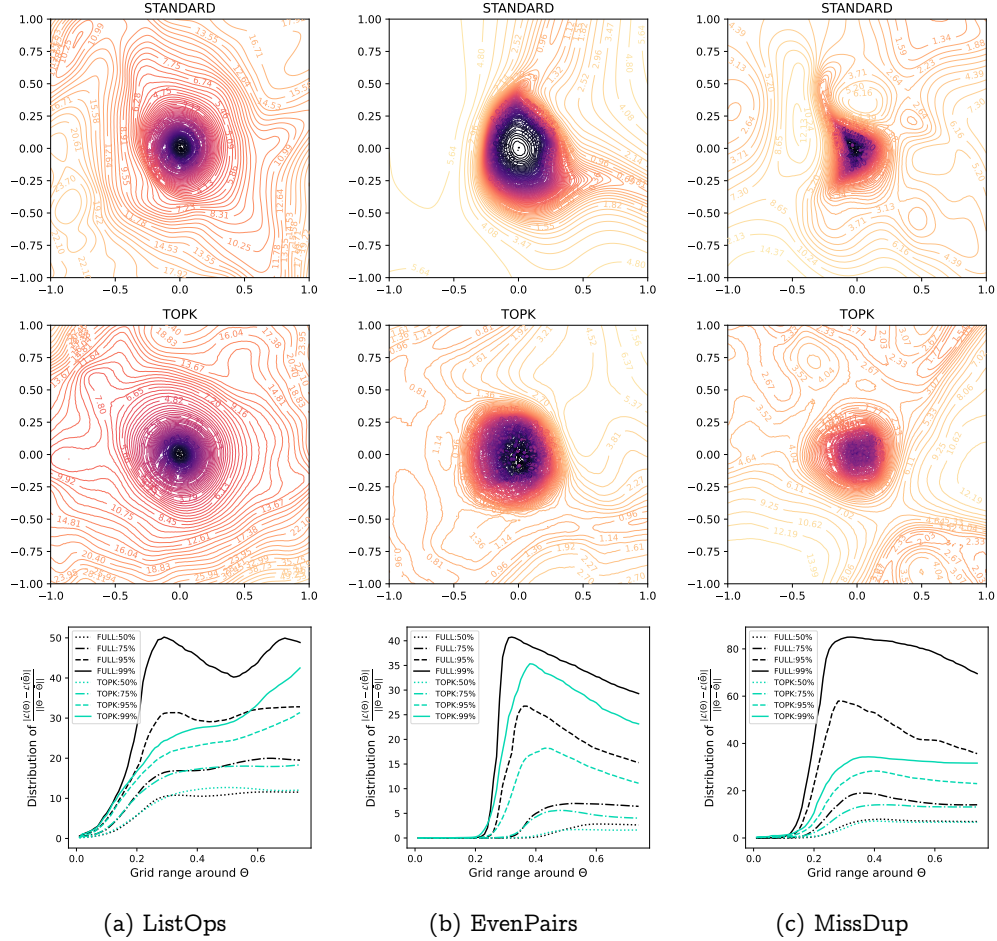


Figure 10: **Top and middle rows:** Loss surfaces of the models with full attention (top row) and top- k attention (middle row) for the tasks considered in figure 2 with the corresponding hyperparameters utilizing the filter-normalized version of the loss landscape visualization. The $(0,0)$ grid point corresponds to the final trained model – the optimum. **Bottom row:** Distribution of the estimated Lipschitz constants computed in the random directions used to generate the loss landscapes. We report the distributions on the vertical axis in terms of the 50-th (dotted), 75-th (dash-dotted), 95-th (dashed) and 99-th (solid) percentiles (lower is better). On the horizontal axis, we denote the distance of the parameters from the optimum on the grid, and visualize how the distributions vary with the distance.

loss for top- k attention has a more favorable Lipschitz continuity compared to full attention, which in turn implies both faster convergence and better generalization guarantees. Thus, our stability-based theoretical investigation in this section appears to align with our empirical observations in section 4.

6 Conclusion

In this paper, we theoretically study the potential advantages and drawbacks of sparse attention over standard attention beyond the currently studied computational perspective. Viewing sparse attention through a lens of stability, we establish conditions under which sparse attention can help learning convergence and generalization. Our findings, based on our theory, and validated with our experiments, show that (i) input-agnostic sparse attention can in general only provide computational benefits, but (ii) specific forms of input-dependent sparse attention – specifically the heavy-hitter kind – can provide significant

improvements over standard attention. We hope that our results provide adequate motivation for exploring such input-dependent heavy-hitter sparse attention in transformers (and thus LLMs) more broadly.

References

- Ashish Vaswani, Noam Shazeer, Niki Parmar, Jakob Uszkoreit, Llion Jones, Aidan N Gomez, Łukasz Kaiser, and Illia Polosukhin. Attention is all you need. *Advances in neural information processing systems*, 30, 2017. URL <https://proceedings.neurips.cc/paper/2017/file/3f5ee243547dee91fbd053c1c4a845aa-Paper.pdf>. 1, 3, 6, 7
- Chulhee Yun, Srinadh Bhojanapalli, Ankit Singh Rawat, Sashank Reddi, and Sanjiv Kumar. Are transformers universal approximators of sequence-to-sequence functions? In *International Conference on Learning Representations*, 2020a. URL <https://openreview.net/forum?id=ByxRMONTvr>. 1, 2, 42
- Yi Tay, Mostafa Dehghani, Dara Bahri, and Donald Metzler. Efficient transformers: A survey. *ACM Computing Surveys*, 55(6), 2022. ISSN 0360-0300. URL <https://doi.org/10.1145/3530811>. 1, 3, 4, 27
- Yi Tay, Mostafa Dehghani, Samira Abnar, Yikang Shen, Dara Bahri, Philip Pham, Jinfeng Rao, Liu Yang, Sebastian Ruder, and Donald Metzler. Long range arena: A benchmark for efficient transformers. In *International Conference on Learning Representations*, 2021. URL <https://openreview.net/forum?id=qVyeW-grC2k>. 1, 2, 4, 7, 27
- LA Jones, PJ Hills, KM Dick, SP Jones, and P Bright. Cognitive Mechanisms Associated with Auditory Sensory Gating. *Brain and cognition*, 102:33–45, 2016. URL <https://www.sciencedirect.com/science/article/pii/S0278262615300440>. 2
- Bernd Fritzsche. *The Senses: A Comprehensive Reference*. Academic Press, 2020. 2
- LL Judd, L McAdams, B Budnick, and DL Braff. Sensory gating deficits in schizophrenia: new results. *The American journal of psychiatry*, 149(4):488–493, 1992. URL <https://pubmed.ncbi.nlm.nih.gov/1554034/>. 2
- Yoshua Bengio. The consciousness prior, 2019. URL <https://arxiv.org/abs/1709.08568>. 2
- 3rd Neuro-Symbolic AI Summer School, 2024. URL <https://neurosymbolic.github.io/nsss2024>. 2
- Dzmitry Bahdanau, Kyunghyun Cho, and Yoshua Bengio. Neural machine translation by jointly learning to align and translate, 2016. URL <https://arxiv.org/abs/1409.0473>. 2
- Gregoire Deletang, Anian Ruoss, Jordi Grau-Moya, Tim Genewein, Li Kevin Wenliang, Elliot Catt, Chris Cundy, Marcus Hutter, Shane Legg, Joel Veness, and Pedro A Ortega. Neural networks and the chomsky hierarchy. In *The Eleventh International Conference on Learning Representations*, 2023. URL <https://openreview.net/forum?id=WbxHAzkeQcn>. 2, 4, 7, 27, 28
- Chulhee Yun, Yin-Wen Chang, Srinadh Bhojanapalli, Ankit Singh Rawat, Sashank Reddi, and Sanjiv Kumar. $O(n)$ connections are expressive enough: Universal approximability of sparse transformers. *Advances in Neural Information Processing Systems*, 33:13783–13794, 2020b. URL https://proceedings.neurips.cc/paper_files/paper/2020/file/9ed27554c893b5bad850a422c3538c15-Paper.pdf. 2, 4, 8
- Joshua Ainslie, Santiago Ontanon, Chris Alberti, Vaclav Cvicek, Zachary Fisher, Philip Pham, Anirudh Ravula, Sumit Sanghai, Qifan Wang, and Li Yang. Etc: Encoding long and structured inputs in transformers. In *Proceedings of the 2020 Conference on Empirical Methods in Natural Language Processing (EMNLP)*, pages 268–284, 2020. URL <https://aclanthology.org/2020.emnlp-main.19/>. 2, 3

- Manzil Zaheer, Guru Guruganesh, Kumar Avinava Dubey, Joshua Ainslie, Chris Alberti, Santiago Ontanon, Philip Pham, Anirudh Ravula, Qifan Wang, Li Yang, et al. Big bird: Transformers for longer sequences. *Advances in neural information processing systems*, 33:17283–17297, 2020. URL https://proceedings.neurips.cc/paper_files/paper/2020/file/c8512d142a2d849725f31a9a7a361ab9-Paper.pdf. 2, 3
- Ankit Gupta, Guy Dar, Shaya Goodman, David Ciprut, and Jonathan Berant. Memory-efficient transformers via top-k attention. In *Proceedings of the Second Workshop on Simple and Efficient Natural Language Processing*, pages 39–52. Association for Computational Linguistics, 2021. doi: 10.18653/v1/2021.sustainlp-1.5. URL <https://aclanthology.org/2021.sustainlp-1.5>. 2, 3, 7, 17, 27, 28
- QIUHAO Zeng, Jerry Huang, Peng Lu, Gezheng Xu, Boxing Chen, Charles Ling, and Boyu Wang. ZETA: Leveraging z -order curves for efficient top- k attention. In *The Thirteenth International Conference on Learning Representations*, 2025. URL <https://openreview.net/forum?id=j9VVzueEbG>. 2
- Olivier Bousquet and André Elisseeff. Algorithmic stability and generalization performance. *Advances in Neural Information Processing Systems*, 13, 2000. URL https://proceedings.neurips.cc/paper_files/paper/2000/file/49ad23d1ec9fa4bd8d77d02681df5cfa-Paper.pdf. 2, 13
- Moritz Hardt, Ben Recht, and Yoram Singer. Train faster, generalize better: Stability of stochastic gradient descent. In *International conference on machine learning*, pages 1225–1234. PMLR, 2016. URL <https://arxiv.org/pdf/1509.01240>. 2, 13
- Mary Phuong and Marcus Hutter. Formal algorithms for transformers. *arXiv preprint arXiv:2207.09238*, 2022. URL <https://arxiv.org/pdf/2207.09238.pdf>. 3
- Tianyang Lin, Yuxin Wang, Xiangyang Liu, and Xipeng Qiu. A survey of transformers. *AI Open*, 2022. URL <https://www.sciencedirect.com/science/article/pii/S2666651022000146>. 3, 4
- Niki Parmar, Ashish Vaswani, Jakob Uszkoreit, Lukasz Kaiser, Noam Shazeer, Alexander Ku, and Dustin Tran. Image transformer. In *International conference on machine learning*, pages 4055–4064. PMLR, 2018. URL <https://proceedings.mlr.press/v80/parmar18a/parmar18a.pdf>. 3, 7, 28
- Jiezhong Qiu, Hao Ma, Omer Levy, Wen-tau Yih, Sinong Wang, and Jie Tang. Blockwise self-attention for long document understanding. In *Findings of the Association for Computational Linguistics: EMNLP 2020*, pages 2555–2565, 2020. URL <https://aclanthology.org/2020.findings-emnlp.232/>. 3, 7, 28
- Iz Beltagy, Matthew E Peters, and Arman Cohan. Longformer: The long-document transformer. *arXiv preprint arXiv:2004.05150*, 2020. URL <https://arxiv.org/abs/2004.05150>. 3
- Rewon Child, Scott Gray, Alec Radford, and Ilya Sutskever. Generating long sequences with sparse transformers. *arXiv preprint arXiv:1904.10509*, 2019. URL <https://arxiv.org/abs/1904.10509>. 3
- Yi Tay, Dara Bahri, Liu Yang, Donald Metzler, and Da-Cheng Juan. Sparse sinkhorn attention. *Proceedings of ICML*, 2020. URL <http://proceedings.mlr.press/v119/tay20a/tay20a.pdf>. 3
- Aurko Roy, Mohammad Saffar, Ashish Vaswani, and David Grangier. Efficient content-based sparse attention with routing transformers. *Transactions of the Association for Computational Linguistics*, 9:53–68, 2021. URL https://direct.mit.edu/tacl/article/doi/10.1162/tacl_a_00353/. 3, 7, 17, 27, 28
- Nikita Kitaev, Lukasz Kaiser, and Anselm Levskaya. Reformer: The efficient transformer. In *International Conference on Learning Representations*, 2020. URL <https://openreview.net/pdf?id=rkgNkKhtvB>. 4, 7, 17, 27, 28

- Najoung Kim and Tal Linzen. COGS: A compositional generalization challenge based on semantic interpretation. In *Proceedings of the 2020 Conference on Empirical Methods in Natural Language Processing (EMNLP)*, pages 9087–9105, 2020. URL <https://aclanthology.org/2020.emnlp-main.731.pdf>. 4
- Brenden Lake and Marco Baroni. Generalization without systematicity: On the compositional skills of sequence-to-sequence recurrent networks. In *International Conference on Machine Learning*, pages 2873–2882. PMLR, 2018. URL <https://proceedings.mlr.press/v80/lake18a.html>. 4
- Ankur Sikarwar, Arkil Patel, and Navin Goyal. When can transformers ground and compose: Insights from compositional generalization benchmarks. In Yoav Goldberg, Zornitsa Kozareva, and Yue Zhang, editors, *Proceedings of the 2022 Conference on Empirical Methods in Natural Language Processing*, pages 648–669, Abu Dhabi, United Arab Emirates, December 2022. Association for Computational Linguistics. doi: 10.18653/v1/2022.emnlp-main.41. URL <https://aclanthology.org/2022.emnlp-main.41>. 4
- Róbert Csordás, Kazuki Irie, and Juergen Schmidhuber. The devil is in the detail: Simple tricks improve systematic generalization of transformers. In Marie-Francine Moens, Xuanjing Huang, Lucia Specia, and Scott Wen-tau Yih, editors, *Proceedings of the 2021 Conference on Empirical Methods in Natural Language Processing*, pages 619–634, Online and Punta Cana, Dominican Republic, November 2021. Association for Computational Linguistics. doi: 10.18653/v1/2021.emnlp-main.49. URL <https://aclanthology.org/2021.emnlp-main.49>. 4
- Santiago Ontanon, Joshua Ainslie, Zachary Fisher, and Vaclav Cvicek. Making transformers solve compositional tasks. In Smaranda Muresan, Preslav Nakov, and Aline Villavicencio, editors, *Proceedings of the 60th Annual Meeting of the Association for Computational Linguistics (Volume 1: Long Papers)*, pages 3591–3607, Dublin, Ireland, May 2022. Association for Computational Linguistics. doi: 10.18653/v1/2022.acl-long.251. URL <https://aclanthology.org/2022.acl-long.251>. 4
- Yichen Jiang and Mohit Bansal. Inducing transformer’s compositional generalization ability via auxiliary sequence prediction tasks. In Marie-Francine Moens, Xuanjing Huang, Lucia Specia, and Scott Wen-tau Yih, editors, *Proceedings of the 2021 Conference on Empirical Methods in Natural Language Processing*, pages 6253–6265, Online and Punta Cana, Dominican Republic, November 2021. Association for Computational Linguistics. doi: 10.18653/v1/2021.emnlp-main.505. URL <https://aclanthology.org/2021.emnlp-main.505>. 4
- Andrew Drozdov, Nathanael Schärli, Ekin Akyürek, Nathan Scales, Xinying Song, Xinyun Chen, Olivier Bousquet, and Denny Zhou. Compositional semantic parsing with large language models. In *The Eleventh International Conference on Learning Representations*, 2023. URL <https://openreview.net/forum?id=gJW8hSGBys8>. 4
- Lena Strobl, William Merrill, Gail Weiss, David Chiang, and Dana Angluin. What formal languages can transformers express? a survey. *Transactions of the Association for Computational Linguistics*, 12: 543–561, 2024. URL https://direct.mit.edu/tacl/article/doi/10.1162/tacl_a_00663/120983. 4
- Satwik Bhattamishra, Kabir Ahuja, and Navin Goyal. On the ability and limitations of transformers to recognize formal languages. In *Proceedings of the 2020 Conference on Empirical Methods in Natural Language Processing (EMNLP)*, pages 7096–7116, 2020. URL <https://aclanthology.org/2020.emnlp-main.576/>. 4
- Michael Hahn. Theoretical limitations of self-attention in neural sequence models. *Transactions of the Association for Computational Linguistics*, 8:156–171, 2020. URL https://direct.mit.edu/tacl/article/doi/10.1162/tacl_a_00306/43545. 4
- Yiding Hao, Dana Angluin, and Robert Frank. Formal language recognition by hard attention transformers: Perspectives from circuit complexity. *Transactions of the Association for Computational Linguistics*, 10:800–810, 2022. URL <https://transacl.org/ojs/index.php/tacl/article/view/3765>. 4

- William Merrill, Ashish Sabharwal, and Noah A Smith. Saturated transformers are constant-depth threshold circuits. *Transactions of the Association for Computational Linguistics*, 10:843–856, 2022. URL <https://transacl.org/ojs/index.php/tacl/article/view/3465>. 4
- David Chiang and Peter Cholak. Overcoming a theoretical limitation of self-attention. In *Proceedings of the 60th Annual Meeting of the Association for Computational Linguistics (Volume 1: Long Papers)*, pages 7654–7664, 2022. URL <https://aclanthology.org/2022.acl-long.527/>. 4
- David Chiang, Peter Cholak, and Anand Pillay. Tighter bounds on the expressivity of transformer encoders. In *International Conference on Machine Learning*, pages 5544–5562. PMLR, 2023. URL <https://proceedings.mlr.press/v202/chiang23a.html>. 4
- Yingcong Li, Muhammed Emrullah Ildiz, Dimitris Papailiopoulos, and Samet Oymak. Transformers as algorithms: Generalization and stability in in-context learning. In Andreas Krause, Emma Brunskill, Kyunghyun Cho, Barbara Engelhardt, Sivan Sabato, and Jonathan Scarlett, editors, *Proceedings of the 40th International Conference on Machine Learning*, volume 202 of *Proceedings of Machine Learning Research*, pages 19565–19594. PMLR, 23–29 Jul 2023. URL <https://proceedings.mlr.press/v202/li23l.html>. 4, 15, 43, 44
- Johannes Von Oswald, Eyvind Niklasson, Ettore Randazzo, João Sacramento, Alexander Mordvintsev, Andrey Zhmoginov, and Max Vladymyrov. Transformers learn in-context by gradient descent. In *International Conference on Machine Learning*, pages 35151–35174. PMLR, 2023. URL <https://proceedings.mlr.press/v202/von-oswald23a/von-oswald23a.pdf>. 4
- Borjan Geshkovski, Cyril Letrouit, Yury Polyanskiy, and Philippe Rigollet. The emergence of clusters in self-attention dynamics. *Advances in Neural Information Processing Systems*, 36, 2023. URL https://proceedings.neurips.cc/paper_files/paper/2023/file/b2b3e1d9840eba17ad9bbf073e009afe-Paper-Conference.pdf. 4
- Kwangjun Ahn, Xiang Cheng, Hadi Daneshmand, and Suvrit Sra. Transformers learn to implement preconditioned gradient descent for in-context learning. *Advances in Neural Information Processing Systems*, 36, 2023. URL https://proceedings.neurips.cc/paper_files/paper/2023/file/8ed3d610ea4b68e7afb30ea7d01422c6-Paper-Conference.pdf. 4
- Ruiqi Zhang, Spencer Frei, and Peter L Bartlett. Trained transformers learn linear models in-context. *Journal of Machine Learning Research*, 25(49):1–55, 2024. URL <https://www.jmlr.org/papers/volume25/23-1042/23-1042.pdf>. 4
- Jingzhao Zhang, Sai Praneeth Karimireddy, Andreas Veit, Seungyeon Kim, Sashank Reddi, Sanjiv Kumar, and Suvrit Sra. Why are adaptive methods good for attention models? *Advances in Neural Information Processing Systems*, 33:15383–15393, 2020. URL https://proceedings.neurips.cc/paper_files/paper/2020/file/b05b57f6add810d3b7490866d74c0053-Paper.pdf. 5
- Yan Pan and Yuanzhi Li. Toward understanding why adam converges faster than SGD for transformers. In *OPT 2022: Optimization for Machine Learning (NeurIPS 2022 Workshop)*, 2022. URL <https://openreview.net/forum?id=Sf1N1V2r6P0>. 5
- Kaiqi Jiang, Dhruv Malik, and Yuanzhi Li. How does adaptive optimization impact local neural network geometry? *Advances in Neural Information Processing Systems*, 36:8305–8384, 2023. URL https://proceedings.neurips.cc/paper_files/paper/2023/file/1a5e6d0441a8e1eda9a50717b0870f94-Paper-Conference.pdf. 5
- Frederik Kunstner, Jacques Chen, Jonathan Wilder Lavington, and Mark Schmidt. Noise is not the main factor behind the gap between sgd and adam on transformers, but sign descent might be. In *The Eleventh*

- International Conference on Learning Representations*, 2023. URL <https://openreview.net/forum?id=a65YK0cqH8g>. 5
- Kwangjun Ahn, Xiang Cheng, Minhak Song, Chulhee Yun, Ali Jadbabaie, and Suvrit Sra. Linear attention is (maybe) all you need (to understand transformer optimization). In *The Twelfth International Conference on Learning Representations*, 2024. URL <https://openreview.net/forum?id=0uI5415ry7>. 5
- Bingrui Li, Wei Huang, Andi Han, Zhanpeng Zhou, Taiji Suzuki, Jun Zhu, and Jianfei Chen. On the optimization and generalization of two-layer transformers with sign gradient descent. In *The Thirteenth International Conference on Learning Representations*, 2025. URL <https://openreview.net/forum?id=97r0QDPmk2>. 5
- Jimmy Lei Ba, Jamie Ryan Kiros, and Geoffrey E Hinton. Layer normalization. *arXiv preprint arXiv:1607.06450*, 2016. URL <https://arxiv.org/pdf/1607.06450>. 5
- Biao Zhang and Rico Sennrich. Root mean square layer normalization. *Advances in Neural Information Processing Systems*, 32, 2019. URL <https://proceedings.neurips.cc/paper/2019/file/1e8a19426224ca89e83cef47f1e7f53b-Paper.pdf>. 5
- Jacob Devlin, Ming-Wei Chang, Kenton Lee, and Kristina Toutanova. BERT: Pre-training of deep bidirectional transformers for language understanding. In *Proceedings of the 2019 Conference of the North American Chapter of the Association for Computational Linguistics: Human Language Technologies, Volume 1 (Long and Short Papers)*, pages 4171–4186. Association for Computational Linguistics, 2019. doi: 10.18653/v1/N19-1423. URL <https://aclanthology.org/N19-1423>. 6
- Dan Hendrycks and Kevin Gimpel. Bridging nonlinearities and stochastic regularizers with gaussian error linear units. *CoRR*, abs/1606.08415, 2016. URL <http://arxiv.org/abs/1606.08415>. 6, 10, 30
- Djork-Arné Clevert, Thomas Unterthiner, and Sepp Hochreiter. Fast and accurate deep network learning by exponential linear units (ELUs). *arXiv preprint arXiv:1511.07289*, 2015. URL <https://arxiv.org/abs/1511.07289>. 6
- Nikita Nangia and Samuel Bowman. Listops: A diagnostic dataset for latent tree learning. In *Proceedings of the 2018 Conference of the North American Chapter of the Association for Computational Linguistics: Student Research Workshop*, pages 92–99, 2018. URL <https://aclanthology.org/N18-4013/>. 7, 27
- Diganta Misra. Mish: A self regularized non-monotonic neural activation function. *CoRR*, abs/1908.08681, 2019. URL <http://arxiv.org/abs/1908.08681>. 10, 31
- Diederik P. Kingma and Jimmy Ba. Adam: A method for stochastic optimization. In *The Third International Conference on Learning Representations*, 2015. URL <http://arxiv.org/abs/1412.6980>. 12
- Hyunjik Kim, George Papamakarios, and Andriy Mnih. The lipschitz constant of self-attention. In *International Conference on Machine Learning*, pages 5562–5571. PMLR, 2021. URL <https://arxiv.org/pdf/2006.04710>. 14, 33
- Guangxiang Zhao, Junyang Lin, Zhiyuan Zhang, Xuancheng Ren, Qi Su, and Xu Sun. Explicit sparse transformer: Concentrated attention through explicit selection. *CoRR*, abs/1912.11637, 2019. URL <http://arxiv.org/abs/1912.11637>. 17
- Hao Li, Zheng Xu, Gavin Taylor, Christoph Studer, and Tom Goldstein. Visualizing the loss landscape of neural nets. *Advances in neural information processing systems*, 31, 2018. URL https://proceedings.neurips.cc/paper_files/paper/2018/file/a41b3bb3e6b050b6c9067c67f663b915-Paper.pdf. 18, 58, 59

- Ido Amos, Jonathan Berant, and Ankit Gupta. Never train from scratch: Fair comparison of long-sequence models requires data-driven priors. In *The Twelfth International Conference on Learning Representations*, 2024. URL <https://openreview.net/forum?id=PdaPky8MUn>. 27
- Yuanzhi Li and Yingyu Liang. Learning overparameterized neural networks via stochastic gradient descent on structured data. *Advances in neural information processing systems*, 31, 2018. URL https://proceedings.neurips.cc/paper_files/paper/2018/file/54fe976ba170c19ebae453679b362263-Paper.pdf. 35
- Zeyuan Allen-Zhu, Yuanzhi Li, and Zhao Song. A convergence theory for deep learning via overparameterization. In *International conference on machine learning*, pages 242–252. PMLR, 2019. URL <https://proceedings.mlr.press/v97/allen-zhu19a/allen-zhu19a.pdf>. 35
- Difan Zou, Yuan Cao, Dongruo Zhou, and Quanguan Gu. Gradient descent optimizes over-parameterized deep relu networks. *Machine learning*, 109:467–492, 2020. URL <https://link.springer.com/content/pdf/10.1007/s10994-019-05839-6.pdf>. 35
- Benjamin Fehrman, Benjamin Gess, and Arnulf Jentzen. Convergence rates for the stochastic gradient descent method for non-convex objective functions. *Journal of Machine Learning Research*, 21(136): 1–48, 2020. URL <https://jmlr.csail.mit.edu/papers/volume21/19-636/19-636.pdf>. 35

Appendix

Table of Contents

A	Discussion of Limitations	27
B	Details on Experimental Setup	27
C	Additional Empirical Results	28
C.1	Detailed Evaluation	28
C.2	Effect of the MLP Activation Function	30
D	Softmax to Lipschitz Continuity: Technical Details	32
D.1	Proof of Lemma 1	32
D.2	Proof of Theorem 1	36
D.3	Proof of Theorem 2	40
D.4	Multi-headed Attention	42
E	Role of Sparse Softmax: Technical Details	43
E.1	Standard Softmax based Attention	43
E.2	Regular Input-agnostic Sparse Softmax based Attention	46
E.3	Heavy-hitter Input-dependent Sparse Softmax based Attention	50
E.4	Comparison of Bounds between Full and Heavy-hitter Attention	56
E.5	Loss Surfaces and Estimated Lipschitz Constants	58

A Discussion of Limitations

Our results imply that there is value in pursuing input-dependent sparse attention [Kitaev et al., 2020, Roy et al., 2021, Gupta et al., 2021] in real world LLMs given that they would be both computationally cheaper while having improved generalization guarantees. However, we would like to list some limitations of our work:

- (1) Our empirical results are limited to benchmarks developed to study transformers under a controlled setup, and do not speak of their capabilities (in terms of improved training speed, equivalent expressivity and improved generalization) in the wild as we are unable to perform such experiments at scale. The potential advantages of this input-dependent sparse attention at scale remains an open question, though our theoretical results and accompanying preliminary experiments provide a strong motivation.
- (2) We study transformers in a supervised learning setup with an encoder-only architecture, where the models are trained from scratch. We do not consider the effect of pretraining, which has been shown to be quite useful with transformers [Amos et al., 2024], and we do not cover how our results would transfer to a sequence-to-sequence learning setup with an encoder-decoder architecture (though the now common decoder-only architecture can be easily analyzed in our framework).
- (3) In our empirical evaluations, we have considered a few representative input-dependent and input-agnostic sparse attention to validate our theoretical results. However, there are various other sparse attention mechanisms [Tay et al., 2022] that we have not considered in our empirical evaluations.
- (4) Our analyses establish upper bounds for the worst case performance (convergence rate or generalization error) for various forms of full and sparse attention, and we compare these upper bounds in our discussion to understand relative behavior. We do support our discussion with empirical evaluations. Furthermore, our study is focused on in-distribution generalization, and does not consider the commonly studied problem of length generalization.
- (5) As with any theoretical analysis involving neural networks, we acknowledge that there might a gap between the theoretical constants (such as Lipschitz constant or weight norm upper bounds) we utilize and the practical estimates of those constants empirically seen with these models. However, much of our analysis is *adaptive* in nature, where an improved value of such a constant can be directly incorporated for improved guarantees.

B Details on Experimental Setup

Tasks. We consider the List Operations or ListOps task [Nangia and Bowman, 2018] from the LRA benchmark [Tay et al., 2021] with sequence lengths between 500 and 600 both for training and testing because we are evaluating in-distribution learning and generalization. This is a 10-class classification problem. We select this task over the other tasks in the LRA benchmark because (i) this is a task where transformers have better than random performance (around 30-40% compared to a random 10% performance), but there is still a significant room for improvement, and (ii) we can control the length of the input sequences and still have a meaningful problem, which is not as straightforward with the other document or image processing tasks in LRA. From the NNCH benchmark [Deletang et al., 2023], we consider 3 tasks that can be solved as a binary classification problem – Parity, Even Pairs, and Missing Duplicates, and 4 tasks that can be solved as a multi-class classification problem – Cycle Navigation, Stack Manipulation, Modular Arithmetic with Brackets and Solve Equation. Parity, Even Pairs and Cycle Navigation are regular languages. Stack Manipulation, Modular Arithmetic and Solve Equation are deterministic context-free languages, while Missing Duplicates is a context-sensitive language. For the NNCH tasks, we consider input sequences of length 40 both for training and testing; Deletang et al. [2023] train on the same length but test on longer to evaluate out-of-distribution length generalization. For all the tasks, we utilize a training / holdout sets of sizes 5000 / 2000.

Sparse attention. While there are various sparse attention mechanisms (as we discussed in section 2), we will consider a representative subset for our empirical evaluations. For input-agnostic sparse attention,

we choose banded attention (figure 1b [Parmar et al., 2018]) and block-local attention (figure 1d [Qiu et al., 2020]), with varying band and block sizes respectively. For input-dependent heavy-hitter sparse attention, we choose top- k attention (figure 1f [Gupta et al., 2021]). The main motivation for selecting top- k over LSH based [Kitaev et al., 2020] or clustering based [Roy et al., 2021] input-dependent sparse attention is that we can then easily ensure that the input-dependent sparse attention attends to exactly the same number of tokens as in the input-agnostic ones – that is, the number of nonzeros in each column of the attention score matrix is exactly the same across all sparse attention patterns we consider. We also consider versions of these input-agnostic sparse attention with varying number of global tokens (figure 1e). Note that, as we have highlighted before, **the number of learnable parameters is exactly the same between the model using standard full attention and the one using sparse attention.** A *minor difference* is with global tokens where we also learn their initial global token embeddings. For this reason, we use *exactly the same hyperparameters* for the full and sparse attention versions of the same model to ablate the effect of the sparse attention.

Compute resources and experimental setup. All our empirical evaluations are performed on a Nvidia V100 GPU (8GB memory). Each experiment was executed with 10 random seeds and all results are aggregated across these 10 trials. Each trial took around 55 hours – ListOps: 21.5, Parity: 10, Missing Duplicates: 2.5, Even Pairs: 1, Stack Manipulation: 2, Modular Arithmetic: 6, Solve Equation: 6, Cycle Navigation: 7.5 – for a total of 550 hours for each of the 3 activation functions considered. Ablation of additional hyperparameters took another 160 hours. The implementation is in Pytorch 2.2 with CUDA 12.4. We implement our own attention block to handle different forms of sparse attention.

Hyperparameters. For the NNCH tasks, we considered the transformer architecture used in Deletang et al. [2023] with (i) $T = 5$ transformer blocks, (ii) embedding dimension $d = 64$ and (iii) the MLP hidden layer $d_{\text{MLP}} = 64$, but with a single head (instead of 8) and a dropout of 0.01. The final classification layer uses the average of all the token representations after the final transformer block. For the ListOps task, we utilize the same architecture but use $T = 10$ transformer blocks for the initial experiment. We also consider varying number of heads and blocks in our experiments studying the effect of hyperparameters. For all problems, we use the **SGD optimizer** and the **StepLR learning rate scheduler** with a decay rate of 0.99 for ListOps and 0.9995 for NNCH tasks and a decay period of 1 epoch. For the NNCH tasks, we use an initial learning rate of 0.1, while we use 1.0 for ListOps. The number of epochs is selected to ensure that standard full attention transformer is able to consistently achieve 100% training accuracy (and thus, the ERM has converged). Thus, we use 100 epochs for Even Pairs, 200 epochs for ListOps and Stack Manipulation, 250 epochs for Missing Duplicates, 600 epochs for Modular Arithmetic and Solve Equation, 750 epochs for Cycle Navigation, and 1000 for Parity.

C Additional Empirical Results

C.1 Detailed Evaluation

In this subsection, we present a detailed view of the results presented in figure 2 and figure 3, where we evaluate different mask sizes (number of nonzeros in each column of the attention matrix) and the number of global tokens included with the input-agnostic sparse attention patterns. We present the trajectories of the training cross-entropy loss in figure 11 and figure 13, and the trajectories of the training accuracies in figure 12 and figure 14. In table 2, we present the best accuracy on the held-out set for each of the sparse attention patterns and contrast it with that of the full attention model. Table 3 presents the number of epochs (aggregated over the 10 repetitions of each experiments) required by each attention pattern to (i) achieve at least 95% training accuracy for the first time (if at all), and (ii) achieve the best held-out accuracy.

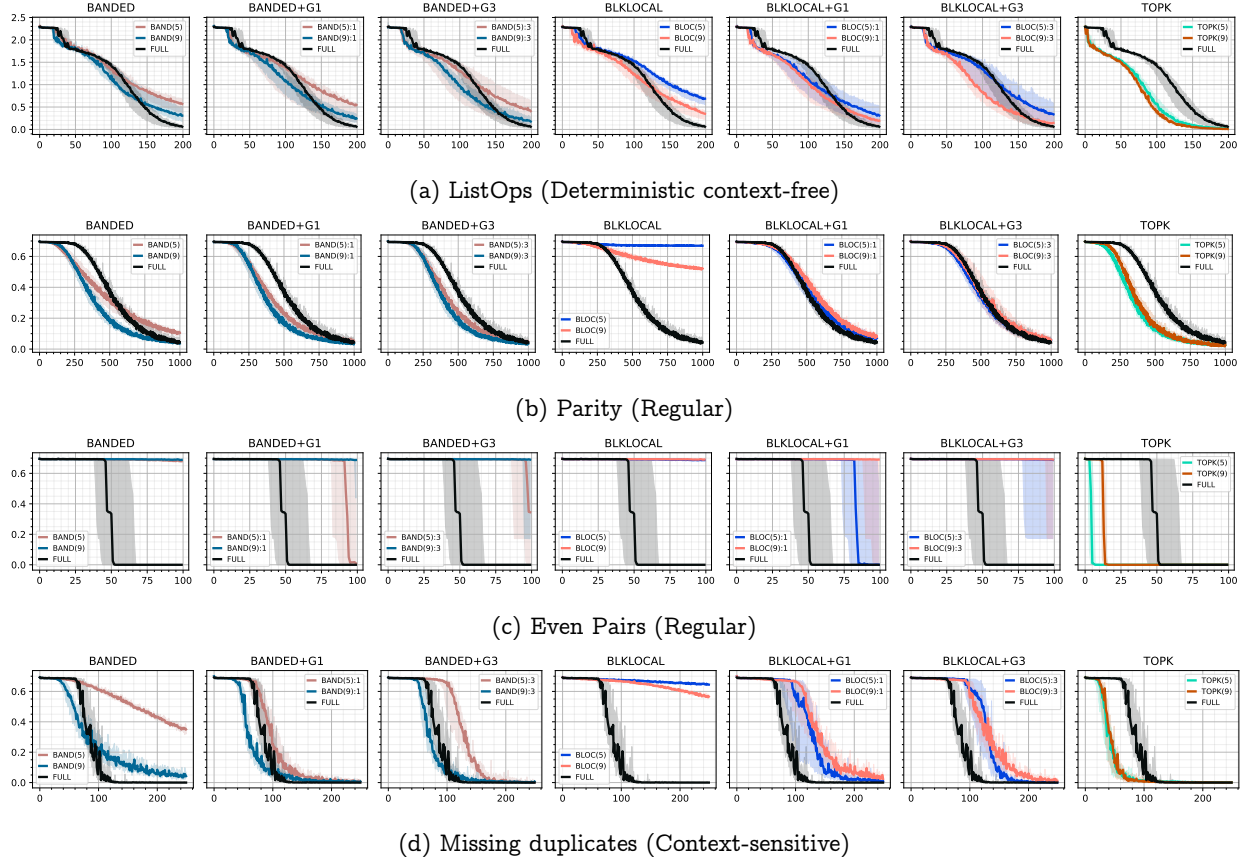


Figure 11: Training cross-entropy (vertical axis, lower is better) vs number of epochs (horizontal axis) across different tasks and sparse attention forms aggregated across 10 repetitions. Each plot contains the training curve for the standard transformers (in black). Sparse attention: Banded (column 1), banded with 1 global token (column 2), banded with 3 global tokens (column 3), block-local (column 4), block-local with 1 global token (column 5), block-local with 3 global tokens (column 6), top- k attention (column 7).

The results in figure 11 and figure 13 (along with figure 12 and figure 14) show that the input-agnostic sparse attention has a slower ERM convergence than standard full attention, being unable to reach even 95% training accuracy with the ListOps and Even Pairs tasks. With the input-agnostic sparse attention, having the global tokens helps convergence in almost all cases, being critical for convergence in the NNCH binary classification tasks (Parity, Even Pairs and Missing Duplicates), especially with the block local attention. In contrast, the ERM convergence of the top- k attention is significantly improved over the standard full attention in all 8 tasks, with improvements (in terms of achieving 95% training accuracy) over standard attention ranging between $1.37\times$ (121 epochs vs 167 epochs) with ListOps to $9.5\times$ (6 epochs vs 53 epochs) with Even Pairs (see table 3 for further results on this).

The results in table 2 show that, in almost all cases, the input-dependent sparse attention has similar (Even Pairs and Missing Duplicates) or better (ListOps) holdout accuracy than the standard full attention. This is true both in terms of the highest holdout accuracy during the training trajectory, and the final holdout accuracy. The latter highlights that the faster ERM convergence of input-dependent sparse attention does not lead to overfitting. In fact, with the ListOps task, the final holdout accuracy with standard attention drops from around $35.1 \pm 0.6\%$ to $28.9 \pm 1.4\%$, while the drop with top- k attention is only from $36.3 \pm 0.3\%$ to $31.3 \pm 0.9\%$. In general, the top- k attention based transformers also have comparatively similar or lower variations in their performance. This set of results align with our theoretical result that the improved stability

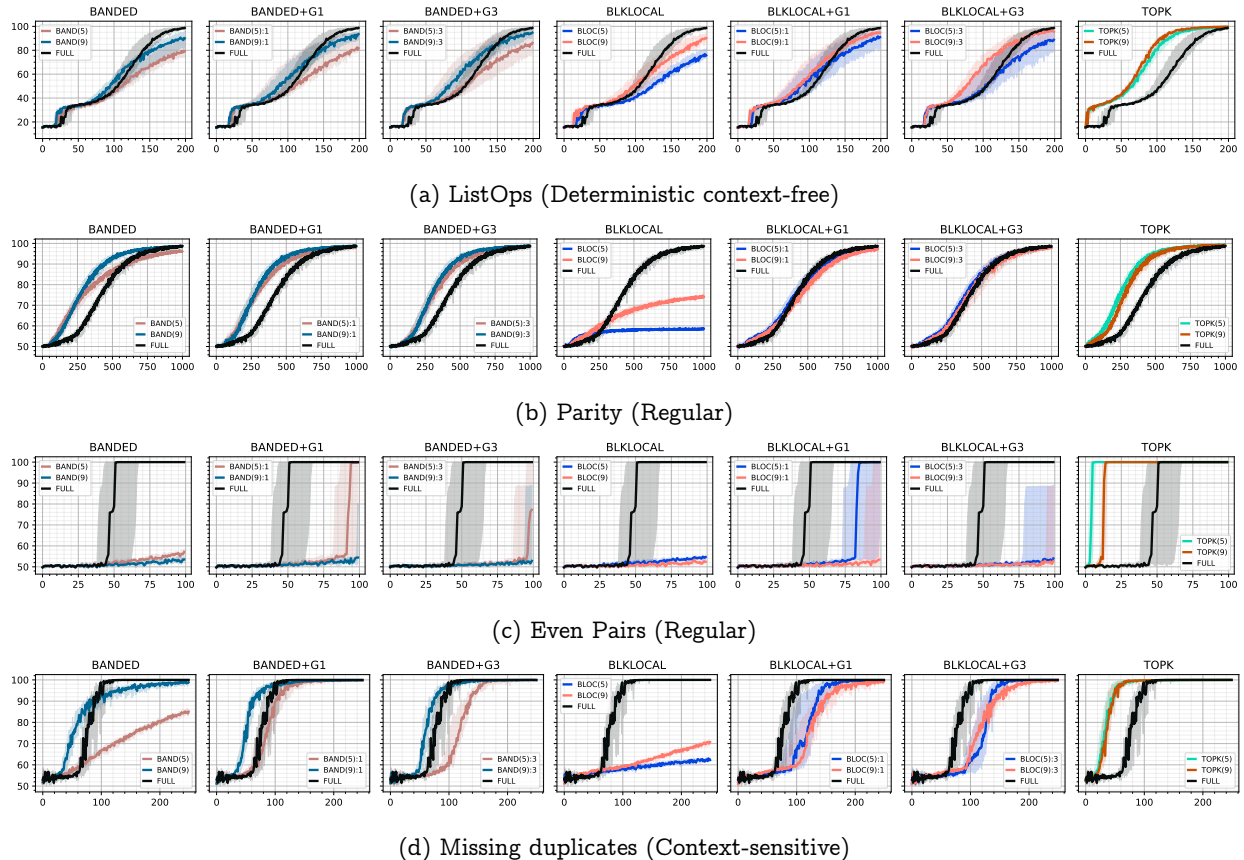


Figure 12: Training accuracy (vertical axis – higher is better) vs number of epochs (horizontal axis) across different tasks and sparse attention aggregated across 10 repetitions (median (line) and inter-quartile range (shaded region)). Each plot contains the training curve for the standard full attention transformer (in black). Sparse attention are as follows with each with $k = 5$ and $k = 9$ nonzeros in each row of the attention score matrix – column 1: banded, column 2: banded with 1 global token, column 3: banded with 3 global tokens, column 4: block-local, column 5: block-local with 1 global token, column 6: block-local with 3 global tokens, column 7: top- k attention.

of the input-dependent sparse attention translates to matching or better generalization error. This does not hold with the Parity, Modular Arithmetic, Solve Equation and Cycle Navigation tasks. However, note that these are tasks for which all forms of attention have very close to random performance (which is 50% for a balanced binary classification problem and 20% for a 5-class classification problem), and thus none of the attention mechanisms are generalizing well. The inability of the input-agnostic sparse attention to obtain high training accuracy within the training budget translates to low holdout error, especially with the Even Pairs task.

C.2 Effect of the MLP Activation Function

Here, we present a detailed view of the results presented in figure 4 and figure 5, where we evaluate different mask sizes (number of nonzeros in each column of the attention matrix) and the number of global tokens included with the input-agnostic sparse attention patterns. We present the trajectories of the training cross-entropy loss with the GELU activation [Hendrycks and Gimpel, 2016] in figure 15 and figure 19 for all 8 tasks, and their corresponding training accuracy trajectories in figure 16 and figure 20. Similar results for

Table 2: Generalization performance (higher is better) for standard full attention (highlighted in green) and sparse attention. We report the mean \pm std aggregated over the 10 trials (same as figure 11 and figure 12). The first set of columns show the best holdout accuracy obtained across the training trajectory, while the second set show the holdout accuracy at the end of training. We highlight methods that have not reached 95% training accuracy at the end of training in blue; among the remaining methods, the highest mean in each column is shown in bold. See figure 11 for the naming of the attention mechanisms.

Attention	Best holdout accuracy			Final holdout accuracy		
	ListOps	MissingDups	EvenPairs	ListOps	MissingDups	EvenPairs
Standard	35.09 \pm 0.60	100.00 \pm 0.00	100.00 \pm 0.00	28.92 \pm 1.40	99.98 \pm 0.02	100.00 \pm 0.00
Banded(5)	34.47 \pm 0.55	58.35 \pm 1.34	52.57 \pm 0.96	28.25 \pm 1.70	54.04 \pm 1.83	50.34 \pm 1.42
Banded(9)	34.82 \pm 0.51	96.53 \pm 1.99	52.06 \pm 1.07	28.40 \pm 1.09	95.35 \pm 2.19	50.42 \pm 1.08
Banded(5)+G1	34.73 \pm 0.43	99.78 \pm 0.34	81.86 \pm 22.36	30.50 \pm 0.58	99.62 \pm 0.35	81.40 \pm 22.88
Banded(9)+G1	35.54 \pm 0.53	99.81 \pm 0.13	64.47 \pm 19.70	31.05 \pm 2.16	99.40 \pm 0.38	63.07 \pm 20.59
Banded(5)+G3	35.23 \pm 0.52	99.92 \pm 0.12	75.94 \pm 24.06	30.99 \pm 1.15	99.80 \pm 0.30	75.48 \pm 24.52
Banded(9)+G3	35.29 \pm 0.60	99.90 \pm 0.10	66.20 \pm 22.13	31.80 \pm 1.41	99.41 \pm 0.48	65.61 \pm 22.52
Blklocal(5)	34.83 \pm 0.42	57.87 \pm 1.16	51.98 \pm 0.98	29.06 \pm 1.33	52.90 \pm 1.12	50.46 \pm 0.81
Blklocal(9)	34.73 \pm 0.25	58.12 \pm 1.21	51.79 \pm 0.84	28.59 \pm 1.21	52.50 \pm 0.71	50.28 \pm 1.00
Blklocal(5)+G1	35.20 \pm 0.55	98.78 \pm 3.28	85.62 \pm 21.89	29.73 \pm 1.63	98.47 \pm 3.75	85.10 \pm 22.69
Blklocal(9)+G1	34.63 \pm 0.43	99.02 \pm 0.74	71.13 \pm 23.56	30.57 \pm 1.07	98.58 \pm 0.81	70.33 \pm 24.22
Blklocal(5)+G3	35.53 \pm 0.66	99.96 \pm 0.09	66.55 \pm 21.93	29.97 \pm 1.35	99.86 \pm 0.13	65.97 \pm 22.33
Blklocal(9)+G3	35.53 \pm 0.61	99.73 \pm 0.22	66.34 \pm 22.05	31.82 \pm 1.35	99.12 \pm 0.73	65.48 \pm 22.63
Topk(5)	36.02 \pm 0.59	100.00 \pm 0.00	100.00 \pm 0.00	31.06 \pm 0.73	99.94 \pm 0.07	100.00 \pm 0.00
Topk(9)	36.25 \pm 0.29	100.00 \pm 0.00	100.00 \pm 0.00	31.33 \pm 0.85	99.95 \pm 0.06	100.00 \pm 0.00

Table 3: Additional generalization/convergence results: We note the number of iterations required during the training (i) to reach 95% training accuracy, with a ‘-’ denoting that we do not reach that training accuracy, and (ii) to reach the highest holdout accuracy. For training that reach 95% training accuracy, the smallest in each column is highlighted in bold.

Attention	Iterations to 95% training accuracy			Iterations to best holdout accuracy		
	ListOps	MissingDups	EvenPairs	ListOps	MissingDups	EvenPairs
Standard	167 \pm 18	96 \pm 21	53 \pm 15	62 \pm 18	174 \pm 55	64 \pm 21
Band(5)	-	-	-	63 \pm 19	38 \pm 69	66 \pm 28
Band(9)	-	114 \pm 30	-	68 \pm 17	236 \pm 6	45 \pm 35
Band(5)+G1	-	114 \pm 13	-	59 \pm 23	236 \pm 6	83 \pm 28
Band(9)+G1	-	72 \pm 11	-	74 \pm 21	231 \pm 12	51 \pm 37
Band(5)+G3	-	137 \pm 16	-	62 \pm 20	227 \pm 24	81 \pm 27
Band(9)+G3	-	80 \pm 9	-	69 \pm 24	224 \pm 16	70 \pm 32
Blklocal(5)	-	-	-	71 \pm 11	5 \pm 4	67 \pm 26
Blklocal(9)	-	-	-	57 \pm 11	3 \pm 2	57 \pm 26
Blklocal(5)+G1	-	-	-	53 \pm 9	238 \pm 7	85 \pm 18
Blklocal(9)+G1	-	154 \pm 26	-	54 \pm 15	235 \pm 12	67 \pm 36
Blklocal(5)+G3	-	134 \pm 20	-	69 \pm 21	230 \pm 19	86 \pm 12
Blklocal(9)+G3	-	146 \pm 18	-	60 \pm 17	234 \pm 9	62 \pm 36
Topk(5)	131 \pm 9	48 \pm 9	6 \pm 3	40 \pm 8	226 \pm 14	18 \pm 0
Topk(9)	122 \pm 8	48 \pm 10	13 \pm 3	41 \pm 7	193 \pm 59	19 \pm 0

4/8 tasks – namely ListOps, Parity, Even Pairs and Missing Duplicates – with the Mish activation [Misra, 2019] in the MLP block are presented in figure 17 (training cross-entropy) and figure 18 (training accuracy).

In all cases, the qualitative results do not seem the change much from the previous results with the ReLU activation in the MLP block presented in figure 11 and figure 13 (and corresponding figure 12 and figure 14). The overall trend continues to be that (i) input-agnostic sparse attention models continue to train and generalize comparitively to the full attention model, and (ii) input-dependent heavy-hitter sparse attention models continue to converge faster (and generalize similarly or better) than the full attention model.

The input-agnostic sparse attention models continue to converge comparably to full attention with ListOps and Missing Duplicates while falling behind in Even Pairs. One marked difference here is that, with ListOps, the full attention model initially converges slower than the other sparse attention models (compare figure 2a with figure 4a and figure 5a). This is more marked with the Mish activation. However, finally

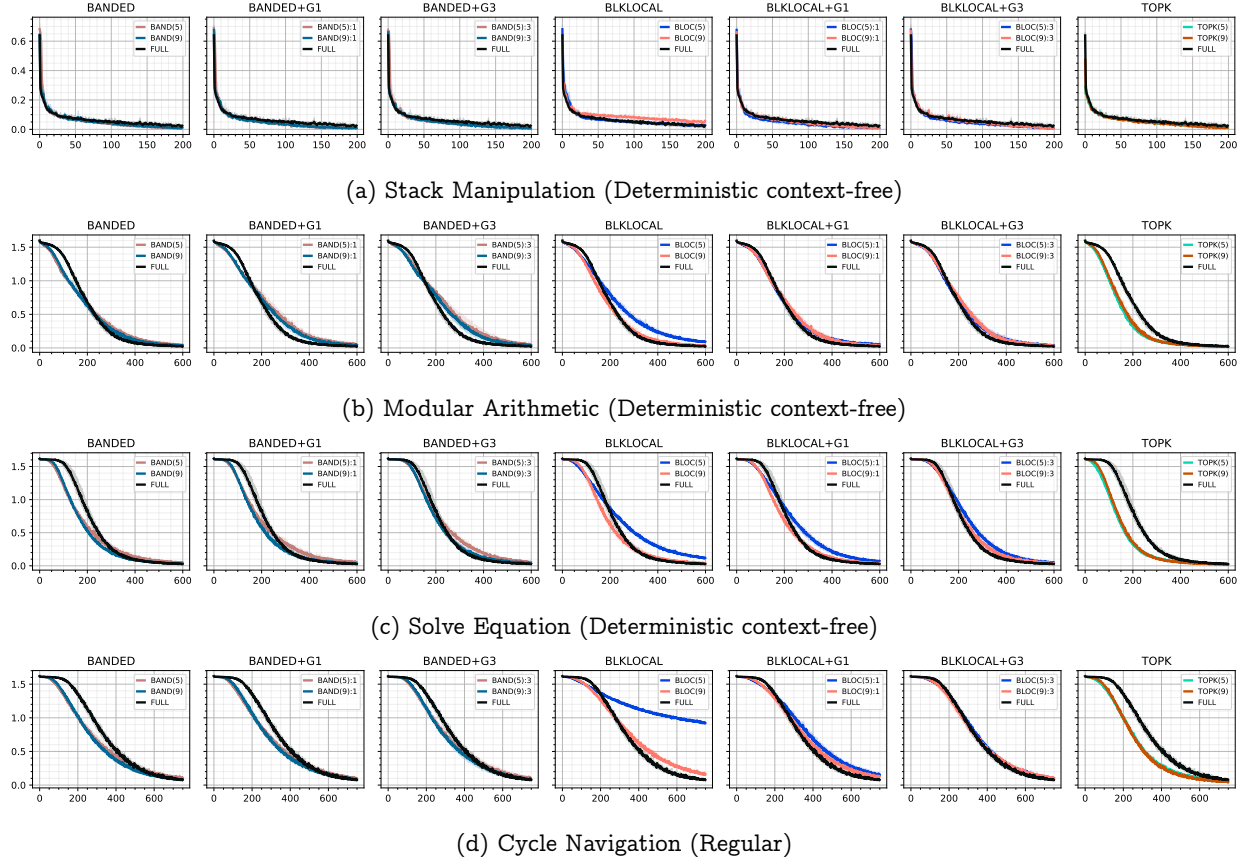


Figure 13: Training cross-entropy (vertical axis, lower is better) vs number of epochs (horizontal axis) across different tasks and sparse attention forms aggregated across 10 repetitions. Each plot contains the training curve for the standard transformers (in black). Sparse attention: Banded (column 1), banded with 1 global token (column 2), banded with 3 global tokens (column 3), block-local (column 4), block-local with 1 global token (column 5), block-local with 3 global tokens (column 6), top- k attention (column 7).

the full attention model convergence catches up to the input-agnostic sparse attention models. This initial slowdown in the convergence is also reflected in the initial lower generalization accuracy. In contrast, the input-dependent heavy-hitter top- k attention continues to consistently converge faster than full attention in terms of the training loss for both these MLP activations, with very little differences from the results with ReLU activation. This form of sparse attention also achieves better generalization performance earlier in the training process. This indicates that the difference in performance is probably due to the differences in the attention mechanism and not an artifact of the MLP block configuration.

D Softmax to Lipschitz Continuity: Technical Details

D.1 Proof of Lemma 1

Lemma S1. Consider the following assumptions:

- (M1) The MLP activation σ is λ_σ Lipschitz with $\sigma(0) = 0$.
- (M2) The MLP parameters have norms bounded by $B > 0$, that is $\|\mathbf{P}\| \leq B$ and $\|\mathbf{R}\| \leq B$.
- (M3) The input \mathbf{x} to the MLP is bounded by $\Xi > 0$, that is $\|\mathbf{x}\| \leq \Xi$.

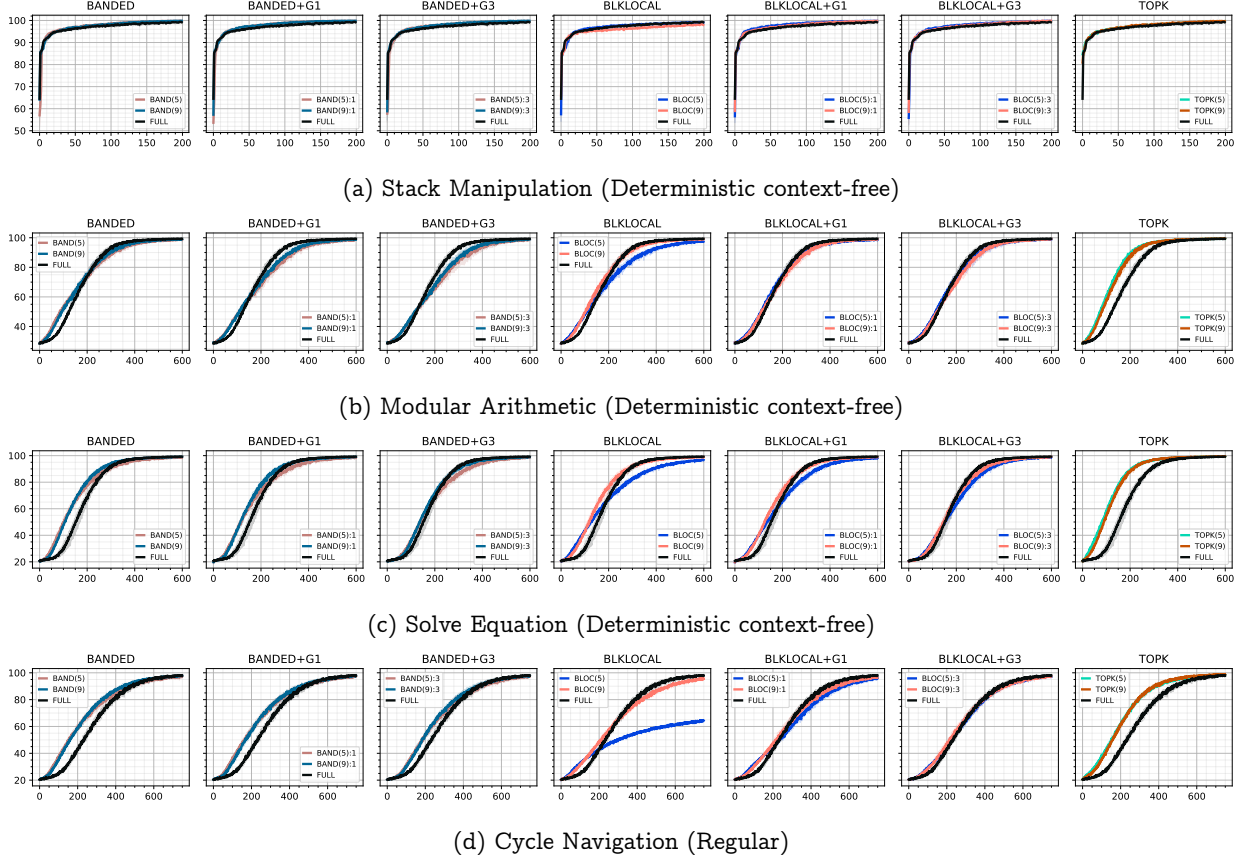


Figure 14: Training accuracy (vertical axis – higher is better) vs number of epochs (horizontal axis) across different tasks and sparse attention aggregated across 10 repetitions (median (line) and inter-quartile range (shaded region)). Each plot contains the training curve for the standard full attention transformer (in black). Sparse attention are as follows with each with $k = 5$ and $k = 9$ nonzeros in each row of the attention score matrix – column 1: banded, column 2: banded with 1 global token, column 3: banded with 3 global tokens, column 4: block-local, column 5: block-local with 1 global token, column 6: block-local with 3 global tokens, column 7: top- k attention.

Then the token-wise MLP and LN operations are Lipschitz with respect to their input and model parameters as follows $\forall \mathbf{x}, \mathbf{x}' \in \mathbb{R}^d, \|\mathbf{x}\|, \|\mathbf{x}'\| \leq \Xi, \mathbf{P}, \bar{\mathbf{P}} \in \mathbb{R}^{d_{\text{MLP}} \times d}, \mathbf{R}, \bar{\mathbf{R}} \in \mathbb{R}^{d_{\text{MLP}} \times d}$:

$$\|\text{MLP}_{\mathbf{P}, \mathbf{R}}(\mathbf{x}) - \text{MLP}_{\mathbf{P}, \mathbf{R}}(\bar{\mathbf{x}})\| \leq \eta_X \|\mathbf{x} - \bar{\mathbf{x}}\|, \quad (26)$$

$$\|\text{MLP}_{\mathbf{P}, \mathbf{R}}(\mathbf{x}) - \text{MLP}_{\bar{\mathbf{P}}, \mathbf{R}}(\mathbf{x})\| \leq \eta_P \|\mathbf{P} - \bar{\mathbf{P}}\|, \quad (27)$$

$$\|\text{MLP}_{\mathbf{P}, \mathbf{R}}(\mathbf{x}) - \text{MLP}_{\mathbf{P}, \bar{\mathbf{R}}}(\mathbf{x})\| \leq \eta_R \|\mathbf{R} - \bar{\mathbf{R}}\|, \quad (28)$$

$$\|\text{LN}(\mathbf{x}) - \text{LN}(\bar{\mathbf{x}})\| \leq \zeta_{\text{LN}} \|\mathbf{x} - \bar{\mathbf{x}}\|, \quad (29)$$

where $\eta_X = B^2 \lambda_\sigma$, $\eta_P = \eta_R = \lambda_\sigma B \Xi$.

Proof. First, the Lipschitz property of the LayerNorm (and the corresponding value of ζ_{LN}) has been previously established in Kim et al. [2021, Appendix N]. With LayerNorm $\text{LN} : \mathbb{R}^d \rightarrow \mathbb{R}^d$ defined as

$$\text{LN}(\mathbf{x}) = \frac{\mathbf{x} - \frac{1}{d}(\sum_{i \in [d]} x_i)}{\sqrt{\epsilon + \frac{1}{d} \left(x_i - \frac{1}{d}(\sum_{i \in [d]} x_i)\right)^2}} \odot \mathbf{a} + \mathbf{b}, \quad (30)$$

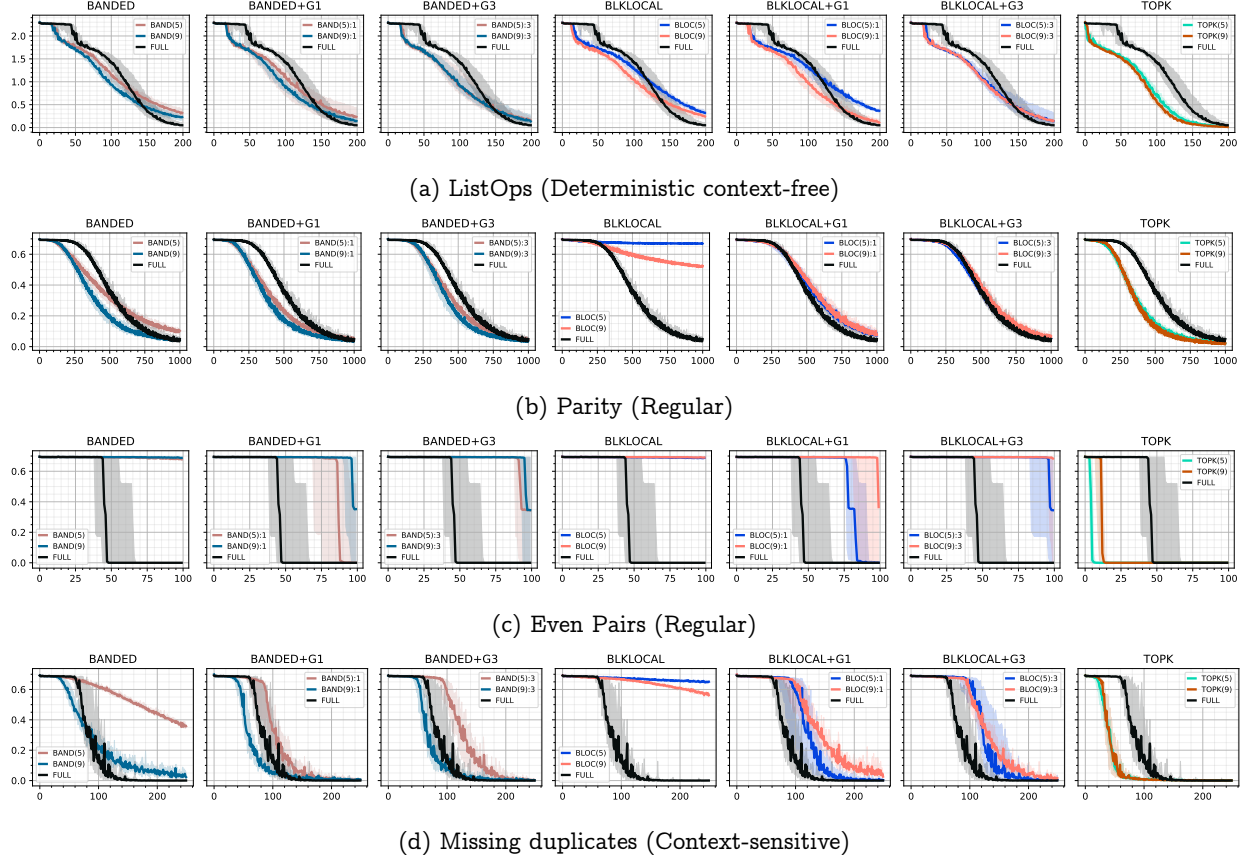


Figure 15: Same as figure 11 with GELU activation in the MLP component of the transformer block.

where \mathbf{a} and \mathbf{b} are the scale and shift hyperparameter. Then LayerNorm is Lipschitz with $\zeta_{\text{LN}} = \epsilon^{-\frac{1}{2}} \|\mathbf{a}\|_{\infty} (d^2 - 2)/d$ in equation (29).

For equation (26), we have the following:

$$\|\text{MLP}_{\mathbf{P}, \mathbf{R}}(\mathbf{x}) - \text{MLP}_{\mathbf{P}, \mathbf{R}}(\bar{\mathbf{x}})\| = \|\mathbf{R}^{\top} \sigma(\mathbf{P}\mathbf{x}) - \mathbf{R}^{\top} \sigma(\mathbf{P}\bar{\mathbf{x}})\| \leq \|\mathbf{R}\| \|\sigma(\mathbf{P}\mathbf{x}) - \sigma(\mathbf{P}\bar{\mathbf{x}})\| \quad (31)$$

$$\leq B \lambda_{\sigma} \|\mathbf{P}(\mathbf{x} - \bar{\mathbf{x}})\| \leq B \lambda_{\sigma} \|\mathbf{P}\| \|\mathbf{x} - \bar{\mathbf{x}}\| \leq B^2 \lambda_{\sigma} \|\mathbf{x} - \bar{\mathbf{x}}\|, \quad (32)$$

where we use the assumption (M1) that $\|\sigma(\mathbf{z}) - \sigma(\bar{\mathbf{z}})\| \leq \lambda_{\sigma} \|\mathbf{z} - \bar{\mathbf{z}}\|$, and assumption (M2) that $\|\mathbf{P}\| \leq B$ and $\|\mathbf{R}\| \leq B$.

For equation (27), we have the following:

$$\|\text{MLP}_{\mathbf{P}, \mathbf{R}}(\mathbf{x}) - \text{MLP}_{\bar{\mathbf{P}}, \mathbf{R}}(\mathbf{x})\| = \|\mathbf{R}^{\top} \sigma(\mathbf{P}\mathbf{x}) - \mathbf{R}^{\top} \sigma(\bar{\mathbf{P}}\mathbf{x})\| \leq \|\mathbf{R}\| \|\sigma(\mathbf{P}\mathbf{x}) - \sigma(\bar{\mathbf{P}}\mathbf{x})\| \quad (33)$$

$$\leq B \lambda_{\sigma} \|(\mathbf{P} - \bar{\mathbf{P}})\mathbf{x}\| \leq B \lambda_{\sigma} \Xi \|\mathbf{P} - \bar{\mathbf{P}}\|, \quad (34)$$

since $\|\mathbf{x}\| \leq \Xi$ for all tokens as per the assumption (M3).

For equation (28), we have the following:

$$\|\text{MLP}_{\mathbf{P}, \mathbf{R}}(\mathbf{x}) - \text{MLP}_{\mathbf{P}, \bar{\mathbf{R}}}(\mathbf{x})\| = \|\mathbf{R}^{\top} \sigma(\mathbf{P}\mathbf{x}) - \bar{\mathbf{R}}^{\top} \sigma(\mathbf{P}\mathbf{x})\| \leq \|(\mathbf{R} - \bar{\mathbf{R}}) \sigma(\mathbf{P}\mathbf{x})\| \leq \|\mathbf{R} - \bar{\mathbf{R}}\| \|\sigma(\mathbf{P}\mathbf{x})\| \quad (35)$$

$$= \|\mathbf{R} - \bar{\mathbf{R}}\| \|\sigma(\mathbf{P}\mathbf{x}) - \sigma(0)\| = \|\mathbf{R} - \bar{\mathbf{R}}\| \lambda_{\sigma} \|\mathbf{P}\mathbf{x}\|, \leq \lambda_{\sigma} B \Xi \|\mathbf{R} - \bar{\mathbf{R}}\|, \quad (36)$$

since $\|\mathbf{x}\| \leq \Xi$ for all tokens as per assumption (M3) and $\sigma(0) = 0$ as per assumption (M1). \square

Note that the $\sigma(0) = 0$ holds for standard activations such as $\text{ReLU}(x) = \max(x, 0)$ and $\text{GELU}(x) = x\Phi(x)$ where $\Phi: \mathbb{R} \rightarrow [0, 1]$ is the cumulative density function of the standard Gaussian distribution.

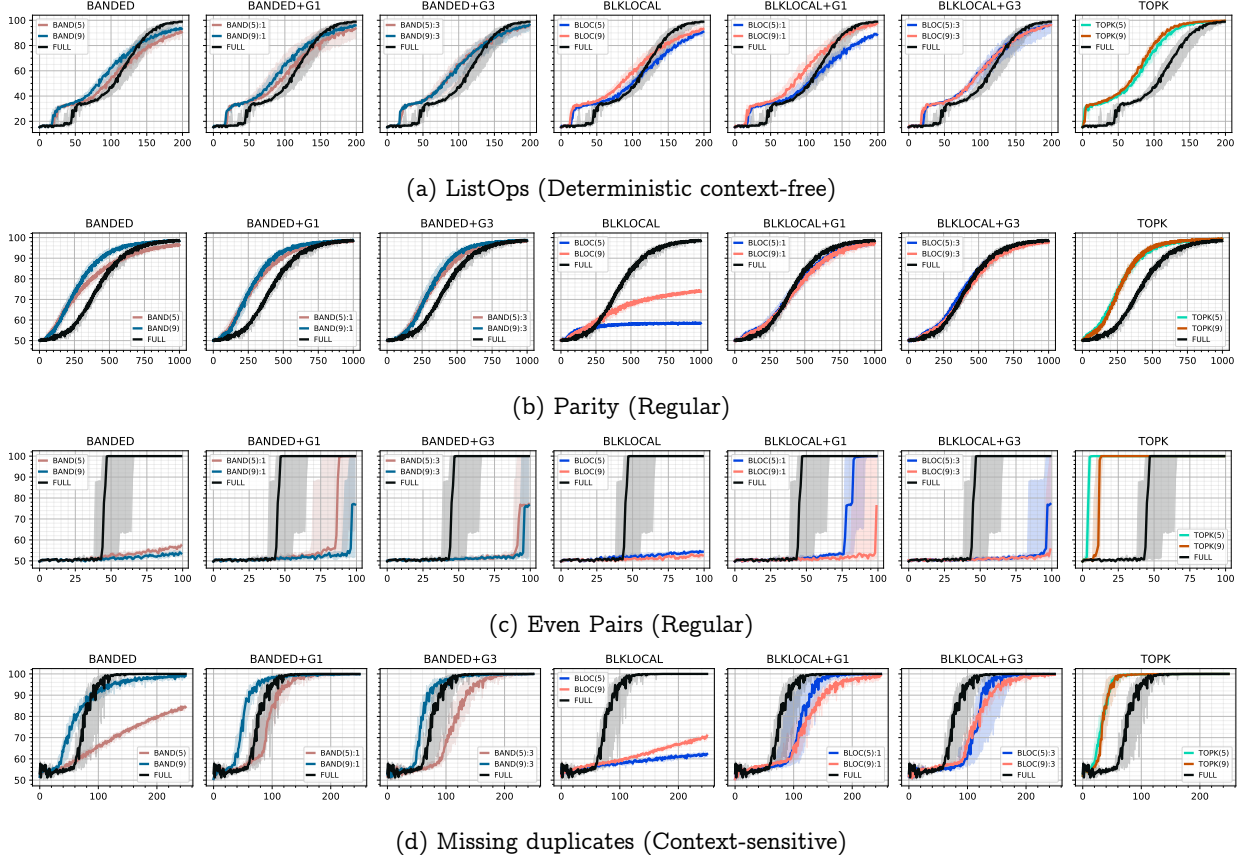


Figure 16: Same as figure 12 with GELU activation in the MLP component of the transformer block.

With activations such as ReLU, the $\text{MLP}(\mathbf{x}) = \mathbf{R}^\top \sigma(\mathbf{P}\mathbf{x})$ are often positive homogeneous such that, for any $\alpha \neq 0$, we have $\mathbf{R}^\top \sigma(\mathbf{P}\mathbf{x}) = \alpha \mathbf{R}^\top \sigma(\alpha^{-1}\mathbf{P}\mathbf{x})$, leading to symmetries in the parameter space, and making analysis of optimization algorithms challenging [Li and Liang, 2018, Allen-Zhu et al., 2019, Zou et al., 2020, Fehrman et al., 2020], and some results focus on the convergence under specific conditions. However, most convergence rates depend on the Lipschitz-ness of the ReLU network, and the Lipschitz constant is not affected by this positive homogeneity as long as we assume that the matrices \mathbf{R}, \mathbf{P} have bounded norms (which we do). As an example, note the following for the Lipschitz-ness with respect to \mathbf{P} :

$$\|\text{MLP}_{\mathbf{P}, \mathbf{R}}(\mathbf{x}) - \text{MLP}_{\bar{\mathbf{P}}, \mathbf{R}}(\mathbf{x})\| \leq \max_{\alpha} \|\text{MLP}_{\alpha^{-1}\mathbf{P}, \alpha\mathbf{R}}(\mathbf{x}) - \text{MLP}_{\alpha^{-1}\bar{\mathbf{P}}, \alpha\mathbf{R}}(\mathbf{x})\| \quad (37)$$

$$= \max_{\alpha} \|\alpha \mathbf{R}^\top \sigma(\alpha^{-1}\mathbf{P}\mathbf{x}) - \alpha \mathbf{R}^\top \sigma(\alpha^{-1}\bar{\mathbf{P}}\mathbf{x})\| \quad (38)$$

$$\leq \max_{\alpha} \|\alpha \mathbf{R}\| \|\sigma(\alpha^{-1}\mathbf{P}\mathbf{x}) - \sigma(\alpha^{-1}\bar{\mathbf{P}}\mathbf{x})\| \quad (39)$$

$$\leq \max_{\alpha} \alpha \|\mathbf{R}\| \lambda_{\sigma} \|\alpha^{-1}(\mathbf{P} - \bar{\mathbf{P}})\mathbf{x}\| \leq \max_{\alpha} \alpha B \lambda_{\sigma} \alpha^{-1} \Xi \|\mathbf{P} - \bar{\mathbf{P}}\| \quad (40)$$

$$= B \lambda_{\sigma} \Xi \|\mathbf{P} - \bar{\mathbf{P}}\|, \quad (41)$$

where we see that the effect of the α is cancelled out and we get the result in lemma S1. Similar result can be shown for Lipschitz-ness with respect to \mathbf{R} .

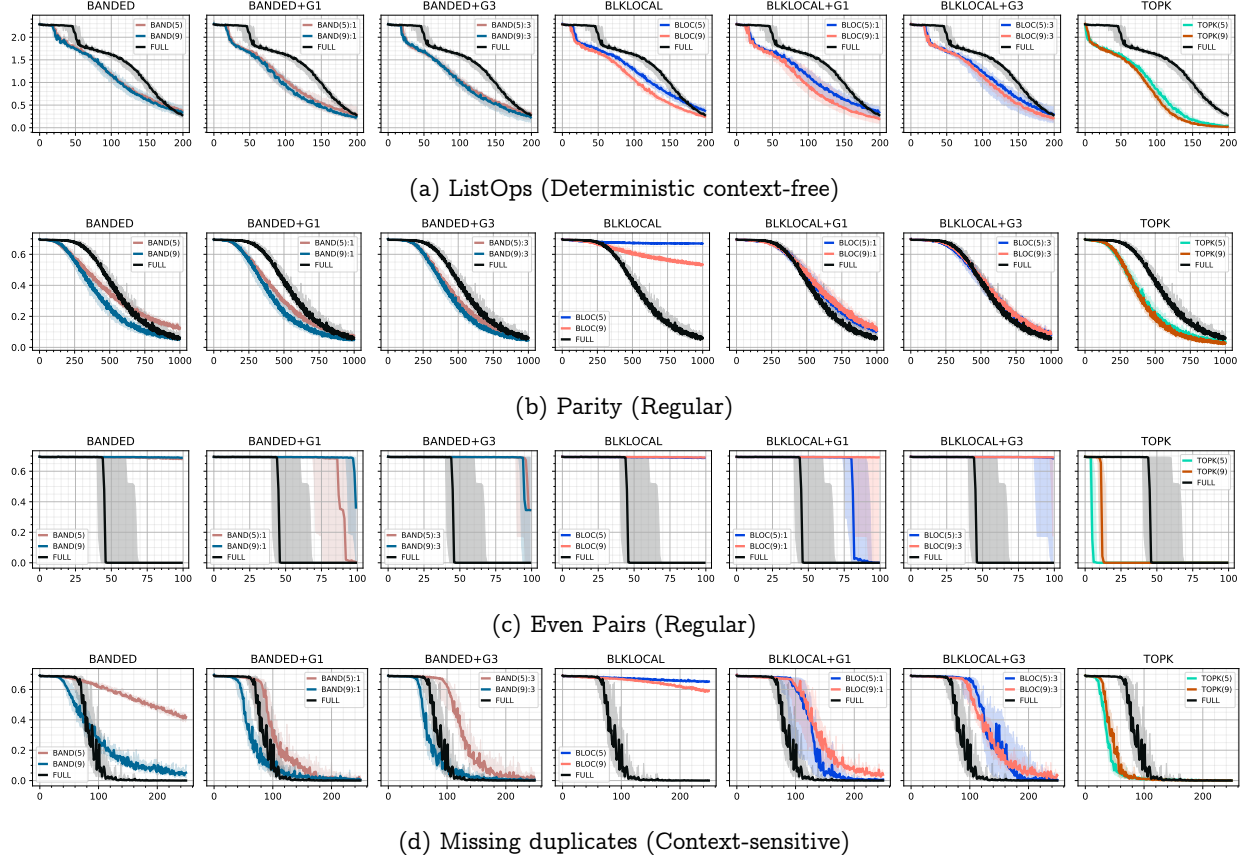


Figure 17: Same as figure 11 with Mish activation in the MLP component of the transformer block.

D.2 Proof of Theorem 1

Theorem S1. *Given definition 1 and lemma 1, a transformer block TF with learnable parameters $\theta = (\mathbf{W}, \mathbf{V}, \mathbf{P}, \mathbf{R})$ is $\lambda_\theta(\xi)$ -Lipschitz with respect to its learnable parameters θ with*

$$\lambda_\theta(\xi) = \zeta_{\text{LN}}(\zeta_{\text{LN}}(1 + \eta_X)(\lambda_W(\xi) + \lambda_V) + L(\eta_P + \eta_R)), \quad (42)$$

and TF is $\lambda_X(\xi)$ -Lipschitz with respect to its input \mathbf{X} with

$$\lambda_X(\xi) = \zeta_{\text{LN}}^2(1 + \eta_X)(1 + \lambda_X(\xi)), \quad (43)$$

where we explicitly note the dependence of the Lipschitz constant with respect to learnable parameters $\lambda_\theta(\xi)$, and input $\lambda_X(\xi)$ to the Lipschitz constant ξ of the (masked) softmax operation.

Proof. Let $\theta = (\mathbf{W}, \mathbf{V}, \mathbf{P}, \mathbf{R})$ and $\bar{\theta} = (\bar{\mathbf{W}}, \bar{\mathbf{V}}, \bar{\mathbf{P}}, \bar{\mathbf{R}})$. Then, we have the following:

$$\begin{aligned} \|\text{TF}_\theta(\mathbf{X}) - \text{TF}_{\bar{\theta}}(\mathbf{X})\|_{2,1} &= \|\text{TF}_{\mathbf{W}, \mathbf{V}, \mathbf{P}, \mathbf{R}}(\mathbf{X}) - \text{TF}_{\bar{\mathbf{W}}, \bar{\mathbf{V}}, \bar{\mathbf{P}}, \bar{\mathbf{R}}}(\mathbf{X})\|_{2,1} & (44) \\ &\leq \|\text{TF}_{\mathbf{W}, \mathbf{V}, \mathbf{P}, \mathbf{R}}(\mathbf{X}) - \text{TF}_{\mathbf{W}, \mathbf{V}, \bar{\mathbf{P}}, \bar{\mathbf{R}}}(\mathbf{X})\|_{2,1} & (T_1) \\ &\quad + \|\text{TF}_{\mathbf{W}, \mathbf{V}, \bar{\mathbf{P}}, \bar{\mathbf{R}}}(\mathbf{X}) - \text{TF}_{\mathbf{W}, \bar{\mathbf{V}}, \bar{\mathbf{P}}, \bar{\mathbf{R}}}(\mathbf{X})\|_{2,1} & (T_2) \\ &\quad + \|\text{TF}_{\mathbf{W}, \bar{\mathbf{V}}, \bar{\mathbf{P}}, \bar{\mathbf{R}}}(\mathbf{X}) - \text{TF}_{\bar{\mathbf{W}}, \bar{\mathbf{V}}, \bar{\mathbf{P}}, \bar{\mathbf{R}}}(\mathbf{X})\|_{2,1} & (T_3) \\ &\quad + \|\text{TF}_{\bar{\mathbf{W}}, \bar{\mathbf{V}}, \bar{\mathbf{P}}, \bar{\mathbf{R}}}(\mathbf{X}) - \text{TF}_{\bar{\mathbf{W}}, \bar{\mathbf{V}}, \bar{\mathbf{P}}, \bar{\mathbf{R}}}(\mathbf{X})\|_{2,1}. & (T_4) \end{aligned}$$

First, processing equation (T_1) , let us denote with $\tilde{\mathbf{X}} = \text{LN}(\mathbf{X} + \mathbf{A}_{\mathbf{W}, \mathbf{V}}(\mathbf{X}))$, then

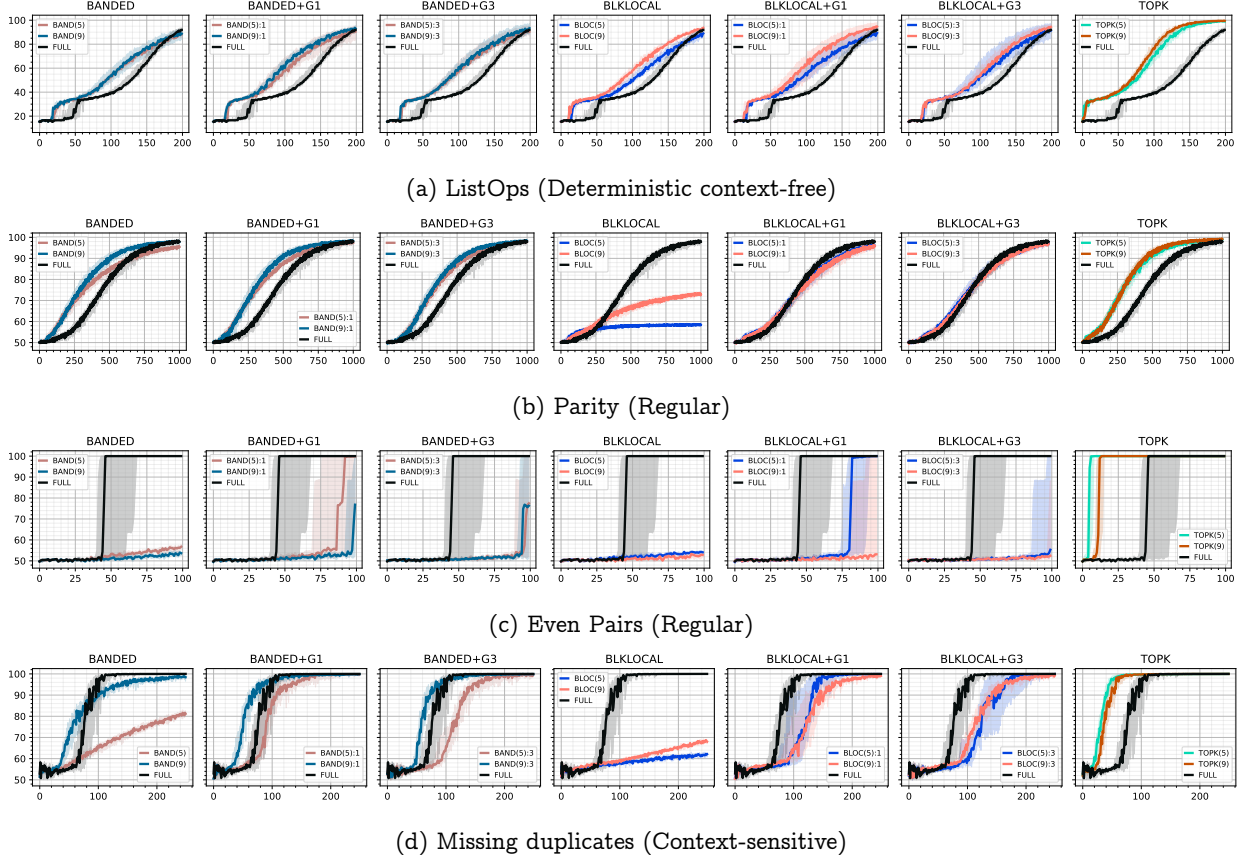


Figure 18: Same as figure 12 with Mish activation in the MLP component of the transformer block.

$$(T_1) = \|\text{TF}_{\mathbf{W},\mathbf{V},\mathbf{P},\mathbf{R}}(\mathbf{X}) - \text{TF}_{\mathbf{W},\mathbf{V},\mathbf{P},\mathbf{R}}(\mathbf{X})\|_{2,1} = \|\text{LN}(\tilde{\mathbf{X}} + \text{MLP}_{\mathbf{P},\mathbf{R}}(\tilde{\mathbf{X}})) - \text{LN}(\tilde{\mathbf{X}} + \text{MLP}_{\mathbf{P},\mathbf{R}}(\tilde{\mathbf{X}}))\|_{2,1} \quad (45)$$

$$= \sum_{i \in \llbracket L \rrbracket} \|\text{LN}(\tilde{\mathbf{X}}_{:i} + \text{MLP}_{\mathbf{P},\mathbf{R}}(\tilde{\mathbf{X}}_{:i})) - \text{LN}(\tilde{\mathbf{X}}_{:i} + \text{MLP}_{\mathbf{P},\mathbf{R}}(\tilde{\mathbf{X}}_{:i}))\| \quad (46)$$

$$\leq \sum_{i \in \llbracket L \rrbracket} \zeta_{\text{LN}} \|\text{MLP}_{\mathbf{P},\mathbf{R}}(\tilde{\mathbf{X}}_{:i}) - \text{MLP}_{\mathbf{P},\mathbf{R}}(\tilde{\mathbf{X}}_{:i})\| \quad (\text{using equation (29)}) \quad (47)$$

$$\leq \sum_{i \in \llbracket L \rrbracket} \zeta_{\text{LN}} \eta_{\mathbf{R}} \|\mathbf{R} - \mathbf{R}\| = L \zeta_{\text{LN}} \eta_{\mathbf{R}} \|\mathbf{R} - \mathbf{R}\| \quad (\text{using equation (28)}). \quad (48)$$

Handling equation (T_2) in a similar fashion, we have

$$(T_2) = \|\text{TF}_{\mathbf{W},\mathbf{V},\mathbf{P},\mathbf{R}}(\mathbf{X}) - \text{TF}_{\mathbf{W},\mathbf{V},\mathbf{P},\mathbf{R}}(\mathbf{X})\|_{2,1} = \|\text{LN}(\tilde{\mathbf{X}} + \text{MLP}_{\mathbf{P},\mathbf{R}}(\tilde{\mathbf{X}})) - \text{LN}(\tilde{\mathbf{X}} + \text{MLP}_{\mathbf{P},\mathbf{R}}(\tilde{\mathbf{X}}))\|_{2,1} \quad (49)$$

$$= \sum_{i \in \llbracket L \rrbracket} \|\text{LN}(\tilde{\mathbf{X}}_{:i} + \text{MLP}_{\mathbf{P},\mathbf{R}}(\tilde{\mathbf{X}}_{:i})) - \text{LN}(\tilde{\mathbf{X}}_{:i} + \text{MLP}_{\mathbf{P},\mathbf{R}}(\tilde{\mathbf{X}}_{:i}))\| \quad (50)$$

$$\leq \sum_{i \in \llbracket L \rrbracket} \zeta_{\text{LN}} \|\text{MLP}_{\mathbf{P},\mathbf{R}}(\tilde{\mathbf{X}}_{:i}) - \text{MLP}_{\mathbf{P},\mathbf{R}}(\tilde{\mathbf{X}}_{:i})\| \quad (\text{using equation (29)}) \quad (51)$$

$$\leq \sum_{i \in \llbracket L \rrbracket} \zeta_{\text{LN}} \eta_{\mathbf{P}} \|\mathbf{P} - \mathbf{P}\| = L \zeta_{\text{LN}} \eta_{\mathbf{P}} \|\mathbf{P} - \mathbf{P}\| \quad (\text{using equation (27)}). \quad (52)$$

For equation (T_3) , let us denote with $\tilde{\mathbf{X}}' = \text{LN}(\mathbf{X} + \mathbf{A}_{\mathbf{W},\mathbf{V}}(\mathbf{X}))$. Then we have

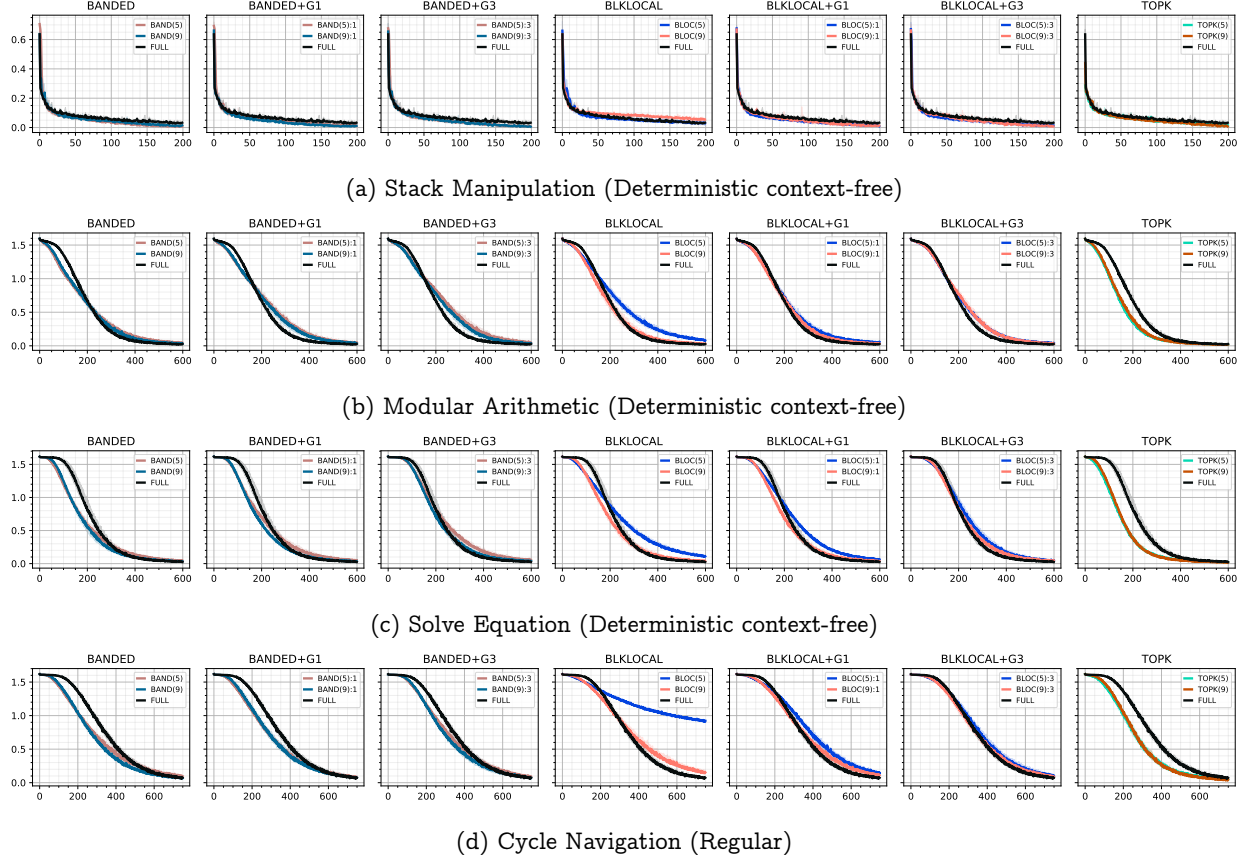


Figure 19: Same as figure 13 with GELU activation in the MLP component of the transformer block.

$$(T_3) = \|\text{TF}_{\mathbf{W}, \mathbf{V}, \bar{\mathbf{P}}, \bar{\mathbf{R}}}(\mathbf{X}) - \text{TF}_{\mathbf{W}, \mathbf{V}, \bar{\mathbf{P}}, \bar{\mathbf{R}}}(\mathbf{X}')\|_{2,1} = \|\text{LN}(\tilde{\mathbf{X}} + \text{MLP}_{\bar{\mathbf{P}}, \bar{\mathbf{R}}}(\tilde{\mathbf{X}})) - \text{LN}(\tilde{\mathbf{X}}' + \text{MLP}_{\bar{\mathbf{P}}, \bar{\mathbf{R}}}(\tilde{\mathbf{X}}'))\|_{2,1} \quad (53)$$

$$= \sum_{i \in [L]} \|\text{LN}(\tilde{\mathbf{X}}_{:i} + \text{MLP}_{\bar{\mathbf{P}}, \bar{\mathbf{R}}}(\tilde{\mathbf{X}}_{:i})) - \text{LN}(\tilde{\mathbf{X}}'_{:i} + \text{MLP}_{\bar{\mathbf{P}}, \bar{\mathbf{R}}}(\tilde{\mathbf{X}}'_{:i}))\| \quad (54)$$

$$\leq \sum_{i \in [L]} \zeta_{\text{LN}} \|(\tilde{\mathbf{X}}_{:i} - \tilde{\mathbf{X}}'_{:i}) + (\text{MLP}_{\bar{\mathbf{P}}, \bar{\mathbf{R}}}(\tilde{\mathbf{X}}_{:i}) - \text{MLP}_{\bar{\mathbf{P}}, \bar{\mathbf{R}}}(\tilde{\mathbf{X}}'_{:i}))\| \quad (\text{using equation (29)}) \quad (55)$$

$$\leq \sum_{i \in [L]} \zeta_{\text{LN}} (1 + \eta_X) \|(\tilde{\mathbf{X}}_{:i} - \tilde{\mathbf{X}}'_{:i})\| \quad (\text{using equation (26)}) \quad (56)$$

$$= \sum_{i \in [L]} \zeta_{\text{LN}} (1 + \eta_X) \|\text{LN}(\mathbf{X}_{:i} + \mathbf{A}_{\mathbf{W}, \mathbf{V}}(\mathbf{X})_{:i}) - \text{LN}(\mathbf{X}'_{:i} + \mathbf{A}_{\mathbf{W}, \mathbf{V}}(\mathbf{X}')_{:i})\| \quad (57)$$

$$\leq \sum_{i \in [L]} \zeta_{\text{LN}} (1 + \eta_X) \zeta_{\text{LN}} \|\mathbf{A}_{\mathbf{W}, \mathbf{V}}(\mathbf{X})_{:i} - \mathbf{A}_{\mathbf{W}, \mathbf{V}}(\mathbf{X}')_{:i}\| \quad (\text{using equation (29)}) \quad (58)$$

$$= \zeta_{\text{LN}} (1 + \eta_X) \zeta_{\text{LN}} \|\mathbf{A}_{\mathbf{W}, \mathbf{V}}(\mathbf{X}) - \mathbf{A}_{\mathbf{W}, \mathbf{V}}(\mathbf{X}')\|_{2,1} \quad (59)$$

$$\leq \zeta_{\text{LN}} (1 + \eta_X) \zeta_{\text{LN}} \lambda_V \|\mathbf{V} - \mathbf{V}'\| \quad (\text{using equation (8) in definition 1}). \quad (60)$$

For equation (T_4) , let us denote with $\tilde{\mathbf{X}}'' = \text{LN}(\mathbf{X} + \mathbf{A}_{\bar{\mathbf{W}}, \bar{\mathbf{V}}}(\mathbf{X}))$. Then we can follow the same procedure as for equation (T_3) and get the following:

$$(T_4) = \|\text{TF}_{\mathbf{W}, \mathbf{V}, \bar{\mathbf{P}}, \bar{\mathbf{R}}}(\mathbf{X}) - \text{TF}_{\bar{\mathbf{W}}, \bar{\mathbf{V}}, \bar{\mathbf{P}}, \bar{\mathbf{R}}}(\mathbf{X})\|_{2,1} \quad (61)$$

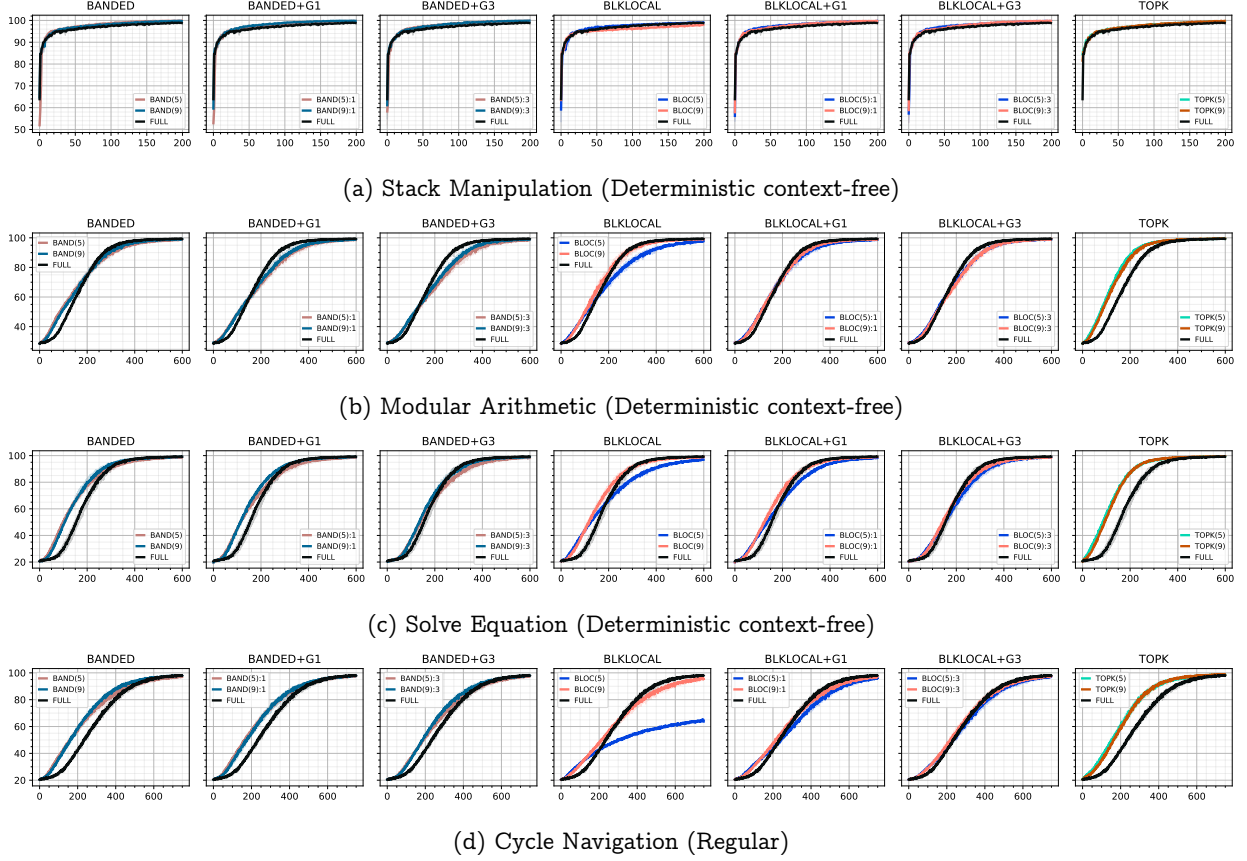


Figure 20: Same as figure 14 with GELU activation in the MLP component of the transformer block.

$$= \|\text{LN}(\tilde{\mathbf{X}}' + \text{MLP}_{\bar{\mathbf{P}}, \bar{\mathbf{R}}}(\tilde{\mathbf{X}}')) - \text{LN}(\tilde{\mathbf{X}}'' + \text{MLP}_{\bar{\mathbf{P}}, \bar{\mathbf{R}}}(\tilde{\mathbf{X}}''))\|_{2,1} \quad (62)$$

$$= \sum_{i \in [L]} \|\text{LN}(\tilde{\mathbf{X}}'_{:i} + \text{MLP}_{\bar{\mathbf{P}}, \bar{\mathbf{R}}}(\tilde{\mathbf{X}}'_{:i})) - \text{LN}(\tilde{\mathbf{X}}''_{:i} + \text{MLP}_{\bar{\mathbf{P}}, \bar{\mathbf{R}}}(\tilde{\mathbf{X}}''_{:i}))\| \quad (63)$$

$$\leq \sum_{i \in [L]} \zeta_{\text{LN}} \|\tilde{\mathbf{X}}'_{:i} - \tilde{\mathbf{X}}''_{:i}\| + (\text{MLP}_{\bar{\mathbf{P}}, \bar{\mathbf{R}}}(\tilde{\mathbf{X}}'_{:i}) - \text{MLP}_{\bar{\mathbf{P}}, \bar{\mathbf{R}}}(\tilde{\mathbf{X}}''_{:i})) \quad (\text{using equation (29)}) \quad (64)$$

$$\leq \sum_{i \in [L]} \zeta_{\text{LN}} (1 + \eta_X) \|\tilde{\mathbf{X}}'_{:i} - \tilde{\mathbf{X}}''_{:i}\| \quad (\text{using equation (26)}) \quad (65)$$

$$= \sum_{i \in [L]} \zeta_{\text{LN}} (1 + \eta_X) \|\text{LN}(\mathbf{X}_{:i} + \mathbf{A}_{\bar{\mathbf{W}}, \bar{\mathbf{V}}}(\mathbf{X}_{:i})) - \text{LN}(\mathbf{X}_{:i} + \mathbf{A}_{\bar{\mathbf{W}}, \bar{\mathbf{V}}}(\mathbf{X}_{:i}))\| \quad (66)$$

$$\leq \sum_{i \in [L]} \zeta_{\text{LN}} (1 + \eta_X) \zeta_{\text{LN}} \|\mathbf{A}_{\bar{\mathbf{W}}, \bar{\mathbf{V}}}(\mathbf{X}_{:i}) - \mathbf{A}_{\bar{\mathbf{W}}, \bar{\mathbf{V}}}(\mathbf{X}_{:i})\| \quad (\text{using equation (29)}) \quad (67)$$

$$= \zeta_{\text{LN}} (1 + \eta_X) \zeta_{\text{LN}} \|\mathbf{A}_{\bar{\mathbf{W}}, \bar{\mathbf{V}}}(\mathbf{X}) - \mathbf{A}_{\bar{\mathbf{W}}, \bar{\mathbf{V}}}(\mathbf{X})\|_{2,1} \quad (68)$$

$$\leq \zeta_{\text{LN}} (1 + \eta_X) \zeta_{\text{LN}} \lambda_W(\xi) \|\mathbf{W} - \bar{\mathbf{W}}\| \quad (\text{using equation (7) in definition 1}). \quad (69)$$

Putting these all together, we have

$$\|\text{TF}_{\theta}(\mathbf{X}) - \text{TF}_{\bar{\theta}}(\mathbf{X})\|_{2,1} \quad (70)$$

$$\leq \zeta_{\text{LN}} L (\eta_R \|\mathbf{R} - \bar{\mathbf{R}}\| + \eta_P \|\mathbf{P} - \bar{\mathbf{P}}\|) + \zeta_{\text{LN}}^2 (1 + \eta_X) (\lambda_V \|\mathbf{V} - \bar{\mathbf{V}}\| + \lambda_W(\xi) \|\mathbf{W} - \bar{\mathbf{W}}\|) \quad (71)$$

$$\leq \zeta_{\text{LN}} L (\eta_R \|\theta - \bar{\theta}\| + \eta_P \|\theta - \bar{\theta}\|) + \zeta_{\text{LN}}^2 (1 + \eta_X) (\lambda_V \|\theta - \bar{\theta}\| + \lambda_W(\xi) \|\theta - \bar{\theta}\|) \quad (72)$$

$$= \zeta_{\text{LN}} (\zeta_{\text{LN}}(1 + \eta_X)(\lambda_W(\xi) + \lambda_V) + L(\eta_P + \eta_R)) \|\theta - \bar{\theta}\|, \quad (73)$$

where we used the definition that, for matrix tuples $\theta, \bar{\theta}$, $\|\theta - \bar{\theta}\| = \max\{\|\mathbf{W} - \bar{\mathbf{W}}\|, \|\mathbf{V} - \bar{\mathbf{V}}\|, \|\mathbf{P} - \bar{\mathbf{P}}\|, \|\mathbf{R} - \bar{\mathbf{R}}\|\}$. This gives us the desired result in equation (42).

For inputs $\mathbf{X}, \bar{\mathbf{X}}$, let $\tilde{\mathbf{X}} = \text{LN}(\mathbf{X} + \mathbf{A}_{\mathbf{W}, \mathbf{V}}(\mathbf{X}))$ and $\tilde{\mathbf{X}}' = \text{LN}(\bar{\mathbf{X}} + \mathbf{A}_{\mathbf{W}, \mathbf{V}}(\bar{\mathbf{X}}))$. Then we have the following:

$$\|\text{TF}_{\theta}(\mathbf{X}) - \text{TF}_{\theta}(\bar{\mathbf{X}})\|_{2,1} = \|\text{LN}(\tilde{\mathbf{X}} + \text{MLP}_{\mathbf{P}, \mathbf{R}}(\tilde{\mathbf{X}})) - \text{LN}(\tilde{\mathbf{X}}' + \text{MLP}_{\mathbf{P}, \mathbf{R}}(\tilde{\mathbf{X}}'))\|_{2,1} \quad (74)$$

$$= \sum_{i \in [L]} \|\text{LN}(\tilde{\mathbf{X}}_{:i} + \text{MLP}_{\mathbf{P}, \mathbf{R}}(\tilde{\mathbf{X}}_{:i})) - \text{LN}(\tilde{\mathbf{X}}'_{:i} + \text{MLP}_{\mathbf{P}, \mathbf{R}}(\tilde{\mathbf{X}}'_{:i}))\| \quad (75)$$

$$\leq \sum_{i \in [L]} \zeta_{\text{LN}} \|\tilde{\mathbf{X}}_{:i} - \tilde{\mathbf{X}}'_{:i}\| + \left(\text{MLP}_{\mathbf{P}, \mathbf{R}}(\tilde{\mathbf{X}}_{:i}) - \text{MLP}_{\mathbf{P}, \mathbf{R}}(\tilde{\mathbf{X}}'_{:i}) \right) \quad (\text{using equation (29)}) \quad (76)$$

$$\leq \sum_{i \in [L]} \zeta_{\text{LN}}(1 + \eta_X) \|\tilde{\mathbf{X}}_{:i} - \tilde{\mathbf{X}}'_{:i}\| \quad (\text{using equation (26)}) \quad (77)$$

$$= \sum_{i \in [L]} \zeta_{\text{LN}}(1 + \eta_X) \|\text{LN}(\mathbf{X}_{:i} + \mathbf{A}_{\mathbf{W}, \mathbf{V}}(\mathbf{X})_{:i}) - \text{LN}(\bar{\mathbf{X}}_{:i} + \mathbf{A}_{\mathbf{W}, \mathbf{V}}(\bar{\mathbf{X}})_{:i})\| \quad (78)$$

$$\leq \sum_{i \in [L]} \zeta_{\text{LN}}^2(1 + \eta_X) \|\mathbf{X}_{:i} - \bar{\mathbf{X}}_{:i}\| + \|\mathbf{A}_{\mathbf{W}, \mathbf{V}}(\mathbf{X})_{:i} - \mathbf{A}_{\mathbf{W}, \mathbf{V}}(\bar{\mathbf{X}})_{:i}\| \quad (\text{using equation (29)}) \quad (79)$$

$$\leq \zeta_{\text{LN}}^2(1 + \eta_X) \|\mathbf{X} - \bar{\mathbf{X}}\| + \|\mathbf{A}_{\mathbf{W}, \mathbf{V}}(\mathbf{X}) - \mathbf{A}_{\mathbf{W}, \mathbf{V}}(\bar{\mathbf{X}})\|_{2,1} \quad (80)$$

$$= \zeta_{\text{LN}}^2(1 + \eta_X) (\|\mathbf{X} - \bar{\mathbf{X}}\|_{2,1} + \|\mathbf{A}_{\mathbf{W}, \mathbf{V}}(\mathbf{X}) - \mathbf{A}_{\mathbf{W}, \mathbf{V}}(\bar{\mathbf{X}})\|_{2,1}) \quad (81)$$

$$\leq \zeta_{\text{LN}}^2(1 + \eta_X) (1 + \lambda_X(\xi)) \|\mathbf{X} - \bar{\mathbf{X}}\|_{2,1} \quad (\text{using equation (6) in definition 1}), \quad (82)$$

which gives us the desired result in equation (43). \square

D.3 Proof of Theorem 2

Theorem S2. Consider the following assumptions:

(L1) The sample wise loss ℓ in equation (4) is α -Lipschitz.

(L2) The final readout layer weights are norm-bounded as $\|\Phi\| \leq 1$ and the per-token output of each transformer block is norm bounded as $\|\mathbf{X}_{:i}^{(t)}\| \leq \Xi$ for all $i \in [L]$ and $t \in [\tau]$.

(L3) The sequence aggregator is $\omega = (1/L)\mathbf{1}_L$.

Under the above assumptions and the conditions of definition 1 and theorem 1, the learning objective \mathcal{L} in equation (4) is $\lambda_{\mathcal{L}}(\xi)$ -Lipschitz with respect to the learnable parameters $\Theta = (\mathbf{T}, \theta^{(1)}, \dots, \theta^{(\tau)}, \Phi)$, where

$$\lambda_{\mathcal{L}}(\xi) = \alpha \left(\Xi + \lambda_X(\xi)^\tau \left(1 + \frac{\lambda_{\theta}(\xi)}{L(\lambda_X(\xi) - 1)} \right) \right). \quad (83)$$

Proof. Let us first denote the model parameter tuples as $\Theta = (\mathbf{T}, \theta^{(1)}, \dots, \theta^{(\tau)}, \Phi)$ and $\bar{\Theta} = (\bar{\mathbf{T}}, \bar{\theta}^{(1)}, \dots, \bar{\theta}^{(\tau)}, \bar{\Phi})$. Let $\mathbf{X}^{(0)} = [\mathbf{T}_{v_1} + \mathbf{E}_1, \dots, \mathbf{T}_{v_L} + \mathbf{E}_L]$ and $\bar{\mathbf{X}}^{(0)} = [\bar{\mathbf{T}}_{v_1} + \mathbf{E}_1, \dots, \bar{\mathbf{T}}_{v_L} + \mathbf{E}_L]$ denote the initial token embeddings for the same input $X = [v_1, \dots, v_L], v_i \in [D]$, with model parameters Θ and $\bar{\Theta}$ respectively. Note that we are not learning the position encoding \mathbf{E} in our setup. For any $t = 1, \dots, \tau$, let $\mathbf{X}^{(t)} = \text{TF}_{\theta^{(t)}}(\mathbf{X}^{(t-1)})$ and $\bar{\mathbf{X}}^{(t)} = \text{TF}_{\bar{\theta}^{(t)}}(\bar{\mathbf{X}}^{(t-1)})$, both defined recursively.

Then, using the loss function \mathcal{L} in equation (4), we have the following:

$$|\mathcal{L}(\Theta) - \mathcal{L}(\bar{\Theta})| = \left| \frac{1}{n} \sum_{(X, y) \in S} (\ell(y, f_{\Theta}(X)) - \ell(y, f_{\bar{\Theta}}(X))) \right| \quad (84)$$

$$\leq \frac{1}{n} \sum_{(X,y) \in S} \alpha |f_{\Theta}(X) - f_{\bar{\Theta}}(X)|, \quad (85)$$

where we utilized the assumption that ℓ is α -Lipschitz. Focusing on the $|f_{\Theta}(X) - f_{\bar{\Theta}}(X)|$ term in equation (85), we see the following:

$$|f_{\Theta}(X) - f_{\bar{\Theta}}(X)| = \left| \Phi(\mathbf{X}^{(\tau)} \boldsymbol{\omega}) - \bar{\Phi}(\bar{\mathbf{X}}^{(\tau)} \boldsymbol{\omega}) \right| = \left| \Phi \left(\frac{1}{L} \sum_{i=1}^L (\mathbf{X}_{:i}^{(\tau)} - \bar{\mathbf{X}}_{:i}^{(\tau)}) \right) + (\Phi - \bar{\Phi}) \left(\frac{1}{L} \sum_{i=1}^L \bar{\mathbf{X}}_{:i}^{(\tau)} \right) \right| \quad (86)$$

$$\leq \|\Phi\| \left(\frac{1}{L} \sum_{i=1}^L \|\mathbf{X}_{:i}^{(\tau)} - \bar{\mathbf{X}}_{:i}^{(\tau)}\| \right) + \|\Phi - \bar{\Phi}\| \left(\frac{1}{L} \sum_{i=1}^L \|\bar{\mathbf{X}}_{:i}^{(\tau)}\| \right) \quad (87)$$

$$\leq \frac{1}{L} \|\mathbf{X}^{(\tau)} - \bar{\mathbf{X}}^{(\tau)}\|_{2,1} + \Xi \|\Phi - \bar{\Phi}\|, \quad (88)$$

where we utilized the assumption that $\|\Phi\| \leq 1$ and $\|\bar{\mathbf{X}}_{:i}\| \leq \Xi \forall i \in \llbracket L \rrbracket$. Considering the $\|\mathbf{X}^{(\tau)} - \bar{\mathbf{X}}^{(\tau)}\|_{2,1}$ in the right-hand-side of equation (88), and noting the recursive definition of $\bar{\mathbf{X}}^{(t)} = \text{TF}_{\bar{\theta}^{(t)}}(\bar{\mathbf{X}}^{(t-1)})$, we have the following:

$$\|\mathbf{X}^{(\tau)} - \bar{\mathbf{X}}^{(\tau)}\|_{2,1} \quad (89)$$

$$= \left\| \text{TF}_{\theta^{(\tau)}}(\text{TF}_{\theta^{(\tau-1)}}(\dots(\text{TF}_{\theta^{(1)}}(\mathbf{X}^{(0)}))) - \text{TF}_{\bar{\theta}^{(\tau)}}(\text{TF}_{\bar{\theta}^{(\tau-1)}}(\dots(\text{TF}_{\bar{\theta}^{(1)}}(\bar{\mathbf{X}}^{(0)}))) \right\|_{2,1} \quad (90)$$

$$\leq \left\| \text{TF}_{\theta^{(\tau)}}(\dots(\text{TF}_{\theta^{(1)}}(\mathbf{X}^{(0)}))) - \text{TF}_{\theta^{(\tau)}}(\dots(\text{TF}_{\theta^{(1)}}(\bar{\mathbf{X}}^{(0)}))) \right\|_{2,1} \quad (P_1)$$

$$+ \sum_{t=1}^{\tau-1} \left\| \text{TF}_{\theta^{(\tau)}}(\dots(\text{TF}_{\theta^{(t)}}(\bar{\mathbf{X}}^{(t-1)}))) - \text{TF}_{\theta^{(\tau)}}(\dots(\text{TF}_{\bar{\theta}^{(t)}}(\bar{\mathbf{X}}^{(t-1)}))) \right\|_{2,1} \quad (P_2)$$

$$+ \left\| \text{TF}_{\theta^{(\tau)}}(\bar{\mathbf{X}}^{(t-1)}) - \text{TF}_{\bar{\theta}^{(\tau)}}(\bar{\mathbf{X}}^{(t-1)}) \right\|_{2,1} \quad (P_3)$$

Utilizing the $\lambda_{\mathbf{X}}(\xi)$ -Lipschitzness of each transformer block with respect to the input (as per theorem 1, equation (14)), and applying it recursively through the τ transformer blocks, we can bound equation (P₁) as:

$$(P_1) \leq \lambda_{\mathbf{X}}(\xi)^{\tau} \|\mathbf{X}^{(0)} - \bar{\mathbf{X}}^{(0)}\|_{2,1} = \lambda_{\mathbf{X}}(\xi)^{\tau} \sum_{i=1}^L \|\mathbf{T}_{v_i} - \bar{\mathbf{T}}_{v_i}\| \quad (91)$$

$$\leq \lambda_{\mathbf{X}}(\xi)^{\tau} \sum_{i=1}^L \|\mathbf{T} - \bar{\mathbf{T}}\| = \lambda_{\mathbf{X}}(\xi)^{\tau} L \|\mathbf{T} - \bar{\mathbf{T}}\|. \quad (92)$$

For equation (P₂), we will again utilize the $\lambda_{\mathbf{X}}(\xi)$ -Lipschitzness of each transformer block with respect to the input recursively to get the following:

$$(P_2) = \sum_{t=1}^{\tau-1} \left\| \text{TF}_{\theta^{(\tau)}}(\dots(\text{TF}_{\theta^{(t)}}(\bar{\mathbf{X}}^{(t-1)}))) - \text{TF}_{\theta^{(\tau)}}(\dots(\text{TF}_{\bar{\theta}^{(t)}}(\bar{\mathbf{X}}^{(t-1)}))) \right\|_{2,1} \quad (93)$$

$$\leq \sum_{t=1}^{\tau-1} \lambda_{\mathbf{X}}(\xi)^{\tau-t} \left\| \text{TF}_{\theta^{(t)}}(\bar{\mathbf{X}}^{(t-1)}) - \text{TF}_{\bar{\theta}^{(t)}}(\bar{\mathbf{X}}^{(t-1)}) \right\|_{2,1} \quad (94)$$

$$\leq \sum_{t=1}^{\tau-1} \lambda_{\mathbf{X}}(\xi)^{\tau-t} \lambda_{\theta}(\xi) \|\theta^{(t)} - \bar{\theta}^{(t)}\|, \quad (95)$$

where we utilize the $\lambda_{\theta}(\xi)$ -Lipschitzness of the transformer block with respect to the parameters in the last inequality.

We can use $\lambda_{\theta}(\xi)$ -Lipschitzness of each transformer block with respect to the parameters (as per theorem 1, equation (13)) to bound equation (P₃) with $\lambda_{\theta}(\xi) \|\theta^{(\tau)} - \bar{\theta}^{(\tau)}\|$.

Substituting this, equation (92) and equation (95) in equation (88), we have

$$|f_{\Theta}(X) - f_{\bar{\Theta}}(X)| \tag{96}$$

$$\leq \frac{1}{L} \left(\lambda_{\mathbf{X}}(\xi)^{\tau} L \|\mathbf{T} - \bar{\mathbf{T}}\| + \left(\lambda_{\theta}(\xi) \sum_{t=1}^{\tau-1} \lambda_{\mathbf{X}}(\xi)^{\tau-t} \|\theta^{(t)} - \bar{\theta}^{(t)}\| \right) + \lambda_{\theta}(\xi) \|\theta^{(\tau)} - \bar{\theta}^{(\tau)}\| \right) + \Xi \|\Phi - \bar{\Phi}\| \tag{97}$$

$$\leq \frac{1}{L} \left(\lambda_{\mathbf{X}}(\xi)^{\tau} L \|\Theta - \bar{\Theta}\| + \left(\lambda_{\theta}(\xi) \sum_{t=1}^{\tau-1} \lambda_{\mathbf{X}}(\xi)^{\tau-t} \|\Theta - \bar{\Theta}\| \right) + \lambda_{\theta}(\xi) \|\Theta - \bar{\Theta}\| \right) + \Xi \|\Theta - \bar{\Theta}\| \tag{98}$$

$$= \left(\Xi + \lambda_{\mathbf{X}}(\xi)^{\tau} \left(1 + \frac{\lambda_{\theta}(\xi)}{L(\lambda_{\mathbf{X}}(\xi) - 1)} \right) \right) \|\Theta - \bar{\Theta}\|. \tag{99}$$

Finally, substituting the above in equation (85) gives us:

$$|\mathcal{L}(\Theta) - \mathcal{L}(\bar{\Theta})| \leq \frac{1}{n} \sum_{(X,y) \in S} \alpha \left(\Xi + \lambda_{\mathbf{X}}(\xi)^{\tau} \left(1 + \frac{\lambda_{\theta}(\xi)}{L(\lambda_{\mathbf{X}}(\xi) - 1)} \right) \right) \|\Theta - \bar{\Theta}\| \tag{100}$$

$$\leq \alpha \left(\Xi + \lambda_{\mathbf{X}}(\xi)^{\tau} \left(1 + \frac{\lambda_{\theta}(\xi)}{L(\lambda_{\mathbf{X}}(\xi) - 1)} \right) \right) \|\Theta - \bar{\Theta}\|. \tag{101}$$

This gives us equation (83) in the statement of the theorem. \square

D.4 Multi-headed Attention

As per Yun et al. [2020a, Section 2, equation 1], we can write multi-headed (self) attention h heads in our notation as:

$$\text{MHA}_{\{\mathbf{W}^{(i)}, \mathbf{V}^{(i)}, \mathbf{H}^{(i)}\}_{i \in \llbracket h \rrbracket}}(\mathbf{X}) = \sum_{i \in \llbracket h \rrbracket} \mathbf{H}^{(i)} \mathbf{A}_{\mathbf{W}^{(i)}, \mathbf{V}^{(i)}}(\mathbf{X}), \tag{102}$$

where $\mathbf{H}^{(i)} \in \mathbb{R}^{d \times d}$ are the head-aggregator matrices. Here we are assuming that each head is of size d , same as the d_{model} . This is for ease of exposition, as we can introduce a new variable for head size and get the same guarantees.

Now, for each of the heads $i \in \llbracket h \rrbracket$, let us assume the following (as in definition 1):

$$\|\mathbf{A}_{\mathbf{W}^{(i)}, \mathbf{V}^{(i)}}(\mathbf{X}) - \mathbf{A}_{\mathbf{W}^{(i)}, \mathbf{V}^{(i)}}(\bar{\mathbf{X}})\|_{2,1} \leq \lambda_X(\xi) \|\mathbf{X} - \bar{\mathbf{X}}\|_{2,1}, \tag{103}$$

$$\|\mathbf{A}_{\mathbf{W}^{(i)}, \mathbf{V}^{(i)}}(\mathbf{X}) - \mathbf{A}_{\bar{\mathbf{W}}^{(i)}, \mathbf{V}^{(i)}}(\mathbf{X})\|_{2,1} \leq \lambda_W(\xi) \|\mathbf{W} - \bar{\mathbf{W}}\|. \tag{104}$$

Then, we can show the following for multi-headed attention, assuming $\|\mathbf{H}^i\| \leq \Lambda$ for all $i \in \llbracket h \rrbracket$:

$$\|\text{MHA}_{\{\mathbf{W}^{(i)}, \mathbf{V}^{(i)}, \mathbf{H}^{(i)}\}_{i \in \llbracket h \rrbracket}}(\mathbf{X}) - \text{MHA}_{\{\mathbf{W}^{(i)}, \mathbf{V}^{(i)}, \mathbf{H}^{(i)}\}_{i \in \llbracket h \rrbracket}}(\bar{\mathbf{X}})\|_{2,1} \tag{105}$$

$$= \left\| \sum_{i=1}^h \mathbf{H}^{(i)} (\mathbf{A}_{\mathbf{W}^{(i)}, \mathbf{V}^{(i)}}(\mathbf{X}) - \mathbf{A}_{\mathbf{W}^{(i)}, \mathbf{V}^{(i)}}(\bar{\mathbf{X}})) \right\|_{2,1} \leq \sum_{i=1}^h \|\mathbf{H}^{(i)}\| \|\mathbf{A}_{\mathbf{W}^{(i)}, \mathbf{V}^{(i)}}(\mathbf{X}) - \mathbf{A}_{\mathbf{W}^{(i)}, \mathbf{V}^{(i)}}(\bar{\mathbf{X}})\|_{2,1} \tag{106}$$

$$\leq \Lambda h \lambda_X(\xi) \|\mathbf{X} - \bar{\mathbf{X}}\|_{2,1}. \tag{107}$$

Thus, the stability of multi-headed attention with respect to its input is preserved as with a single head, but with additional constant factors.

Furthermore, in terms of Lipschitz-ness with respect to its parameters, such as \mathbf{W} , we can see that

$$\|\text{MHA}_{\{\mathbf{W}^{(i)}, \mathbf{V}^{(i)}, \mathbf{H}^{(i)}\}_{i \in \llbracket h \rrbracket}}(\mathbf{X}) - \text{MHA}_{\{\bar{\mathbf{W}}^{(i)}, \mathbf{V}^{(i)}, \mathbf{H}^{(i)}\}_{i \in \llbracket h \rrbracket}}(\mathbf{X})\|_{2,1} \tag{108}$$

$$= \left\| \sum_{i=1}^h \mathbf{H}^{(i)} (\mathbf{A}_{\mathbf{W}^{(i)}, \mathbf{V}^{(i)}}(\mathbf{X}) - \mathbf{A}_{\bar{\mathbf{W}}^{(i)}, \mathbf{V}^{(i)}}(\mathbf{X})) \right\|_{2,1} \leq \sum_{i=1}^h \|\mathbf{H}^{(i)}\| \|\mathbf{A}_{\mathbf{W}^{(i)}, \mathbf{V}^{(i)}}(\mathbf{X}) - \mathbf{A}_{\bar{\mathbf{W}}^{(i)}, \mathbf{V}^{(i)}}(\mathbf{X})\|_{2,1} \tag{109}$$

$$\leq \Lambda \lambda_W(\xi) \sum_{i \in \llbracket h \rrbracket} \|\mathbf{W}^{(i)} - \bar{\mathbf{W}}^{(i)}\|, \quad (110)$$

where we utilize equation (104) for the $\mathbf{W}^{(i)}$ parameters for each of the heads. This shows us that we can establish results for multi-headed attention analogous to those we study for single head attention. The driving factors continue to be $\lambda_X(\xi)$ and $\lambda_W(\xi)$ which are tied to the properties of the masked softmax functions. However, both the terms get multiplicatively magnified with increasing number of heads, and thus any improvement in the stability of the masked softmax function will get more pronounced as the number of heads increase. This intuition is supported by our results in figure 6b.

E Role of Sparse Softmax: Technical Details

E.1 Standard Softmax based Attention

Lemma S2 (adapted from Li et al. [2023] Lemma B.1). *For any $\mathbf{z}, \bar{\mathbf{z}} \in \mathbb{R}^L$ with*

$$\max_{i,j \in \llbracket L \rrbracket} z_i - z_j \leq \delta, \quad \text{and} \quad \max_{i,j \in \llbracket L \rrbracket} \bar{z}_i - \bar{z}_j \leq \delta, \quad (111)$$

for a positive constant $\delta > 0$, we have the following:

$$\|\text{softmax}(\mathbf{z})\|_\infty \leq \frac{e^\delta}{L}, \quad \|\text{softmax}(\mathbf{z}) - \text{softmax}(\bar{\mathbf{z}})\|_1 \leq \frac{e^\delta}{L} \|\mathbf{z} - \bar{\mathbf{z}}\|_1. \quad (112)$$

Proof. For any $\mathbf{z} \in \mathbb{R}^L$, without loss of generality, let the first entry z_1 be the largest, and the second entry z_2 be the smallest. By equation (111), $z_1 - z_2 \leq \delta$. With $\mathbf{s} = \text{softmax}(\mathbf{z})$, the first entry s_1 will be the largest. Thus:

$$\|\text{softmax}(\mathbf{z})\|_\infty = s_1 = \frac{\exp(z_1)}{\exp(z_1) + \sum_{i=2}^L \exp(z_i)} \quad (113)$$

$$\leq \frac{\exp(z_1)}{\exp(z_1) + \sum_{i=2}^L \exp(z_2)} = \frac{\exp(z_1 - z_2)}{\exp(z_1 - z_2) + (L - 1)} \leq \frac{\exp(\delta)}{L}. \quad (114)$$

Now we can write $\text{softmax}(\mathbf{z}) - \text{softmax}(\bar{\mathbf{z}})$ as an aggregation of infinitesimal steps along the gradient of the softmax in the direction $\bar{\mathbf{z}} - \mathbf{z}$:

$$\text{softmax}(\mathbf{z}) - \text{softmax}(\bar{\mathbf{z}}) = \int_0^1 \nabla_\varepsilon \text{softmax}(\mathbf{z} + \varepsilon(\bar{\mathbf{z}} - \mathbf{z})) d\varepsilon \quad (115)$$

$$\|\text{softmax}(\mathbf{z}) - \text{softmax}(\bar{\mathbf{z}})\|_1 \leq \left\| \int_0^1 \nabla_\varepsilon \text{softmax}(\mathbf{z} + \varepsilon(\bar{\mathbf{z}} - \mathbf{z})) d\varepsilon \right\|_1 \quad (116)$$

$$\leq \int_0^1 \|\nabla_\varepsilon \text{softmax}(\mathbf{z} + \varepsilon(\bar{\mathbf{z}} - \mathbf{z}))\|_1 d\varepsilon. \quad (117)$$

Considering the $\|\nabla_\varepsilon \text{softmax}(\mathbf{z} + \varepsilon(\bar{\mathbf{z}} - \mathbf{z}))\|_1$ term, and denoting $\mathbf{z}(\varepsilon) = \mathbf{z} + \varepsilon(\bar{\mathbf{z}} - \mathbf{z})$ and $\mathbf{s}(\varepsilon) = \text{softmax}(\mathbf{z}(\varepsilon))$, we have

$$\|\nabla_\varepsilon \text{softmax}(\mathbf{z}(\varepsilon))\|_1 = \|[\text{diag}(\mathbf{s}(\varepsilon)) - \mathbf{s}(\varepsilon)\mathbf{s}(\varepsilon)^\top](\bar{\mathbf{z}} - \mathbf{z})\|_1 \quad (118)$$

$$= \sum_{i=1}^L \left| (s(\varepsilon)_i - s(\varepsilon)_i^2)(\bar{z}_i - z_i) - \sum_{j \in \llbracket L \rrbracket, j \neq i} s(\varepsilon)_i s(\varepsilon)_j (\bar{z}_j - z_j) \right| \quad (119)$$

$$\leq \sum_{i=1}^L |s(\varepsilon)_i (\bar{z}_i - z_i)|, \quad (120)$$

since all the $s(\varepsilon)_i, s(\varepsilon)_j \in [0, 1]$. Noting that $s(\varepsilon)_i \leq \|\text{softmax}(\mathbf{s}(\varepsilon))\|_\infty \leq \exp(\delta)/L$, we have

$$\|\nabla_\varepsilon \text{softmax}(\mathbf{z}(\varepsilon))\|_1 \leq \sum_{i=1}^L |(\exp(\delta)/L)(\bar{z}_i - z_i)| = \frac{\exp(\delta)}{L} \|\mathbf{z} - \bar{\mathbf{z}}\|_1. \quad (121)$$

Thus

$$\|\text{softmax}(\mathbf{z}) - \text{softmax}(\bar{\mathbf{z}})\|_1 \leq \int_0^1 \|\nabla_\varepsilon \text{softmax}(\mathbf{z} + \varepsilon(\bar{\mathbf{z}} - \mathbf{z}))\|_1 d\varepsilon \quad (122)$$

$$\leq \int_0^1 \frac{\exp(\delta)}{L} \|\mathbf{z} - \bar{\mathbf{z}}\|_1 d\varepsilon = \frac{\exp(\delta)}{L} \|\mathbf{z} - \bar{\mathbf{z}}\|_1, \quad (123)$$

thus giving us equation (112). \square

Theorem S3. Consider the self-attention operation $\mathbf{A} : \mathbb{R}^{d \times L} \rightarrow \mathbb{R}^{d \times L}$ with input \mathbf{X} of L token representations and parameters $\mathbf{W}, \mathbf{V} \in \mathbb{R}^{d \times d}$. Consider the following assumptions:

- (S1) The per-token Euclidean norms are bounded as $\|\mathbf{X}_{:i}\| \leq \Xi \forall i \in \llbracket L \rrbracket$, and the parameter norms are bounded at $\|\mathbf{W}\| \leq \Gamma$ and $\|\mathbf{V}\| \leq \Upsilon$.
- (S2) The per-query semantic dispersion (definition 2) is bounded by δ_s , that is:

$$\forall i \in \llbracket L \rrbracket, \max_{j, j' \in \llbracket L \rrbracket} (\mathbf{X}_{:j}^\top \mathbf{W} \mathbf{X}_{:i} - \mathbf{X}_{:j'}^\top \mathbf{W} \mathbf{X}_{:i}) \leq \delta_s. \quad (124)$$

Then the standard softmax is ξ_s -Lipschitz with $\xi_s = e^{\delta_s}/L$, and the standard attention is Lipschitz with respect to its input and parameters as following for any input pair $\mathbf{X}, \bar{\mathbf{X}} \in \mathbb{R}^{d \times L}$ with $\|\bar{\mathbf{X}}_{:i}\| \leq 1 \forall i \in \llbracket L \rrbracket$, and parameter pairs $\mathbf{W}, \bar{\mathbf{W}}, \mathbf{V}, \bar{\mathbf{V}} \in \mathbb{R}^{d \times d}$ with $\|\mathbf{W}\| \leq \Gamma, \|\bar{\mathbf{W}}\| \leq \Gamma$ and $\|\mathbf{V}\| \leq \Upsilon, \|\bar{\mathbf{V}}\| \leq \Upsilon$:

$$\|\mathbf{A}_{\mathbf{W}, \mathbf{V}}(\mathbf{X}) - \mathbf{A}_{\mathbf{W}, \mathbf{V}}(\bar{\mathbf{X}})\|_{2,1} \leq \xi_s \Upsilon L (2\Gamma \Xi^2 + 1) \|\mathbf{X} - \bar{\mathbf{X}}\|_{2,1}, \quad (125)$$

$$\|\mathbf{A}_{\mathbf{W}, \mathbf{V}}(\mathbf{X}) - \mathbf{A}_{\bar{\mathbf{W}}, \mathbf{V}}(\mathbf{X})\|_{2,1} \leq \xi_s \Upsilon L^2 \Xi^3 \|\mathbf{W} - \bar{\mathbf{W}}\|, \quad (126)$$

$$\|\mathbf{A}_{\mathbf{W}, \mathbf{V}}(\mathbf{X}) - \mathbf{A}_{\mathbf{W}, \bar{\mathbf{V}}}(\mathbf{X})\|_{2,1} \leq L \Xi \|\mathbf{V} - \bar{\mathbf{V}}\|. \quad (127)$$

Proof. Now, given the upper bound on the per-query semantic dispersion δ_s in equation (124), we can apply Lemma S2 with $\delta = \delta_s$, giving us a ξ_s -Lipschitz softmax with $\xi_s = \exp(\delta_s)/L$.

Next, we can show equation (125) utilizing lemma S2 and adapting Li et al. [2023, Lemma B.2].

$$\|\mathbf{A}_{\mathbf{W}, \mathbf{V}}(\mathbf{X}) - \mathbf{A}_{\mathbf{W}, \mathbf{V}}(\bar{\mathbf{X}})\|_{2,1} = \|\mathbf{V} \mathbf{X} \text{softmax}(\mathbf{X}^\top \mathbf{W} \mathbf{X}) - \mathbf{V} \bar{\mathbf{X}} \text{softmax}(\bar{\mathbf{X}}^\top \mathbf{W} \bar{\mathbf{X}})\|_{2,1} \quad (128)$$

$$\leq \|\mathbf{V} \mathbf{X} \text{softmax}(\mathbf{X}^\top \mathbf{W} \mathbf{X}) - \mathbf{V} \bar{\mathbf{X}} \text{softmax}(\mathbf{X}^\top \mathbf{W} \mathbf{X})\|_{2,1} \quad (A_1)$$

$$+ \|\mathbf{V} \bar{\mathbf{X}} \text{softmax}(\mathbf{X}^\top \mathbf{W} \mathbf{X}) - \mathbf{V} \bar{\mathbf{X}} \text{softmax}(\mathbf{X}^\top \mathbf{W} \bar{\mathbf{X}})\|_{2,1} \quad (A_2)$$

$$+ \|\mathbf{V} \bar{\mathbf{X}} \text{softmax}(\mathbf{X}^\top \mathbf{W} \bar{\mathbf{X}}) - \mathbf{V} \bar{\mathbf{X}} \text{softmax}(\bar{\mathbf{X}}^\top \mathbf{W} \bar{\mathbf{X}})\|_{2,1}. \quad (A_3)$$

We will handle each of the equation (A₁), equation (A₂), and equation (A₃) individually. We will use a_{ji} to denote the j -th entry of $\text{softmax}(\mathbf{X}^\top \mathbf{W} \mathbf{X}_{:i})$, and a_{ji}, \bar{a}_{ji} to denote the j -th entry of $\text{softmax}(\mathbf{X}^\top \mathbf{W} \bar{\mathbf{X}}_{:i})$ and $\text{softmax}(\bar{\mathbf{X}}^\top \mathbf{W} \bar{\mathbf{X}}_{:i})$ respectively. Note that, by lemma S2 and equation (124), all $a_{ji}, \bar{a}_{ji}, \bar{a}_{ji} \leq \xi_s = \exp(\delta_s)/L$.

$$(A_1) = \|\mathbf{V}(\mathbf{X} - \bar{\mathbf{X}}) \text{softmax}(\mathbf{X}^\top \mathbf{W} \mathbf{X})\|_{2,1} = \sum_{i=1}^L \|\mathbf{V}(\mathbf{X} - \bar{\mathbf{X}}) \text{softmax}(\mathbf{X}^\top \mathbf{W} \mathbf{X}_{:i})\| \quad (129)$$

$$= \sum_{i=1}^L \|\mathbf{V} \sum_{j=1}^L (\mathbf{X}_{:j} - \bar{\mathbf{X}}_{:j}) a_{ji}\| \leq \|\mathbf{V}\| \sum_{i=1}^L \left\| \sum_{j=1}^L (\mathbf{X}_{:j} - \bar{\mathbf{X}}_{:j}) a_{ji} \right\| \leq \|\mathbf{V}\| \sum_{i=1}^L \sum_{j=1}^L \|\mathbf{X}_{:j} - \bar{\mathbf{X}}_{:j}\| |a_{ji}| \quad (130)$$

$$\leq \Upsilon \xi_s \sum_{i=1}^L \sum_{j=1}^L \|\mathbf{X}_{:j} - \bar{\mathbf{X}}_{:j}\| = \Upsilon \xi_s \sum_{i=1}^L \|\mathbf{X} - \bar{\mathbf{X}}\|_{2,1} = \Upsilon \xi_s L \|\mathbf{X} - \bar{\mathbf{X}}\|_{2,1}, \quad (131)$$

where we utilize the fact that $\|\mathbf{V}\| \leq \Upsilon$.

$$(A_2) = \|\mathbf{V}\bar{\mathbf{X}} [\text{softmax}(\mathbf{X}^\top \mathbf{W}\mathbf{X}) - \text{softmax}(\mathbf{X}^\top \mathbf{W}\bar{\mathbf{X}})]\|_{2,1} \quad (132)$$

$$= \sum_{i=1}^L \|\mathbf{V}\bar{\mathbf{X}} [\text{softmax}(\mathbf{X}^\top \mathbf{W}\mathbf{X}_{:i}) - \text{softmax}(\mathbf{X}^\top \mathbf{W}\bar{\mathbf{X}}_{:i})]\| = \sum_{i=1}^L \|\mathbf{V} \sum_{j=1}^L \bar{\mathbf{X}}_{:j} (a_{ji} - \bar{a}_{ji})\| \quad (133)$$

$$\leq \|\mathbf{V}\| \sum_{i=1}^L \sum_{j=1}^L \|\bar{\mathbf{X}}_{:j}\| |a_{ji} - \bar{a}_{ji}| \leq \Upsilon \Xi \sum_{i=1}^L \sum_{j=1}^L |a_{ji} - \bar{a}_{ji}| \quad (134)$$

$$= \Upsilon \Xi \sum_{i=1}^L \|\text{softmax}(\mathbf{X}^\top \mathbf{W}\mathbf{X}_{:i}) - \text{softmax}(\mathbf{X}^\top \mathbf{W}\bar{\mathbf{X}}_{:i})\|_1 \quad (135)$$

$$\leq \Upsilon \Xi \xi_s \sum_{i=1}^L \|\mathbf{X}^\top \mathbf{W}(\mathbf{X}_{:i} - \bar{\mathbf{X}}_{:i})\|_1 = \Upsilon \Xi \xi_s \sum_{i=1}^L \sum_{j=1}^L |\mathbf{X}_{:j}^\top \mathbf{W}(\mathbf{X}_{:i} - \bar{\mathbf{X}}_{:i})| \quad (136)$$

$$\leq \Upsilon \Xi \xi_s \sum_{i=1}^L \sum_{j=1}^L \|\mathbf{X}_{:j}^\top \mathbf{W}\| \|\mathbf{X}_{:i} - \bar{\mathbf{X}}_{:i}\| = \Upsilon \Xi \xi_s \sum_{i=1}^L \|\mathbf{X}_{:i} - \bar{\mathbf{X}}_{:i}\| \left(\sum_{j=1}^L \|\mathbf{X}_{:j}^\top \mathbf{W}\| \right) \quad (137)$$

$$\leq \Upsilon \Xi \xi_s \sum_{i=1}^L \|\mathbf{X}_{:i} - \bar{\mathbf{X}}_{:i}\| \|\mathbf{W}\| \left(\sum_{j=1}^L \|\mathbf{X}_{:j}\| \right) \leq \Upsilon \Xi^2 \xi_s \Gamma L \sum_{i=1}^L \|\mathbf{X}_{:i} - \bar{\mathbf{X}}_{:i}\| = \Upsilon \Xi^2 \xi_s \Gamma L \|\mathbf{X} - \bar{\mathbf{X}}\|_{2,1}, \quad (138)$$

utilizing equation (112) and the assumption that $\|\mathbf{W}\| \leq \Gamma$ and $\|\mathbf{X}_{:i}\| \leq \Xi$ for all $i \in [L]$.

$$(A_3) = \|\mathbf{V}\bar{\mathbf{X}} [\text{softmax}(\mathbf{X}^\top \mathbf{W}\bar{\mathbf{X}}) - \text{softmax}(\bar{\mathbf{X}}^\top \mathbf{W}\bar{\mathbf{X}})]\|_{2,1} \quad (139)$$

$$= \sum_{i=1}^L \|\mathbf{V}\bar{\mathbf{X}} [\text{softmax}(\mathbf{X}^\top \mathbf{W}\bar{\mathbf{X}}_{:i}) - \text{softmax}(\bar{\mathbf{X}}^\top \mathbf{W}\bar{\mathbf{X}}_{:i})]\| = \sum_{i=1}^L \|\mathbf{V} \sum_{j=1}^L \bar{\mathbf{X}}_{:j} (a_{ji} - \bar{a}_{ji})\| \quad (140)$$

$$\leq \|\mathbf{V}\| \sum_{i=1}^L \sum_{j=1}^L \|\bar{\mathbf{X}}_{:j}\| |a_{ji} - \bar{a}_{ji}| \leq \Upsilon \Xi \sum_{i=1}^L \sum_{j=1}^L |a_{ji} - \bar{a}_{ji}| \quad (141)$$

$$= \Upsilon \Xi \sum_{i=1}^L \|\text{softmax}(\mathbf{X}^\top \mathbf{W}\bar{\mathbf{X}}_{:i}) - \text{softmax}(\bar{\mathbf{X}}^\top \mathbf{W}\bar{\mathbf{X}}_{:i})\|_1 \quad (142)$$

$$\leq \Upsilon \Xi \xi_s \sum_{i=1}^L \|\mathbf{X}^\top \mathbf{W}\bar{\mathbf{X}}_{:i} - \bar{\mathbf{X}}^\top \mathbf{W}\bar{\mathbf{X}}_{:i}\|_1 = \Upsilon \Xi \xi_s \sum_{i=1}^L \sum_{j=1}^L |(\mathbf{X}_{:j} - \bar{\mathbf{X}}_{:j})^\top \mathbf{W}\bar{\mathbf{X}}_{:i}| \quad (143)$$

$$\leq \Upsilon \Xi \xi_s \sum_{i=1}^L \sum_{j=1}^L \|\mathbf{X}_{:j} - \bar{\mathbf{X}}_{:j}\| \|\mathbf{W}\bar{\mathbf{X}}_{:i}\| = \Upsilon \Xi \xi_s \sum_{i=1}^L \|\mathbf{W}\bar{\mathbf{X}}_{:i}\| \left(\sum_{j=1}^L \|\mathbf{X}_{:j} - \bar{\mathbf{X}}_{:j}\| \right) \quad (144)$$

$$= \Upsilon \Xi \xi_s \sum_{i=1}^L \|\mathbf{W}\bar{\mathbf{X}}_{:i}\| \|\mathbf{X} - \bar{\mathbf{X}}\|_{2,1} \leq \Upsilon \Xi \xi_s \|\mathbf{W}\| \|\mathbf{X} - \bar{\mathbf{X}}\|_{2,1} \sum_{i=1}^L \|\bar{\mathbf{X}}_{:i}\| \leq \Upsilon \Xi^2 \xi_s \Gamma L \|\mathbf{X} - \bar{\mathbf{X}}\|_{2,1} \quad (145)$$

Combining the individual bounds on equation (A₁), equation (A₂), and equation (A₃), we have the following bound as per equation (125):

$$\|\mathbf{A}_{\mathbf{W},\mathbf{V}}(\mathbf{X}) - \mathbf{A}_{\mathbf{W},\mathbf{V}}(\bar{\mathbf{X}})\|_{2,1} \leq \xi_s \Upsilon L (2\Gamma \Xi^2 + 1) \|\mathbf{X} - \bar{\mathbf{X}}\|_{2,1}, \quad (146)$$

For equation (126), we note the following:

$$\|\mathbf{A}_{\mathbf{W},\mathbf{V}}(\mathbf{X}) - \mathbf{A}_{\bar{\mathbf{W}},\mathbf{V}}(\mathbf{X})\|_{2,1} = \|\mathbf{V}\mathbf{X} \text{softmax}(\mathbf{X}^\top \mathbf{W}\mathbf{X}) - \mathbf{V}\mathbf{X} \text{softmax}(\mathbf{X}^\top \bar{\mathbf{W}}\mathbf{X})\|_{2,1} \quad (147)$$

$$= \sum_{i=1}^L \|\mathbf{V}\mathbf{X} (\text{softmax}(\mathbf{X}^\top \mathbf{W}\mathbf{X}_{:i}) - \text{softmax}(\mathbf{X}^\top \bar{\mathbf{W}}\mathbf{X}_{:i}))\| \quad (148)$$

$$\leq \|\mathbf{V}\| \sum_{i=1}^L \|\mathbf{X}(\text{softmax}(\mathbf{X}^\top \mathbf{W}\mathbf{X}_{:i}) - \text{softmax}(\mathbf{X}^\top \bar{\mathbf{W}}\mathbf{X}_{:i}))\|. \quad (149)$$

Denoting a_{ji} as the j -th entry of $\text{softmax}(\mathbf{X}^\top \mathbf{W}\mathbf{X}_{:i})$ and \bar{a}_{ji} as the j -th entry of $\text{softmax}(\mathbf{X}^\top \bar{\mathbf{W}}\mathbf{X}_{:i})$, and using the assumption that $\|\mathbf{V}\| \leq \Upsilon$, we have

$$\|\mathbf{A}_{\mathbf{W},\mathbf{V}}(\mathbf{X}) - \mathbf{A}_{\bar{\mathbf{W}},\mathbf{V}}(\mathbf{X})\|_{2,1} \leq \Upsilon \sum_{i=1}^L \left\| \sum_{j=1}^L (a_{ji} - \bar{a}_{ji}) \mathbf{X}_{:j} \right\| \leq \Upsilon \sum_{i=1}^L \sum_{j=1}^L \|(a_{ji} - \bar{a}_{ji}) \mathbf{X}_{:j}\| \quad (150)$$

$$\leq \Upsilon \sum_{i=1}^L \sum_{j=1}^L |a_{ji} - \bar{a}_{ji}| \|\mathbf{X}_{:j}\| \quad (151)$$

$$\leq \Upsilon \Xi \sum_{i=1}^L \|\text{softmax}(\mathbf{X}^\top \mathbf{W}\mathbf{X}_{:i}) - \text{softmax}(\mathbf{X}^\top \bar{\mathbf{W}}\mathbf{X}_{:i})\|_1, \quad (152)$$

where we use the assumption that $\|\mathbf{X}_{:j}\| \leq \Xi$. Now, utilizing lemma S2, we have

$$\|\mathbf{A}_{\mathbf{W},\mathbf{V}}(\mathbf{X}) - \mathbf{A}_{\bar{\mathbf{W}},\mathbf{V}}(\mathbf{X})\|_{2,1} \leq \Upsilon \Xi \sum_{i=1}^L \xi_s \|\mathbf{X}^\top \mathbf{W}\mathbf{X}_{:i} - \mathbf{X}^\top \bar{\mathbf{W}}\mathbf{X}_{:i}\|_1 \quad (153)$$

$$= \Upsilon \Xi \xi_s \sum_{i=1}^L \sum_{j=1}^L |\mathbf{X}_{:j}^\top \mathbf{W}\mathbf{X}_{:i} - \mathbf{X}_{:j}^\top \bar{\mathbf{W}}\mathbf{X}_{:i}| \quad (154)$$

$$\leq \Upsilon \Xi \xi_s \sum_{i=1}^L \sum_{j=1}^L \|\mathbf{X}_{:j}^\top \mathbf{W} - \mathbf{X}_{:j}^\top \bar{\mathbf{W}}\| \|\mathbf{X}_{:i}\| \leq \Upsilon \Xi^2 \xi_s \sum_{i=1}^L \sum_{j=1}^L \|\mathbf{X}_{:j}^\top \mathbf{W} - \mathbf{X}_{:j}^\top \bar{\mathbf{W}}\| \quad (155)$$

$$\leq \Upsilon \Xi^2 \xi_s \sum_{i=1}^L \sum_{j=1}^L \|\mathbf{X}_{:j}\| \|\mathbf{W} - \bar{\mathbf{W}}\| \leq \xi_s L^2 \Upsilon \Xi^3 \|\mathbf{W} - \bar{\mathbf{W}}\|, \quad (156)$$

where we utilize $\|\mathbf{X}_{:j}\| \leq \Xi$ twice, thus giving us equation (126).

For equation (127), we note that

$$\|\mathbf{A}_{\mathbf{W},\mathbf{V}}(\mathbf{X}) - \mathbf{A}_{\bar{\mathbf{W}},\bar{\mathbf{V}}}(\mathbf{X})\|_{2,1} = \|\mathbf{V}\mathbf{X}\text{softmax}(\mathbf{X}^\top \mathbf{W}\mathbf{X}) - \bar{\mathbf{V}}\mathbf{X}\text{softmax}(\mathbf{X}^\top \mathbf{W}\mathbf{X})\|_{2,1} \quad (157)$$

$$= \sum_{i=1}^L \|(\mathbf{V} - \bar{\mathbf{V}})\mathbf{X}\text{softmax}(\mathbf{X}^\top \mathbf{W}\mathbf{X}_{:i})\| \quad (158)$$

$$\leq \|\mathbf{V} - \bar{\mathbf{V}}\| \sum_{i=1}^L \|\mathbf{X}\text{softmax}(\mathbf{X}^\top \mathbf{W}\mathbf{X}_{:i})\|. \quad (159)$$

Noting the fact that $\mathbf{X}\text{softmax}(\mathbf{X}^\top \mathbf{W}\mathbf{X}_{:i})$ is a convex sum of the columns of \mathbf{X} , its maximum Euclidean norm is bounded by maximum Euclidean norm of the individual columns, $\max_j \|\mathbf{X}_{:j}\|$, which itself is bounded from above by Ξ . This simplifies the right-hand-side above to $L\Xi\|\mathbf{V} - \bar{\mathbf{V}}\|$, giving us equation (127). \square

Remark S1. For the Lipschitz constants in definition 1, $\lambda_X(\xi_s) = \xi_s L \Upsilon (2\Gamma \Xi^2 + 1) = \exp(\delta_s) \Upsilon (2\Gamma \Xi^2 + 1)$, $\lambda_W(\xi_s) = \xi_s \Upsilon L^2 \Xi^3 = \exp(\delta_s) \Upsilon L \Xi^3$ and $\lambda_V = L\Xi$ with $\xi_s = \exp(\delta_s)/L$ and δ_s defined in equation (124). Under the assumption (S2) of theorem S3, $\delta_s \leq 2\Gamma \Xi^2$.

E.2 Regular Input-agnostic Sparse Softmax based Attention

Lemma S3. Given a mask $\mathbf{b} \in \{0, 1\}^L$ with k nonzeros, define the i -th entry of the masked softmax $\text{softmax}_{\mathbf{b}} : \mathbb{R}^L \rightarrow S_L$ for an input $\mathbf{z} \in \mathbb{R}^d$ as:

$$\text{softmax}_{\mathbf{b}}(\mathbf{z})_i = \frac{\exp(z_i) b_i}{\sum_{j=1}^L \exp(z_j) b_j}. \quad (160)$$

Now, for any $\mathbf{z}, \bar{\mathbf{z}} \in \mathbb{R}^L$ with

$$\max_{i,j \in \llbracket L \rrbracket: b_i=b_j=1} z_i - z_j \leq \delta, \quad \text{and} \quad \max_{i,j \in \llbracket L \rrbracket: b_i=b_j=1} \bar{z}_i - \bar{z}_j \leq \delta, \quad (161)$$

for a constant $\delta > 0$, we have the following:

$$\|\text{softmax}_{\mathbf{b}}(\mathbf{z})\|_{\infty} \leq \frac{e^{\delta}}{k}, \quad \|\text{softmax}_{\mathbf{b}}(\mathbf{z}) - \text{softmax}_{\mathbf{b}}(\bar{\mathbf{z}})\|_1 \leq \frac{e^{\delta}}{k} \|\mathbf{b} \odot (\mathbf{z} - \bar{\mathbf{z}})\|_1 \leq \frac{e^{\delta}}{k} \|\mathbf{z} - \bar{\mathbf{z}}\|_1, \quad (162)$$

where \odot denotes the elementwise multiplication of two vectors.

Proof. For any $\mathbf{z}, \bar{\mathbf{z}} \in \mathbb{R}^L$ and a fixed mask $\mathbf{b} \in \{0, 1\}^L$ with k nonzeros, let $\mathbf{z}[\mathbf{b}], \bar{\mathbf{z}}[\mathbf{b}] \in \mathbb{R}^k$ denote the k -dimensional vectors corresponding to the unmasked entries of $\mathbf{z}, \bar{\mathbf{z}}$. Then, utilizing lemma S2 for a softmax operation over a k -length vector with equation (161), we have the following:

$$\|\text{softmax}_{\mathbf{b}}(\mathbf{z})\|_{\infty} = \|\text{softmax}(\mathbf{z}[\mathbf{b}])\|_{\infty} \leq \frac{\exp(\delta)}{k}. \quad (163)$$

Furthermore,

$$\|\text{softmax}_{\mathbf{b}}(\mathbf{z}) - \text{softmax}_{\mathbf{b}}(\bar{\mathbf{z}})\|_1 = \|\text{softmax}(\mathbf{z}[\mathbf{b}]) - \text{softmax}(\bar{\mathbf{z}}[\mathbf{b}])\|_1 \quad (164)$$

$$\leq \frac{\exp(\delta)}{k} \|\mathbf{z}[\mathbf{b}] - \bar{\mathbf{z}}[\mathbf{b}]\|_1 \quad (165)$$

$$= \frac{\exp(\delta)}{k} \|\mathbf{b} \odot (\mathbf{z} - \bar{\mathbf{z}})\|_1 \quad (166)$$

$$\leq \frac{\exp(\delta)}{k} \|\mathbf{z} - \bar{\mathbf{z}}\|_1, \quad (167)$$

where the last inequality is from the fact that ℓ_1 distance between masked vectors is smaller than the ℓ_1 distance over the full vectors. \square

Theorem S4. Consider the self-attention operation $\mathbf{A} : \mathbb{R}^{d \times L} \rightarrow \mathbb{R}^{d \times L}$ with input \mathbf{X} of L token representations and parameters $\mathbf{W}, \mathbf{V} \in \mathbb{R}^{d \times d}$ utilizing a k -regular input sparse agnostic masking function $m : \mathbb{R}^{L \times L} \rightarrow \{0, 1\}^{L \times L}$ where $m(\mathbf{D}) = \mathbf{M}\mathbf{V}\mathbf{D} \in \mathbb{R}^{L \times L}$. Consider the following assumptions:

(R1) The per-token Euclidean norms are bounded as $\|\mathbf{X}_{:i}\| \leq \Xi \forall i \in \llbracket L \rrbracket$, and the parameter norms are bounded at $\|\mathbf{W}\| \leq \Gamma$ and $\|\mathbf{V}\| \leq \Upsilon$.

(R2) The per-query semantic dispersion (definition 2) is bounded by δ_r , that is:

$$\forall i \in \llbracket L \rrbracket, \quad \max_{j,j' \in \llbracket L \rrbracket, M_{ji}=M_{j'i}=1} (\mathbf{X}_{:j}^{\top} \mathbf{W} \mathbf{X}_{:i} - \mathbf{X}_{:j'}^{\top} \mathbf{W} \mathbf{X}_{:i}) \leq \delta_r. \quad (168)$$

Then the masked softmax is ξ_r -Lipschitz with $\xi_r = e^{\delta_r}/k$, and the masked attention is Lipschitz with respect to its input and parameters as following for any input pair $\mathbf{X}, \bar{\mathbf{X}} \in \mathbb{R}^{d \times L}$ with $\|\bar{\mathbf{X}}_{:i}\| \leq 1 \forall i \in \llbracket L \rrbracket$, and parameter pairs $\mathbf{W}, \bar{\mathbf{W}}, \mathbf{V}, \bar{\mathbf{V}} \in \mathbb{R}^{d \times d}$ with $\|\mathbf{W}\| \leq \Gamma, \|\bar{\mathbf{W}}\| \leq \Gamma$ and $\|\mathbf{V}\| \leq \Upsilon, \|\bar{\mathbf{V}}\| \leq \Upsilon$:

$$\|\mathbf{A}_{\mathbf{W}, \mathbf{V}}(\mathbf{X}) - \mathbf{A}_{\mathbf{W}, \mathbf{V}}(\bar{\mathbf{X}})\|_{2,1} \leq \xi_r \Upsilon k (2\Gamma \Xi^2 + 1) \|\mathbf{X} - \bar{\mathbf{X}}\|_{2,1}, \quad (169)$$

$$\|\mathbf{A}_{\mathbf{W}, \mathbf{V}}(\mathbf{X}) - \mathbf{A}_{\bar{\mathbf{W}}, \mathbf{V}}(\mathbf{X})\|_{2,1} \leq \xi_r \Upsilon L k \Xi^3 \|\mathbf{W} - \bar{\mathbf{W}}\|, \quad (170)$$

$$\|\mathbf{A}_{\mathbf{W}, \mathbf{V}}(\mathbf{X}) - \mathbf{A}_{\mathbf{W}, \bar{\mathbf{V}}}(\mathbf{X})\|_{2,1} \leq L \Xi \|\mathbf{V} - \bar{\mathbf{V}}\|. \quad (171)$$

Proof. Now, given the upper bound on the per-query semantic dispersion δ_r in equation (168), we can apply Lemma S3 with $\delta = \delta_r$, giving us a ξ_r -Lipschitz softmax with $\xi_r = \exp(\delta_r)/k$.

Note that, given a k -regular input agnostic masking function m and the corresponding mask matrix \mathbf{M} , we know that, for any column $\mathbf{M}_{:i}, i \in \llbracket L \rrbracket, \sum_{j=1}^L M_{ji} = k$, and for any row $\mathbf{M}_{i,:}, i \in \llbracket L \rrbracket, \sum_{j=1}^L M_{ij} = k -$ the mask matrix has k nonzeros in each row and each column. We denote the masked softmax with a mask

matrix \mathbf{M} of a dot-product matrix $\mathbf{D} \in \mathbb{R}^{L \times L}$ as $\text{softmax}_{\mathbf{M}}(\mathbf{D})$, defined as the columnwise masked softmax, which itself is denoted as $\text{softmax}_{\mathbf{M},i}(\mathbf{D}:i)$ and defined in equation (160).

For equation (169), we proceed as follows:

$$\|\mathbf{A}_{\mathbf{W},\mathbf{V}}(\mathbf{X}) - \mathbf{A}_{\mathbf{W},\mathbf{V}}(\bar{\mathbf{X}})\|_{2,1} = \|\mathbf{V}\mathbf{X}\text{softmax}_{\mathbf{M}}(\mathbf{X}^{\top}\mathbf{W}\mathbf{X}) - \mathbf{V}\bar{\mathbf{X}}\text{softmax}_{\mathbf{M}}(\bar{\mathbf{X}}^{\top}\mathbf{W}\bar{\mathbf{X}})\|_{2,1} \quad (172)$$

$$\leq \|\mathbf{V}\mathbf{X}\text{softmax}_{\mathbf{M}}(\mathbf{X}^{\top}\mathbf{W}\mathbf{X}) - \mathbf{V}\bar{\mathbf{X}}\text{softmax}_{\mathbf{M}}(\mathbf{X}^{\top}\mathbf{W}\mathbf{X})\|_{2,1} \quad (B_1)$$

$$+ \|\mathbf{V}\bar{\mathbf{X}}\text{softmax}_{\mathbf{M}}(\mathbf{X}^{\top}\mathbf{W}\mathbf{X}) - \mathbf{V}\bar{\mathbf{X}}\text{softmax}_{\mathbf{M}}(\mathbf{X}^{\top}\mathbf{W}\bar{\mathbf{X}})\|_{2,1} \quad (B_2)$$

$$+ \|\mathbf{V}\bar{\mathbf{X}}\text{softmax}_{\mathbf{M}}(\mathbf{X}^{\top}\mathbf{W}\bar{\mathbf{X}}) - \mathbf{V}\bar{\mathbf{X}}\text{softmax}_{\mathbf{M}}(\bar{\mathbf{X}}^{\top}\mathbf{W}\bar{\mathbf{X}})\|_{2,1}. \quad (B_3)$$

We will handle each of the equation (B₁), equation (B₂), and equation (B₃) individually. We will use a_{ji} to denote the j -th entry of masked $\text{softmax}_{\mathbf{M},i}(\mathbf{X}^{\top}\mathbf{W}\mathbf{X}:i)$, and a_{ji} , \bar{a}_{ji} to denote the j -th entry of $\text{softmax}_{\mathbf{M},i}(\mathbf{X}^{\top}\mathbf{W}\bar{\mathbf{X}}:i)$ and $\text{softmax}_{\mathbf{M},i}(\bar{\mathbf{X}}^{\top}\mathbf{W}\bar{\mathbf{X}}:i)$ respectively. Note that, by lemma S3 and equation (168), all $a_{ji}, \bar{a}_{ji}, a_{ji}, \bar{a}_{ji} \leq \xi_r = \exp(\delta_r)/k$.

$$(B_1) = \|\mathbf{V}(\mathbf{X} - \bar{\mathbf{X}})\text{softmax}_{\mathbf{M}}(\mathbf{X}^{\top}\mathbf{W}\mathbf{X})\|_{2,1} = \sum_{i=1}^L \|\mathbf{V}(\mathbf{X} - \bar{\mathbf{X}})\text{softmax}_{\mathbf{M},i}(\mathbf{X}^{\top}\mathbf{W}\mathbf{X}:i)\| \quad (173)$$

$$= \sum_{i=1}^L \|\mathbf{V} \sum_{j=1, M_{ji}=1}^L (\mathbf{X}_{:j} - \bar{\mathbf{X}}_{:j})a_{ji}\| \leq \|\mathbf{V}\| \sum_{i=1}^L \left\| \sum_{j=1, M_{ji}=1}^L (\mathbf{X}_{:j} - \bar{\mathbf{X}}_{:j})a_{ji} \right\| \quad (174)$$

$$\leq \|\mathbf{V}\| \sum_{i=1}^L \sum_{j=1, M_{ji}=1}^L \|\mathbf{X}_{:j} - \bar{\mathbf{X}}_{:j}\| |a_{ji}| \leq \Upsilon \xi_r \sum_{i=1}^L \sum_{j=1, M_{ji}=1}^L \|\mathbf{X}_{:j} - \bar{\mathbf{X}}_{:j}\| \quad (175)$$

$$= \Upsilon \xi_r \sum_{i=1}^L \sum_{j=1}^L \mathbb{I}(M_{ji} = 1) \|\mathbf{X}_{:j} - \bar{\mathbf{X}}_{:j}\| = \Upsilon \xi_r \sum_{j=1}^L \sum_{i=1}^L \mathbb{I}(M_{ji} = 1) \|\mathbf{X}_{:j} - \bar{\mathbf{X}}_{:j}\| \quad (176)$$

$$= \Upsilon \xi_r \sum_{j=1}^L \|\mathbf{X}_{:j} - \bar{\mathbf{X}}_{:j}\| \left(\sum_{i=1}^L \mathbb{I}(M_{ji} = 1) \right) = \Upsilon \xi_r \sum_{j=1}^L \|\mathbf{X}_{:j} - \bar{\mathbf{X}}_{:j}\| k = \Upsilon \xi_r k \|\mathbf{X} - \bar{\mathbf{X}}\|_{2,1} \quad (177)$$

where we utilize the fact that $\|\mathbf{V}\| \leq \Upsilon$, and the row sum of the mask matrix is exactly equal to k .

$$(B_2) = \|\mathbf{V}\bar{\mathbf{X}} [\text{softmax}_{\mathbf{M}}(\mathbf{X}^{\top}\mathbf{W}\mathbf{X}) - \text{softmax}_{\mathbf{M}}(\mathbf{X}^{\top}\mathbf{W}\bar{\mathbf{X}})]\|_{2,1} \quad (178)$$

$$= \sum_{i=1}^L \|\mathbf{V}\bar{\mathbf{X}} [\text{softmax}_{\mathbf{M},i}(\mathbf{X}^{\top}\mathbf{W}\mathbf{X}:i) - \text{softmax}_{\mathbf{M},i}(\mathbf{X}^{\top}\mathbf{W}\bar{\mathbf{X}}:i)]\| \quad (179)$$

$$= \sum_{i=1}^L \|\mathbf{V} \sum_{j=1, M_{ji}=1}^L \bar{\mathbf{X}}_{:j} (a_{ji} - \bar{a}_{ji})\| \leq \|\mathbf{V}\| \sum_{i=1}^L \sum_{j=1, M_{ji}=1}^L \|\bar{\mathbf{X}}_{:j}\| |a_{ji} - \bar{a}_{ji}| \quad (180)$$

$$\leq \Upsilon \Xi \sum_{i=1}^L \sum_{j=1, M_{ji}=1}^L |a_{ji} - \bar{a}_{ji}| = \Upsilon \Xi \sum_{i=1}^L \|\text{softmax}_{\mathbf{M},i}(\mathbf{X}^{\top}\mathbf{W}\mathbf{X}:i) - \text{softmax}_{\mathbf{M},i}(\mathbf{X}^{\top}\mathbf{W}\bar{\mathbf{X}}:i)\|_1 \quad (181)$$

$$\leq \Upsilon \Xi \xi_r \sum_{i=1}^L \|\mathbf{M}_{:i} \odot \mathbf{X}^{\top}\mathbf{W}(\mathbf{X}_{:i} - \bar{\mathbf{X}}_{:i})\|_1 = \Upsilon \Xi \xi_r \sum_{i=1}^L \sum_{j=1, M_{ji}=1}^L |\mathbf{X}_{:j}^{\top}\mathbf{W}(\mathbf{X}_{:i} - \bar{\mathbf{X}}_{:i})| \quad (182)$$

$$\leq \Upsilon \Xi \xi_r \sum_{i=1}^L \sum_{j=1, M_{ji}=1}^L \|\mathbf{X}_{:j}^{\top}\mathbf{W}\| \|\mathbf{X}_{:i} - \bar{\mathbf{X}}_{:i}\| = \Upsilon \Xi \xi_r \sum_{i=1}^L \|\mathbf{X}_{:i} - \bar{\mathbf{X}}_{:i}\| \left(\sum_{j=1, M_{ji}=1}^L \|\mathbf{X}_{:j}^{\top}\mathbf{W}\| \right) \quad (183)$$

$$\leq \Upsilon \Xi \xi_r \sum_{i=1}^L \|\mathbf{X}_{:i} - \bar{\mathbf{X}}_{:i}\| \|\mathbf{W}\| \left(\sum_{j=1, M_{ji}=1}^L \|\mathbf{X}_{:j}\| \right) \leq \Upsilon \Xi^2 k \xi_r \Gamma \sum_{i=1}^L \|\mathbf{X}_{:i} - \bar{\mathbf{X}}_{:i}\| = \Upsilon \Xi^2 \xi_r \Gamma k \|\mathbf{X} - \bar{\mathbf{X}}\|_{2,1}, \quad (184)$$

utilizing equation (162), the assumption that $\|\mathbf{W}\| \leq \Gamma$, $\|\mathbf{X}_{:i}\| \leq \Xi$ for all $i \in \llbracket L \rrbracket$, and that the column sum of \mathbf{M} is k .

$$(B_3) = \|\mathbf{V}\bar{\mathbf{X}} [\text{softmax}_{\mathbf{M}}(\mathbf{X}^\top \mathbf{W}\bar{\mathbf{X}}) - \text{softmax}_{\mathbf{M}}(\bar{\mathbf{X}}^\top \mathbf{W}\bar{\mathbf{X}})]\|_{2,1} \quad (185)$$

$$= \sum_{i=1}^L \|\mathbf{V}\bar{\mathbf{X}} [\text{softmax}_{\mathbf{M}_{:i}}(\mathbf{X}^\top \mathbf{W}\bar{\mathbf{X}}_{:i}) - \text{softmax}_{\mathbf{M}_{:i}}(\bar{\mathbf{X}}^\top \mathbf{W}\bar{\mathbf{X}}_{:i})]\| \quad (186)$$

$$= \sum_{i=1}^L \|\mathbf{V}\| \sum_{j=1, M_{ji}=1}^L \bar{\mathbf{X}}_{:j} (a_{ji} - \bar{a}_{ji}) \leq \|\mathbf{V}\| \sum_{i=1}^L \sum_{j=1, M_{ji}=1}^L \|\bar{\mathbf{X}}_{:j}\| |a_{ji} - \bar{a}_{ji}| \quad (187)$$

$$\leq \Upsilon \Xi \sum_{i=1}^L \sum_{j=1, M_{ji}=1}^L |a_{ji} - \bar{a}_{ji}| = \Upsilon \Xi \sum_{i=1}^L \|\text{softmax}_{\mathbf{M}_{:i}}(\mathbf{X}^\top \mathbf{W}\bar{\mathbf{X}}_{:i}) - \text{softmax}_{\mathbf{M}_{:i}}(\bar{\mathbf{X}}^\top \mathbf{W}\bar{\mathbf{X}}_{:i})\|_1 \quad (188)$$

$$\leq \Upsilon \Xi \xi_r \sum_{i=1}^L \|\mathbf{M}_{:i} \odot (\mathbf{X}^\top \mathbf{W}\bar{\mathbf{X}}_{:i} - \bar{\mathbf{X}}^\top \mathbf{W}\bar{\mathbf{X}}_{:i})\|_1 = \Upsilon \Xi \xi_r \sum_{i=1}^L \sum_{j=1, M_{ji}=1}^L |(\mathbf{X}_{:j} - \bar{\mathbf{X}}_{:j})^\top \mathbf{W}\bar{\mathbf{X}}_{:i}| \quad (189)$$

$$\leq \Upsilon \Xi \xi_r \sum_{i=1}^L \sum_{j=1, M_{ji}=1}^L \|\mathbf{X}_{:j} - \bar{\mathbf{X}}_{:j}\| \|\mathbf{W}\bar{\mathbf{X}}_{:i}\| = \Upsilon \Xi \xi_r \sum_{i=1}^L \|\mathbf{W}\bar{\mathbf{X}}_{:i}\| \left(\sum_{j=1, M_{ji}=1}^L \|\mathbf{X}_{:j} - \bar{\mathbf{X}}_{:j}\| \right) \quad (190)$$

$$\leq \Upsilon \Xi \xi_r \sum_{i=1}^L \|\mathbf{W}\| \|\bar{\mathbf{X}}_{:i}\| \left(\sum_{j=1, M_{ji}=1}^L \|\mathbf{X}_{:j} - \bar{\mathbf{X}}_{:j}\| \right) \leq \Upsilon \Xi^2 \xi_r \|\mathbf{W}\| \sum_{i=1}^L \left(\sum_{j=1, M_{ji}=1}^L \|\mathbf{X}_{:j} - \bar{\mathbf{X}}_{:j}\| \right) \quad (191)$$

$$\leq \Upsilon \Xi^2 \xi_r \Gamma \sum_{i=1}^L \sum_{j=1}^L \mathbb{I}(M_{ji} = 1) \|\mathbf{X}_{:j} - \bar{\mathbf{X}}_{:j}\| = \Upsilon \Xi^2 \xi_r \Gamma \sum_{j=1}^L \|\mathbf{X}_{:j} - \bar{\mathbf{X}}_{:j}\| \left(\sum_{i=1}^L \mathbb{I}(M_{ji} = 1) \right) \quad (192)$$

$$= \Upsilon \Xi^2 \xi_r \Gamma \sum_{j=1}^L \|\mathbf{X}_{:j} - \bar{\mathbf{X}}_{:j}\| k = \Upsilon \Xi^2 \xi_r \Gamma k \|\mathbf{X} - \bar{\mathbf{X}}\|_{2,1} \quad (193)$$

Combining the individual bounds on equation (B₁), equation (B₂), and equation (B₃), we have the following bound as per equation (169):

$$\|\mathbf{A}_{\mathbf{W}, \mathbf{V}}(\mathbf{X}) - \mathbf{A}_{\mathbf{W}, \mathbf{V}}(\bar{\mathbf{X}})\|_{2,1} \leq \xi_r \Upsilon k (2\Gamma \Xi^2 + 1) \|\mathbf{X} - \bar{\mathbf{X}}\|_{2,1}, \quad (194)$$

For equation (170), we note the following:

$$\|\mathbf{A}_{\mathbf{W}, \mathbf{V}}(\mathbf{X}) - \mathbf{A}_{\bar{\mathbf{W}}, \mathbf{V}}(\mathbf{X})\|_{2,1} = \|\mathbf{V}\mathbf{X} \text{softmax}_{\mathbf{M}}(\mathbf{X}^\top \mathbf{W}\mathbf{X}) - \mathbf{V}\mathbf{X} \text{softmax}_{\mathbf{M}}(\mathbf{X}^\top \bar{\mathbf{W}}\mathbf{X})\|_{2,1} \quad (195)$$

$$= \sum_{i=1}^L \|\mathbf{V}\mathbf{X} (\text{softmax}_{\mathbf{M}_{:i}}(\mathbf{X}^\top \mathbf{W}\mathbf{X}_{:i}) - \text{softmax}_{\mathbf{M}_{:i}}(\mathbf{X}^\top \bar{\mathbf{W}}\mathbf{X}_{:i}))\| \quad (196)$$

$$\leq \|\mathbf{V}\| \sum_{i=1}^L \|\mathbf{X} (\text{softmax}_{\mathbf{M}_{:i}}(\mathbf{X}^\top \mathbf{W}\mathbf{X}_{:i}) - \text{softmax}_{\mathbf{M}_{:i}}(\mathbf{X}^\top \bar{\mathbf{W}}\mathbf{X}_{:i}))\|. \quad (197)$$

Denoting a_{ji} as the j -th entry of masked $\text{softmax}_{\mathbf{M}_{:i}}(\mathbf{X}^\top \mathbf{W}\mathbf{X}_{:i})$ and \bar{a}_{ji} as the j -th entry of the masked $\text{softmax}_{\mathbf{M}_{:i}}(\mathbf{X}^\top \bar{\mathbf{W}}\mathbf{X}_{:i})$, and using the assumption that $\|\mathbf{V}\| \leq \Upsilon$, we have

$$\|\mathbf{A}_{\mathbf{W}, \mathbf{V}}(\mathbf{X}) - \mathbf{A}_{\bar{\mathbf{W}}, \mathbf{V}}(\mathbf{X})\|_{2,1} \leq \Upsilon \sum_{i=1}^L \left\| \sum_{j=1, M_{ji}=1}^L (a_{ji} - \bar{a}_{ji}) \mathbf{X}_{:j} \right\| \leq \Upsilon \sum_{i=1}^L \sum_{j=1, M_{ji}=1}^L \|(a_{ji} - \bar{a}_{ji}) \mathbf{X}_{:j}\| \quad (198)$$

$$\leq \Upsilon \sum_{i=1}^L \sum_{j=1, M_{ji}=1}^L |a_{ji} - \bar{a}_{ji}| \|\mathbf{X}_{:j}\| \quad (199)$$

$$\leq \Upsilon \Xi \sum_{i=1}^L \|\text{softmax}_{\mathbf{M}_{:i}}(\mathbf{X}^\top \mathbf{W}\mathbf{X}_{:i}) - \text{softmax}_{\mathbf{M}_{:i}}(\mathbf{X}^\top \bar{\mathbf{W}}\mathbf{X}_{:i})\|_1, \quad (200)$$

where we use the assumption that $\|\mathbf{X}_{:j}\| \leq \Xi$. Now, utilizing lemma S3, we have

$$\|A_{\mathbf{W},\mathbf{V}}(\mathbf{X}) - A_{\bar{\mathbf{W}},\mathbf{V}}(\mathbf{X})\|_{2,1} \leq \Upsilon \Xi \sum_{i=1}^L \xi_r \|\mathbf{M}_{:i} \odot (\mathbf{X}^\top \mathbf{W} \mathbf{X}_{:i} - \mathbf{X}^\top \bar{\mathbf{W}} \mathbf{X}_{:i})\|_1 \quad (201)$$

$$= \Upsilon \Xi \xi_r \sum_{i=1}^L \sum_{j=1, M_{ji}=1}^L |\mathbf{X}_{:j}^\top \mathbf{W} \mathbf{X}_{:i} - \mathbf{X}_{:j}^\top \bar{\mathbf{W}} \mathbf{X}_{:i}| \quad (202)$$

$$\leq \Upsilon \Xi \xi_r \sum_{i=1}^L \sum_{j=1, M_{ji}=1}^L \|\mathbf{X}_{:j}^\top \mathbf{W} - \mathbf{X}_{:j}^\top \bar{\mathbf{W}}\| \|\mathbf{X}_{:i}\| \quad (203)$$

$$\leq \Upsilon \Xi^2 \xi_r \sum_{i=1}^L \sum_{j=1, M_{ji}=1}^L \|\mathbf{X}_{:j}^\top \mathbf{W} - \mathbf{X}_{:j}^\top \bar{\mathbf{W}}\| \quad (204)$$

$$\leq \Upsilon \Xi^2 \xi_r \sum_{i=1}^L \sum_{j=1, M_{ji}=1}^L \|\mathbf{X}_{:j}\| \|\mathbf{W} - \bar{\mathbf{W}}\| \leq \xi_r \Xi^3 L k \Upsilon \|\mathbf{W} - \bar{\mathbf{W}}\|, \quad (205)$$

where we utilize $\|\mathbf{X}_{:j}\| \leq \Xi$ twice, thus giving us equation (170).

For equation (171), we note that

$$\|A_{\mathbf{W},\mathbf{V}}(\mathbf{X}) - A_{\bar{\mathbf{W}},\mathbf{V}}(\mathbf{X})\|_{2,1} = \|\mathbf{V} \mathbf{X}_{\text{softmax}_M}(\mathbf{X}^\top \mathbf{W} \mathbf{X}) - \bar{\mathbf{V}} \mathbf{X}_{\text{softmax}_M}(\mathbf{X}^\top \mathbf{W} \mathbf{X})\|_{2,1} \quad (206)$$

$$= \sum_{i=1}^L \|(\mathbf{V} - \bar{\mathbf{V}}) \mathbf{X}_{\text{softmax}_{M:i}}(\mathbf{X}^\top \mathbf{W} \mathbf{X}_{:i})\| \quad (207)$$

$$\leq \|\mathbf{V} - \bar{\mathbf{V}}\| \sum_{i=1}^L \|\mathbf{X}_{\text{softmax}_{M:i}}(\mathbf{X}^\top \mathbf{W} \mathbf{X}_{:i})\|. \quad (208)$$

Noting the fact that $\mathbf{X}_{\text{softmax}_{M:i}}(\mathbf{X}^\top \mathbf{W} \mathbf{X}_{:i})$ is a (sparse) convex sum of the columns of \mathbf{X} , its maximum Euclidean norm is bounded by maximum Euclidean norm of the individual columns, $\max_j \|\mathbf{X}_{:j}\|$, which itself is bounded from above by Ξ . This simplifies the right-hand-side above to $L \Xi \|\mathbf{V} - \bar{\mathbf{V}}\|$, giving us equation (171). \square

Remark S2. For the Lipschitz constants in definition 1, $\lambda_X(\xi_r) = \xi_r k \Upsilon (2\Gamma \Xi^2 + 1) = \exp(\delta_r) \Upsilon (2\Gamma \Xi^2 + 1)$, $\lambda_W(\xi_r) = \xi_r \Upsilon L k \Xi^3 = \exp(\delta_r) \Upsilon L \Xi^3$ and $\lambda_V = L \Xi$ with $\xi_r = \exp(\delta_r)/k$ and δ_r defined in equation (168). Under the assumption (R2) of theorem S4, $\delta_r \leq 2\Gamma \Xi^2$.

Remark S3. Note that, with $k \rightarrow L$, which corresponds to standard-softmax based attention, $\delta_r \rightarrow \delta_s$, and the results in theorem S4 reduce to the results in theorem S3.

E.3 Heavy-hitter Input-dependent Sparse Softmax based Attention

Lemma S4. Given a k -heavy-hitter masking function $m : \mathbb{R}^L \rightarrow \{0, 1\}$ such that, for any $\mathbf{z} \in \mathbb{R}^L$, with the corresponding mask $\mathbf{b} = m(\mathbf{z})$, the number of nonzeros in \mathbf{b} is exactly k , and

$$\min_{i,j \in [L]: b_i=1, b_j=0} z_i - z_j \geq \Delta, \quad (209)$$

where $\Delta > 0$ denotes the smallest gap between the k heavy-hitter unmasked values in \mathbf{z} and remaining masked values. Furthermore, for any $\mathbf{z}, \bar{\mathbf{z}} \in \mathbb{R}^L$ with corresponding input dependent masks $\mathbf{b} = m(\mathbf{z})$ and $\bar{\mathbf{b}} = m(\bar{\mathbf{z}})$ respectively,

$$\max_{i,j \in [L]: b_i=b_j=1} z_i - z_j \leq \delta, \quad \text{and} \quad \max_{i,j \in [L]: \bar{b}_i=\bar{b}_j=1} \bar{z}_i - \bar{z}_j \leq \delta, \quad (210)$$

for a constant $\delta > 0$. Denoting the combined masked vector as $\mathbf{c} = \mathbf{b} \vee \bar{\mathbf{b}}$ with $c_i = \mathbb{I}(b_i = 1 \vee \bar{b}_i = 1)$, we have the following:

$$\|\text{softmax}_{\mathbf{b}}(\mathbf{z})\|_{\infty} \leq \frac{e^{\delta}}{k}, \quad \|\text{softmax}_{\mathbf{b}}(\mathbf{z}) - \text{softmax}_{\bar{\mathbf{b}}}(\bar{\mathbf{z}})\|_1 \leq (1 + 1/\Delta) \frac{e^{\delta}}{k} \|\mathbf{c} \odot (\mathbf{z} - \bar{\mathbf{z}})\|_1 \quad (211)$$

where \odot denotes the elementwise multiplication of two vectors.

Proof. For any $\mathbf{z}, \bar{\mathbf{z}} \in \mathbb{R}^L$ with input dependent masks $\mathbf{b}, \bar{\mathbf{b}} \in \{0, 1\}^L$ with k nonzeros, let $\mathbf{z}[\mathbf{b}], \bar{\mathbf{z}}[\bar{\mathbf{b}}] \in \mathbb{R}^k$ denote the k -dimensional vectors corresponding to the unmasked entries of $\mathbf{z}, \bar{\mathbf{z}}$. Then, utilizing lemma S2 for a softmax operation over a k -length vector with equation (161), we have the following:

$$\|\text{softmax}_{\mathbf{b}}(\mathbf{z})\|_{\infty} = \|\text{softmax}(\mathbf{z}[\mathbf{b}])\|_{\infty} \leq \frac{\exp(\delta)}{k}. \quad (212)$$

Furthermore,

$$\|\text{softmax}_{\mathbf{b}}(\mathbf{z}) - \text{softmax}_{\bar{\mathbf{b}}}(\bar{\mathbf{z}})\|_1 \leq \|\text{softmax}_{\mathbf{b}}(\mathbf{z}) - \text{softmax}_{\mathbf{b}}(\bar{\mathbf{z}})\|_1 + \|\text{softmax}_{\mathbf{b}}(\bar{\mathbf{z}}) - \text{softmax}_{\bar{\mathbf{b}}}(\bar{\mathbf{z}})\|_1 \quad (213)$$

$$\leq \frac{\exp(\delta)}{k} \|\mathbf{b} \odot (\mathbf{z} - \bar{\mathbf{z}})\|_1 + \|\text{softmax}_{\mathbf{b}}(\bar{\mathbf{z}}) - \text{softmax}_{\bar{\mathbf{b}}}(\bar{\mathbf{z}})\|_1, \quad (214)$$

where we utilized lemma S3 with the fixed mask \mathbf{b} . Now the second term is the masked softmax with two different masks \mathbf{b} and $\bar{\mathbf{b}}$ on the same input $\bar{\mathbf{z}}$. Then the maximum change between the two masked softmax occurs when the entries that go from being masked to being unmasked (or vice versa) – the $i \in [L]$ such that $b_i \otimes \bar{b}_i = 1$ – have the highest values. That is,

$$\|\text{softmax}_{\mathbf{b}}(\bar{\mathbf{z}}) - \text{softmax}_{\bar{\mathbf{b}}}(\bar{\mathbf{z}})\|_1 \leq \sum_{i \in [L]: b_i \otimes \bar{b}_i = 1} |\text{softmax}_{\mathbf{b}}(\bar{\mathbf{z}})_i - \text{softmax}_{\bar{\mathbf{b}}}(\bar{\mathbf{z}})_i| \quad (215)$$

$$\leq \sum_{i \in [L]: b_i \otimes \bar{b}_i = 1} \|\text{softmax}_{\mathbf{b}}(\bar{\mathbf{z}})\|_{\infty} \quad (216)$$

$$\leq \|\mathbf{b} - \bar{\mathbf{b}}\|_1 \|\text{softmax}_{\mathbf{b}}(\bar{\mathbf{z}})\|_{\infty}. \quad (217)$$

Let $k' = \|\mathbf{b} - \bar{\mathbf{b}}\|_1$ denote the change in the mask when the input to the mask changes from \mathbf{z} to $\bar{\mathbf{z}}$. Without loss of generality, assume that \mathbf{z} is such that $b_i = 1, \forall i \in [k]$ – that is the first k entries of \mathbf{z} are the heavy-hitters. Similarly, assume that for $\bar{\mathbf{z}}$, the corresponding mask $\bar{\mathbf{b}}$ overlaps with the last k'' entries of \mathbf{b} and $\bar{b}_i = 1 \forall i \in [k - k'' + 1, 2k - k'']$. Given that $k' = \|\mathbf{b} - \bar{\mathbf{b}}\|_1 = 2(k - k'')$, we can show that $k'' = (k - k')/2$.

Note that, by equation (209), we know that there exists thresholds $t, \bar{t} \in \mathbb{R}$ such that

$$\mathbf{z} : \begin{cases} z_i \geq t, i \in [k] \\ z_i \leq t - \Delta, i \in [k + 1, L] \end{cases}, \quad \bar{\mathbf{z}} : \begin{cases} \bar{z}_i \geq \bar{t}, i \in [k - k'' + 1, 2k - k''] \\ \bar{z}_i \leq \bar{t} - \Delta, i \in [1, k - k''] \cup [2k - k'' + 1, L] \end{cases}. \quad (218)$$

Now we will just consider the first $(2k - k'')$ entries of \mathbf{z} and $\bar{\mathbf{z}}$. We see that

$$(z_i - \bar{z}_i) \begin{cases} \geq (t - \bar{t} + \Delta), i \in [1, k - k''] \\ \leq (-t + \Delta - \bar{t}), i \in [k + 1, 2k - k''] \end{cases} \quad (219)$$

Thus the ℓ_1 norm between such two \mathbf{z} and $\bar{\mathbf{z}}$ is lower bounded as

$$\|\mathbf{z} - \bar{\mathbf{z}}\|_1 \geq \|\mathbf{c} \odot (\mathbf{z} - \bar{\mathbf{z}})\|_1 = \sum_{i=1}^{2k-k''} |z_i - \bar{z}_i| \quad (220)$$

$$= \sum_{i=1}^{k-k''} |(z_i - \bar{z}_i)| + \sum_{i=k-k''+1}^k |(z_i - \bar{z}_i)| + \sum_{i=k+1}^{2k-k''} |(z_i - \bar{z}_i)| \quad (221)$$

$$\geq \sum_{i=1}^{k-k''} |(z_i - \bar{z}_i)| + \sum_{i=k+1}^{2k-k''} |(z_i - \bar{z}_i)| \quad (222)$$

$$\geq \sum_{i=1}^{k-k''} |(t - \bar{t}) + \Delta| + \sum_{i=k+1}^{2k-k''} |(t - \bar{t}) - \Delta| \quad (223)$$

$$= (k - k'') (|(t - \bar{t}) + \Delta| + |(t - \bar{t}) - \Delta|). \quad (224)$$

Denoting $(t - \bar{t})$ as ε , consider the term $(|\varepsilon + \Delta| + |\varepsilon - \Delta|)$ and note that $\Delta > 0$. We can see that, if $|\varepsilon| \leq \Delta$, the term is equal to $\Delta + |\varepsilon| + \Delta - |\varepsilon| = 2\Delta$. If $|\varepsilon| > \Delta$, then term is equal to $|\varepsilon| + \Delta + |\varepsilon| - \Delta = 2|\varepsilon| > 2\Delta$.

Thus we have

$$\|\mathbf{c} \odot (\mathbf{z} - \bar{\mathbf{z}})\|_1 \geq (k - k'') (|(t - \bar{t}) + \Delta| + |(t - \bar{t}) - \Delta|). \quad (225)$$

$$\geq 2(k - k'')\Delta = k'\Delta = \|\mathbf{b} - \bar{\mathbf{b}}\|_1\Delta, \quad (226)$$

giving us $\|\mathbf{b} - \bar{\mathbf{b}}\|_1 \leq (1/\Delta)\|\mathbf{c} \odot (\mathbf{z} - \bar{\mathbf{z}})\|_1$. Utilizing this in combination with equation (214) and equation (217), we have

$$\|\text{softmax}_{\mathbf{b}}(\mathbf{z}) - \text{softmax}_{\bar{\mathbf{b}}}(\bar{\mathbf{z}})\|_1 \leq \frac{\exp(\delta)}{k} \|\mathbf{b} \odot (\mathbf{z} - \bar{\mathbf{z}})\|_1 + (1/\Delta) \frac{\exp(\delta)}{k} \|\mathbf{c} \odot (\mathbf{z} - \bar{\mathbf{z}})\|_1 \quad (227)$$

$$\leq \frac{\exp(\delta)}{k} (1 + 1/\Delta) \|\mathbf{c} \odot (\mathbf{z} - \bar{\mathbf{z}})\|_1, \quad (228)$$

since $\|\mathbf{b} \odot (\mathbf{z} - \bar{\mathbf{z}})\|_1 \leq \|\mathbf{c} \odot (\mathbf{z} - \bar{\mathbf{z}})\|_1$ as \mathbf{b} is contained with \mathbf{c} . This gives us the desired result in equation (211). \square

Theorem S5. Consider the self-attention operation $\mathbf{A} : \mathbb{R}^{d \times L} \rightarrow \mathbb{R}^{d \times L}$ with input \mathbf{X} of L token representations and parameters $\mathbf{W}, \mathbf{V} \in \mathbb{R}^{d \times d}$ utilizing a k -heavy-hitter input-dependent masking function $m : \mathbb{R}^L \rightarrow \{0, 1\}^L$, applied columnwise to the dot-product matrix to get a mask matrix $\mathbf{M} \in \{0, 1\}^{L \times L}$. Consider the following assumptions:

(H1) For any query-key pairs $\mathbf{X}, \bar{\mathbf{X}} \in \mathbb{R}^{d \times L}$, the k -heavy-hitter mask $\mathbf{M} = m(\bar{\mathbf{X}}^\top \mathbf{W} \mathbf{X})$ (applied columnwise) has a minimum per-query semantic separation (definition 3) of $\Delta_h > 0$, that is

$$\forall i \in \llbracket L \rrbracket, \min_{j, j' \in \llbracket L \rrbracket, M_{ji}=1, M_{j'i}=0} (\bar{\mathbf{X}}_{:j}^\top \mathbf{W} \mathbf{X}_{:i} - \bar{\mathbf{X}}_{:j'}^\top \mathbf{W} \mathbf{X}_{:i}) \geq \Delta_h. \quad (229)$$

(H2) A maximum of $\beta k, \beta > 1$ query tokens attend to a single key token, that is, $\|\mathbf{M}_{:i}\|_1 \leq \beta k$ for any $i \in \llbracket L \rrbracket$.

(H3) The per-token Euclidean norms are bounded as $\|\mathbf{X}_{:i}\| \leq \Xi \forall i \in \llbracket L \rrbracket$, and the parameter norms are bounded at $\|\mathbf{W}\| \leq \Gamma$ and $\|\mathbf{V}\| \leq \Upsilon$.

(H4) The per-query semantic dispersion (definition 2) is bounded by δ_h , that is:

$$\forall i \in \llbracket L \rrbracket, \max_{j, j' \in \llbracket L \rrbracket, M_{ji}=M_{j'i}=1} (\mathbf{X}_{:j}^\top \mathbf{W} \mathbf{X}_{:i} - \mathbf{X}_{:j'}^\top \mathbf{W} \mathbf{X}_{:i}) \leq \delta_h. \quad (230)$$

Then the masked softmax is ξ_h -Lipschitz with $\xi_h = (e^{\delta_h}/k) (1 + 1/\Delta_h)$, and the masked attention is Lipschitz with respect to its input and parameters as following for any input pair $\mathbf{X}, \bar{\mathbf{X}} \in \mathbb{R}^{d \times L}$ with $\|\bar{\mathbf{X}}_{:i}\| \leq 1 \forall i \in \llbracket L \rrbracket$, and parameter pairs $\mathbf{W}, \bar{\mathbf{W}}, \mathbf{V}, \bar{\mathbf{V}} \in \mathbb{R}^{d \times d}$ with $\|\mathbf{W}\| \leq \Gamma, \|\bar{\mathbf{W}}\| \leq \Gamma$ and $\|\mathbf{V}\| \leq \Upsilon, \|\bar{\mathbf{V}}\| \leq \Upsilon$:

$$\|\mathbf{A}_{\mathbf{W}, \mathbf{V}}(\mathbf{X}) - \mathbf{A}_{\mathbf{W}, \mathbf{V}}(\bar{\mathbf{X}})\|_{2,1} \leq \xi_h \Upsilon k \left(2\Gamma \Xi^2 (\beta + 1) + \frac{\beta}{1 + 1/\Delta_h} \right) \|\mathbf{X} - \bar{\mathbf{X}}\|_{2,1}, \quad (231)$$

$$\|\mathbf{A}_{\mathbf{W}, \mathbf{V}}(\mathbf{X}) - \mathbf{A}_{\bar{\mathbf{W}}, \mathbf{V}}(\mathbf{X})\|_{2,1} \leq 2\xi_h \Upsilon L k \Xi^3 \|\mathbf{W} - \bar{\mathbf{W}}\|, \quad (232)$$

$$\|\mathbf{A}_{\mathbf{W}, \mathbf{V}}(\mathbf{X}) - \mathbf{A}_{\mathbf{W}, \bar{\mathbf{V}}}(\mathbf{X})\|_{2,1} \leq L \Xi \|\mathbf{V} - \bar{\mathbf{V}}\|. \quad (233)$$

Proof. Now, given the upper bound on the per-query semantic dispersion δ_h in equation (230), and the per-query semantic separation Δ_h in equation (229), we can apply Lemma S4 with $\delta = \delta_h$ and $\Delta = \Delta_h$, giving us a ξ_h -Lipschitz softmax with $\xi_h = \exp(\delta_h)(1 + 1/\Delta_h)/k$.

Note that, given a k -heavy-hitter input-dependent masking function m and the corresponding mask matrix \mathbf{M} , we know that, for any column $\mathbf{M}_{:i}$, $i \in \llbracket L \rrbracket$, $\sum_{j=1}^L M_{ji} = k$. However, unlike the k -regular input-agnostic mask, for any row $\mathbf{M}_{i:}$, $i \in \llbracket L \rrbracket$, $\sum_{j=1}^L M_{ij} \neq k$. Here, we will utilize assumption H2 which states that, for any row $\mathbf{M}_{i:}$, $\sum_{j=1}^L M_{ij} \leq \beta k$.

For equation (231), we note that the mask matrix is input-dependent, and thus will denote as mask matrices $\mathbf{M}, \hat{\mathbf{M}}, \bar{\mathbf{M}}$ for the following dot-product matrices $(\mathbf{X}^\top \mathbf{W} \mathbf{X})$, $(\mathbf{X}^\top \mathbf{W} \bar{\mathbf{X}})$ and $(\bar{\mathbf{X}}^\top \mathbf{W} \bar{\mathbf{X}})$ respectively. That is, $\mathbf{M} = m(\mathbf{X}^\top \mathbf{W} \mathbf{X})$, $\hat{\mathbf{M}} = m(\mathbf{X}^\top \mathbf{W} \bar{\mathbf{X}})$, $\bar{\mathbf{M}} = m(\bar{\mathbf{X}}^\top \mathbf{W} \bar{\mathbf{X}})$, where the masking function m is applied columnwise to the dot-product matrices. Given this, we proceed as follows:

$$\|\mathbf{A}_{\mathbf{W}, \mathbf{V}}(\mathbf{X}) - \mathbf{A}_{\mathbf{W}, \mathbf{V}}(\bar{\mathbf{X}})\|_{2,1} = \|\mathbf{V} \mathbf{X} \text{softmax}_{\mathbf{M}}(\mathbf{X}^\top \mathbf{W} \mathbf{X}) - \mathbf{V} \bar{\mathbf{X}} \text{softmax}_{\bar{\mathbf{M}}}(\bar{\mathbf{X}}^\top \mathbf{W} \bar{\mathbf{X}})\|_{2,1} \quad (234)$$

$$\leq \|\mathbf{V} \mathbf{X} \text{softmax}_{\mathbf{M}}(\mathbf{X}^\top \mathbf{W} \mathbf{X}) - \mathbf{V} \bar{\mathbf{X}} \text{softmax}_{\mathbf{M}}(\mathbf{X}^\top \mathbf{W} \mathbf{X})\|_{2,1} \quad (C_1)$$

$$+ \|\mathbf{V} \bar{\mathbf{X}} \text{softmax}_{\mathbf{M}}(\mathbf{X}^\top \mathbf{W} \mathbf{X}) - \mathbf{V} \bar{\mathbf{X}} \text{softmax}_{\hat{\mathbf{M}}}(\mathbf{X}^\top \mathbf{W} \bar{\mathbf{X}})\|_{2,1} \quad (C_2)$$

$$+ \|\mathbf{V} \bar{\mathbf{X}} \text{softmax}_{\hat{\mathbf{M}}}(\mathbf{X}^\top \mathbf{W} \bar{\mathbf{X}}) - \mathbf{V} \bar{\mathbf{X}} \text{softmax}_{\bar{\mathbf{M}}}(\bar{\mathbf{X}}^\top \mathbf{W} \bar{\mathbf{X}})\|_{2,1}. \quad (C_3)$$

We will handle each of the equation (C1), equation (C2), and equation (C3) individually. We will use a_{ji} to denote the j -th entry of masked $\text{softmax}_{\mathbf{M}_{:i}}(\mathbf{X}^\top \mathbf{W} \mathbf{X}_{:i})$, and \mathbf{a}_{ji} , $\bar{\mathbf{a}}_{ji}$ to denote the j -th entry of $\text{softmax}_{\hat{\mathbf{M}}_{:i}}(\mathbf{X}^\top \mathbf{W} \bar{\mathbf{X}}_{:i})$ and $\text{softmax}_{\bar{\mathbf{M}}_{:i}}(\bar{\mathbf{X}}^\top \mathbf{W} \bar{\mathbf{X}}_{:i})$ respectively. Note that, by lemma S4 and equation (230) in assumption H4, all $a_{ji}, \mathbf{a}_{ji}, \bar{\mathbf{a}}_{ji} \leq \exp(\delta_h)/k = \xi_h/(1 + 1/\Delta_h)$.

$$(C_1) = \|\mathbf{V}(\mathbf{X} - \bar{\mathbf{X}}) \text{softmax}_{\mathbf{M}}(\mathbf{X}^\top \mathbf{W} \mathbf{X})\|_{2,1} = \sum_{i=1}^L \|\mathbf{V}(\mathbf{X} - \bar{\mathbf{X}}) \text{softmax}_{\mathbf{M}_{:i}}(\mathbf{X}^\top \mathbf{W} \mathbf{X}_{:i})\| \quad (235)$$

$$= \sum_{i=1}^L \|\mathbf{V} \sum_{j=1, M_{ji}=1}^L (\mathbf{X}_{:j} - \bar{\mathbf{X}}_{:j}) a_{ji}\| \leq \|\mathbf{V}\| \sum_{i=1}^L \left\| \sum_{j=1, M_{ji}=1}^L (\mathbf{X}_{:j} - \bar{\mathbf{X}}_{:j}) a_{ji} \right\| \quad (236)$$

$$\leq \|\mathbf{V}\| \sum_{i=1}^L \sum_{j=1, M_{ji}=1}^L \|\mathbf{X}_{:j} - \bar{\mathbf{X}}_{:j}\| |a_{ji}| \leq \Upsilon \frac{\xi_h}{1 + 1/\Delta_h} \sum_{i=1}^L \sum_{j=1, M_{ji}=1}^L \|\mathbf{X}_{:j} - \bar{\mathbf{X}}_{:j}\| \quad (237)$$

$$= \Upsilon \frac{\xi_h}{1 + 1/\Delta_h} \sum_{i=1}^L \sum_{j=1}^L \mathbb{I}(M_{ji} = 1) \|\mathbf{X}_{:j} - \bar{\mathbf{X}}_{:j}\| = \Upsilon \frac{\xi_h}{1 + 1/\Delta_h} \sum_{j=1}^L \sum_{i=1}^L \mathbb{I}(M_{ji} = 1) \|\mathbf{X}_{:j} - \bar{\mathbf{X}}_{:j}\| \quad (238)$$

$$= \Upsilon \frac{\xi_h}{1 + 1/\Delta_h} \sum_{j=1}^L \|\mathbf{X}_{:j} - \bar{\mathbf{X}}_{:j}\| \left(\sum_{i=1}^L \mathbb{I}(M_{ji} = 1) \right) \quad (239)$$

$$\leq \Upsilon \frac{\xi_h}{1 + 1/\Delta_h} \sum_{j=1}^L \|\mathbf{X}_{:j} - \bar{\mathbf{X}}_{:j}\| \beta k = \frac{\Upsilon \xi_h \beta k}{1 + 1/\Delta_h} \|\mathbf{X} - \bar{\mathbf{X}}\|_{2,1} \quad (240)$$

where we utilize the fact that $\|\mathbf{V}\| \leq \Upsilon$, and the row sum of the mask matrix is upper bounded by βk from assumption H2.

We handle equation (C2) in the following manner:

$$(C_2) = \|\mathbf{V} \bar{\mathbf{X}} [\text{softmax}_{\mathbf{M}}(\mathbf{X}^\top \mathbf{W} \mathbf{X}) - \text{softmax}_{\hat{\mathbf{M}}}(\mathbf{X}^\top \mathbf{W} \bar{\mathbf{X}})]\|_{2,1} \quad (241)$$

$$= \sum_{i=1}^L \|\mathbf{V} \bar{\mathbf{X}} [\text{softmax}_{\mathbf{M}_{:i}}(\mathbf{X}^\top \mathbf{W} \mathbf{X}_{:i}) - \text{softmax}_{\hat{\mathbf{M}}_{:i}}(\mathbf{X}^\top \mathbf{W} \bar{\mathbf{X}}_{:i})]\| \quad (242)$$

$$= \sum_{i=1}^L \|\mathbf{V} \sum_{j=1, M_{ji}=1 \vee \hat{M}_{ji}=1}^L \bar{\mathbf{X}}_{:j} (a_{ji} - \mathbf{a}_{ji})\| \leq \|\mathbf{V}\| \sum_{i=1}^L \sum_{j=1, M_{ji}=1 \vee \hat{M}_{ji}=1}^L \|\bar{\mathbf{X}}_{:j}\| |a_{ji} - \mathbf{a}_{ji}| \quad (243)$$

$$\leq \Upsilon \Xi \sum_{i=1}^L \sum_{j=1, M_{ji}=1 \vee \hat{M}_{ji}=1}^L |a_{ji} - \bar{a}_{ji}| \quad (244)$$

$$= \Upsilon \Xi \sum_{i=1}^L \|\text{softmax}_{\mathbf{M}_{:i}}(\mathbf{X}^\top \mathbf{W} \mathbf{X}_{:i}) - \text{softmax}_{\hat{\mathbf{M}}_{:i}}(\mathbf{X}^\top \mathbf{W} \bar{\mathbf{X}}_{:i})\|_1 \quad (245)$$

$$\leq \Upsilon \Xi \xi_h \sum_{i=1}^L \|(\mathbf{M}_{:i} \vee \hat{\mathbf{M}}_{:i}) \odot \mathbf{X}^\top \mathbf{W} (\mathbf{X}_{:i} - \bar{\mathbf{X}}_{:i})\|_1 = \Upsilon \Xi \xi_h \sum_{i=1}^L \sum_{j=1, M_{ji}=1 \vee \hat{M}_{ji}=1}^L |\mathbf{X}_{:j}^\top \mathbf{W} (\mathbf{X}_{:i} - \bar{\mathbf{X}}_{:i})| \quad (246)$$

$$\leq \Upsilon \Xi \xi_h \sum_{i=1}^L \sum_{j=1, M_{ji}=1 \vee \hat{M}_{ji}=1}^L \|\mathbf{X}_{:j}^\top \mathbf{W}\| \|\mathbf{X}_{:i} - \bar{\mathbf{X}}_{:i}\| \quad (247)$$

$$= \Upsilon \Xi \xi_h \sum_{i=1}^L \|\mathbf{X}_{:i} - \bar{\mathbf{X}}_{:i}\| \left(\sum_{j=1, M_{ji}=1 \vee \hat{M}_{ji}=1}^L \|\mathbf{X}_{:j}^\top \mathbf{W}\| \right) \quad (248)$$

$$\leq \Upsilon \Xi \xi_h \sum_{i=1}^L \|\mathbf{X}_{:i} - \bar{\mathbf{X}}_{:i}\| \|\mathbf{W}\| \left(\sum_{j=1, M_{ji}=1 \vee \hat{M}_{ji}=1}^L \|\mathbf{X}_{:j}\| \right) \quad (249)$$

$$\leq \Upsilon \Xi \xi_h \Gamma \sum_{i=1}^L \|\mathbf{X}_{:i} - \bar{\mathbf{X}}_{:i}\| \cdot (2k\Xi) = 2\Upsilon \xi_h \Gamma k \Xi^2 \|\mathbf{X} - \bar{\mathbf{X}}\|_{2,1}, \quad (250)$$

utilizing equation (211), the assumption H3 that $\|\mathbf{W}\| \leq \Gamma$, $\|\mathbf{X}_{:i}\| \leq \Xi$ for all $i \in \llbracket L \rrbracket$, and that the column sum of \mathbf{M} is k , thus $\sum_{j=1}^L \mathbb{I}(M_{ji} = 1 \vee \hat{M}_{ji} = 1) \leq 2k$.

We handle equation (C₃) in the following manner:

$$(C_3) = \|\mathbf{V} \bar{\mathbf{X}} [\text{softmax}_{\mathbf{M}}(\mathbf{X}^\top \mathbf{W} \bar{\mathbf{X}}) - \text{softmax}_{\bar{\mathbf{M}}}(\bar{\mathbf{X}}^\top \mathbf{W} \bar{\mathbf{X}})]\|_{2,1} \quad (251)$$

$$= \sum_{i=1}^L \|\mathbf{V} \bar{\mathbf{X}} [\text{softmax}_{\hat{\mathbf{M}}_{:i}}(\mathbf{X}^\top \mathbf{W} \bar{\mathbf{X}}_{:i}) - \text{softmax}_{\bar{\mathbf{M}}_{:i}}(\bar{\mathbf{X}}^\top \mathbf{W} \bar{\mathbf{X}}_{:i})]\| \quad (252)$$

$$= \sum_{i=1}^L \|\mathbf{V}\| \sum_{j=1, \hat{M}_{ji}=1 \vee \bar{M}_{ji}=1}^L \bar{\mathbf{X}}_{:j} (a_{ji} - \bar{a}_{ji}) \leq \|\mathbf{V}\| \sum_{i=1}^L \sum_{j=1, \hat{M}_{ji}=1 \vee \bar{M}_{ji}=1}^L \|\bar{\mathbf{X}}_{:j}\| |a_{ji} - \bar{a}_{ji}| \quad (253)$$

$$\leq \Upsilon \Xi \sum_{i=1}^L \sum_{j=1, \hat{M}_{ji}=1 \vee \bar{M}_{ji}=1}^L |a_{ji} - \bar{a}_{ji}| \quad (254)$$

$$= \Upsilon \Xi \sum_{i=1}^L \|\text{softmax}_{\hat{\mathbf{M}}_{:i}}(\mathbf{X}^\top \mathbf{W} \bar{\mathbf{X}}_{:i}) - \text{softmax}_{\bar{\mathbf{M}}_{:i}}(\bar{\mathbf{X}}^\top \mathbf{W} \bar{\mathbf{X}}_{:i})\|_1 \quad (255)$$

$$\leq \Upsilon \Xi \xi_h \sum_{i=1}^L \|(\hat{\mathbf{M}}_{:i} \vee \bar{\mathbf{M}}_{:i}) \odot (\mathbf{X}^\top \mathbf{W} \bar{\mathbf{X}}_{:i} - \bar{\mathbf{X}}^\top \mathbf{W} \bar{\mathbf{X}}_{:i})\|_1 \quad (256)$$

$$= \Upsilon \Xi \xi_h \sum_{i=1}^L \sum_{j=1, \hat{M}_{ji}=1 \vee \bar{M}_{ji}=1}^L |(\mathbf{X}_{:j} - \bar{\mathbf{X}}_{:j})^\top \mathbf{W} \bar{\mathbf{X}}_{:i}| \quad (257)$$

$$\leq \Upsilon \Xi \xi_h \sum_{i=1}^L \sum_{j=1, \hat{M}_{ji}=1 \vee \bar{M}_{ji}=1}^L \|\mathbf{X}_{:j} - \bar{\mathbf{X}}_{:j}\| \|\mathbf{W} \bar{\mathbf{X}}_{:i}\| \quad (258)$$

$$= \Upsilon \Xi \xi_h \sum_{i=1}^L \|\mathbf{W} \bar{\mathbf{X}}_{:i}\| \left(\sum_{j=1, \hat{M}_{ji}=1 \vee \bar{M}_{ji}=1}^L \|\mathbf{X}_{:j} - \bar{\mathbf{X}}_{:j}\| \right) \quad (259)$$

$$\leq \Upsilon \Xi \xi_h \sum_{i=1}^L \|\mathbf{W}\| \|\bar{\mathbf{X}}_{:i}\| \left(\sum_{j=1, \hat{M}_{ji}=1 \vee \bar{M}_{ji}=1}^L \|\mathbf{X}_{:j} - \bar{\mathbf{X}}_{:j}\| \right) \quad (260)$$

$$\leq \Upsilon \Xi^2 \xi_h \|\mathbf{W}\| \sum_{i=1}^L \left(\sum_{j=1, \hat{M}_{ji}=1 \vee \bar{M}_{ji}=1}^L \|\mathbf{X}_{:j} - \bar{\mathbf{X}}_{:j}\| \right) \quad (261)$$

$$\leq \Upsilon \Xi^2 \xi_h \Gamma \sum_{i=1}^L \sum_{j=1}^L \mathbb{I}(\hat{M}_{ji}=1 \vee \bar{M}_{ji}=1) \|\mathbf{X}_{:j} - \bar{\mathbf{X}}_{:j}\| \quad (262)$$

$$= \Upsilon \Xi^2 \xi_h \Gamma \sum_{j=1}^L \|\mathbf{X}_{:j} - \bar{\mathbf{X}}_{:j}\| \left(\sum_{i=1}^L \mathbb{I}(\hat{M}_{ji}=1 \vee \bar{M}_{ji}=1) \right) \quad (263)$$

$$\leq \Upsilon \Xi^2 \xi_h \Gamma \sum_{j=1}^L \|\mathbf{X}_{:j} - \bar{\mathbf{X}}_{:j}\| \left(\sum_{i=1}^L \mathbb{I}(\hat{M}_{ji}=1) + \sum_{i=1}^L \mathbb{I}(\bar{M}_{ji}=1) \right) \quad (264)$$

$$\leq \Upsilon \Xi^2 \xi_h \Gamma \sum_{j=1}^L \|\mathbf{X}_{:j} - \bar{\mathbf{X}}_{:j}\| (\beta k + \beta k) \quad (265)$$

$$= 2\Upsilon \Xi^2 \xi_h \Gamma \beta k \sum_{j=1}^L \|\mathbf{X}_{:j} - \bar{\mathbf{X}}_{:j}\| k = 2\Upsilon \Xi^2 \xi_h \Gamma \beta k \|\mathbf{X} - \bar{\mathbf{X}}\|_{2,1} \quad (266)$$

Combining the individual bounds on equation (C₁), equation (C₂), and equation (C₃), we have the following bound as per equation (231):

$$\|A_{\mathbf{W}, \mathbf{V}}(\mathbf{X}) - A_{\mathbf{W}, \mathbf{V}}(\bar{\mathbf{X}})\|_{2,1} \leq \Upsilon \xi_h k \left(2\Gamma \Xi^2 (\beta + 1) + \frac{\beta}{1 + 1/\Delta_h} \right) \|\mathbf{X} - \bar{\mathbf{X}}\|_{2,1}. \quad (267)$$

First, let us denote the input-dependent mask matrices as \mathbf{M} and $\bar{\mathbf{M}}$ for the dot-product matrices ($\mathbf{X}^\top \mathbf{W} \mathbf{X}$) and ($\mathbf{X}^\top \bar{\mathbf{W}} \mathbf{X}$) results. Thus $\mathbf{M} = m(\mathbf{X}^\top \mathbf{W} \mathbf{X})$ and $\bar{\mathbf{M}} = m(\mathbf{X}^\top \bar{\mathbf{W}} \mathbf{X})$. Utilizing this for the left-hand-side of equation (232), we note the following:

$$\|A_{\mathbf{W}, \mathbf{V}}(\mathbf{X}) - A_{\bar{\mathbf{W}}, \mathbf{V}}(\mathbf{X})\|_{2,1} = \|\mathbf{V} \mathbf{X} \text{softmax}_{\mathbf{M}}(\mathbf{X}^\top \mathbf{W} \mathbf{X}) - \mathbf{V} \mathbf{X} \text{softmax}_{\bar{\mathbf{M}}}(\mathbf{X}^\top \bar{\mathbf{W}} \mathbf{X})\|_{2,1} \quad (268)$$

$$= \sum_{i=1}^L \|\mathbf{V} \mathbf{X} (\text{softmax}_{\mathbf{M}_{:i}}(\mathbf{X}^\top \mathbf{W} \mathbf{X}_{:i}) - \text{softmax}_{\bar{\mathbf{M}}_{:i}}(\mathbf{X}^\top \bar{\mathbf{W}} \mathbf{X}_{:i}))\| \quad (269)$$

$$\leq \|\mathbf{V}\| \sum_{i=1}^L \|\mathbf{X} (\text{softmax}_{\mathbf{M}_{:i}}(\mathbf{X}^\top \mathbf{W} \mathbf{X}_{:i}) - \text{softmax}_{\bar{\mathbf{M}}_{:i}}(\mathbf{X}^\top \bar{\mathbf{W}} \mathbf{X}_{:i}))\|. \quad (270)$$

Denoting a_{ji} as the j -th entry of masked $\text{softmax}_{\mathbf{M}_{:i}}(\mathbf{X}^\top \mathbf{W} \mathbf{X}_{:i})$ and \bar{a}_{ji} as the j -th entry of the masked $\text{softmax}_{\bar{\mathbf{M}}_{:i}}(\mathbf{X}^\top \bar{\mathbf{W}} \mathbf{X}_{:i})$, and using the assumption that $\|\mathbf{V}\| \leq \Upsilon$, we have

$$\|A_{\mathbf{W}, \mathbf{V}}(\mathbf{X}) - A_{\bar{\mathbf{W}}, \mathbf{V}}(\mathbf{X})\|_{2,1} \leq \Upsilon \sum_{i=1}^L \left\| \sum_{j=1, M_{ji}=1 \vee \bar{M}_{ji}=1}^L (a_{ji} - \bar{a}_{ji}) \mathbf{X}_{:j} \right\| \quad (271)$$

$$\leq \Upsilon \sum_{i=1}^L \sum_{j=1, M_{ji}=1 \vee \bar{M}_{ji}=1}^L \|(a_{ji} - \bar{a}_{ji}) \mathbf{X}_{:j}\| \quad (272)$$

$$\leq \Upsilon \sum_{i=1}^L \sum_{j=1, M_{ji}=1 \vee \bar{M}_{ji}=1}^L |a_{ji} - \bar{a}_{ji}| \|\mathbf{X}_{:j}\| \quad (273)$$

$$\leq \Upsilon \Xi \sum_{i=1}^L \|\text{softmax}_{\mathbf{M}_{:i}}(\mathbf{X}^\top \mathbf{W} \mathbf{X}_{:i}) - \text{softmax}_{\bar{\mathbf{M}}_{:i}}(\mathbf{X}^\top \bar{\mathbf{W}} \mathbf{X}_{:i})\|_1, \quad (274)$$

where we use the assumption that $\|\mathbf{X}_{:j}\| \leq \Xi$. Now, utilizing lemma S4, we have

$$\|\mathbf{A}_{\mathbf{W},\mathbf{V}}(\mathbf{X}) - \mathbf{A}_{\bar{\mathbf{W}},\mathbf{V}}(\mathbf{X})\|_{2,1} \leq \Upsilon\Xi \sum_{i=1}^L \xi_h \|(\mathbf{M}_{:i} \vee \bar{\mathbf{M}}_{:i}) \odot (\mathbf{X}^\top \mathbf{W} \mathbf{X}_{:i} - \mathbf{X}^\top \bar{\mathbf{W}} \mathbf{X}_{:i})\|_1 \quad (275)$$

$$= \Upsilon\Xi \xi_h \sum_{i=1}^L \sum_{j=1, M_{ji}=1 \vee \bar{M}_{ji}=1}^L |\mathbf{X}_{:j}^\top \mathbf{W} \mathbf{X}_{:i} - \mathbf{X}_{:j}^\top \bar{\mathbf{W}} \mathbf{X}_{:i}| \quad (276)$$

$$\leq \Upsilon\Xi \xi_h \sum_{i=1}^L \sum_{j=1, M_{ji}=1 \vee \bar{M}_{ji}=1}^L \|\mathbf{X}_{:j}^\top \mathbf{W} - \mathbf{X}_{:j}^\top \bar{\mathbf{W}}\| \|\mathbf{X}_{:i}\| \quad (277)$$

$$\leq \Upsilon\Xi^2 \xi_h \sum_{i=1}^L \sum_{j=1, M_{ji}=1 \vee \bar{M}_{ji}=1}^L \|\mathbf{X}_{:j}^\top \mathbf{W} - \mathbf{X}_{:j}^\top \bar{\mathbf{W}}\| \quad (278)$$

$$\leq \Upsilon\Xi^2 \xi_h \sum_{i=1}^L \sum_{j=1, M_{ji}=1 \vee \bar{M}_{ji}=1}^L \|\mathbf{X}_{:j}\| \|\mathbf{W} - \bar{\mathbf{W}}\| \quad (279)$$

$$\leq \xi_h \Upsilon\Xi^2 \|\mathbf{W} - \bar{\mathbf{W}}\| \sum_{i=1}^L \left(\sum_{j=1, M_{ji}=1 \vee \bar{M}_{ji}=1}^L \|\mathbf{X}_{:j}\| \right), \quad (280)$$

$$\leq \xi_h \Upsilon\Xi^2 \|\mathbf{W} - \bar{\mathbf{W}}\| \sum_{i=1}^L (2k\Xi), = 2k\xi_h \Upsilon L\Xi^3 \|\mathbf{W} - \bar{\mathbf{W}}\|, \quad (281)$$

where we utilize $\|\mathbf{X}_{:j}\| \leq \Xi$ twice, thus giving us equation (232).

Denote the input-dependent mask matrix as $\mathbf{M} = m(\mathbf{X}^\top \mathbf{W} \mathbf{X})$ for the dot-product matrix $(\mathbf{X}^\top \mathbf{W} \mathbf{X})$, we can express equation (233) as following:

$$\|\mathbf{A}_{\mathbf{W},\mathbf{V}}(\mathbf{X}) - \mathbf{A}_{\bar{\mathbf{W}},\bar{\mathbf{V}}}(\mathbf{X})\|_{2,1} = \|\mathbf{V} \mathbf{X}_{\text{softmax}_{\mathbf{M}}}(\mathbf{X}^\top \mathbf{W} \mathbf{X}) - \bar{\mathbf{V}} \mathbf{X}_{\text{softmax}_{\mathbf{M}}}(\mathbf{X}^\top \mathbf{W} \mathbf{X})\|_{2,1} \quad (282)$$

$$= \sum_{i=1}^L \|(\mathbf{V} - \bar{\mathbf{V}}) \mathbf{X}_{\text{softmax}_{\mathbf{M},i}}(\mathbf{X}^\top \mathbf{W} \mathbf{X}_{:i})\| \quad (283)$$

$$\leq \|\mathbf{V} - \bar{\mathbf{V}}\| \sum_{i=1}^L \|\mathbf{X}_{\text{softmax}_{\mathbf{M},i}}(\mathbf{X}^\top \mathbf{W} \mathbf{X}_{:i})\|. \quad (284)$$

Noting the fact that $\mathbf{X}_{\text{softmax}_{\mathbf{M},i}}(\mathbf{X}^\top \mathbf{W} \mathbf{X}_{:i})$ is a (sparse) convex sum of the columns of \mathbf{X} , its maximum Euclidean norm is bounded by maximum Euclidean norm of the individual columns, $\max_j \|\mathbf{X}_{:j}\|$, which itself is bounded from above by Ξ . This simplifies the right-hand-side above to $L\Xi \|\mathbf{V} - \bar{\mathbf{V}}\|$, giving us equation (233). \square

Remark S4. For the Lipschitz constants in definition 1,

$$\lambda_X(\xi_h) = \xi_h \Upsilon k \left(2\Gamma\Xi^2(1 + \beta) + \frac{\beta}{(1 + 1/\Delta_h)} \right) = \exp(\delta_h) \Upsilon (1 + 1/\Delta_h) \left(2\Gamma\Xi^2(1 + \beta) + \frac{\beta}{(1 + 1/\Delta_h)} \right), \quad (285)$$

and $\lambda_W(\xi_h) = 2\xi_h \Upsilon Lk\Xi^3 = 2\exp(\delta_h) \Upsilon L\Xi^3 (1 + 1/\Delta_h)$ and $\lambda_V = L\Xi$ with $\xi_h = \exp(\delta_h) (1 + 1/\Delta_h) / k$ and δ_h defined in equation (230). Under the assumptions (H1) and (H3) of theorem S5, $\delta_h \leq 2\Gamma\Xi^2 - \Delta_h$.

E.4 Comparison of Bounds between Full and Heavy-hitter Attention

To compare the stability constants for all different forms of attention, we have put them together in table 1. To characterize the conditions when the stability constants for the heavy-hitter sparse attention provides improved guarantees over full attention, we have the following result:

Table 4: Bounds for ξ , $\lambda_X(\xi)$, $\lambda_W(\xi)$, λ_V from definition 1 for different forms of attention. Note that $\lambda_V = L\Xi$ for all forms of attention, and thus elided from this table.

Attention	ξ	$\lambda_X(\xi)$	$\lambda_W(\xi)$
Full (theorem 3)	$\frac{e^{\delta_s}}{L}$	$e^{\delta_s} \Upsilon(2\Gamma\Xi^2 + 1)$	$e^{\delta_s} \Upsilon L\Xi^3$
k -regular (theorem 4)	$\frac{e^{\delta_r}}{k}$	$e^{\delta_r} \Upsilon(2\Gamma\Xi^2 + 1)$	$e^{\delta_r} \Upsilon L\Xi^3$
k -heavy-hitter (theorem 5)	$\frac{e^{\delta_h}}{k} (1 + 1/\Delta_h)$	$e^{\delta_h} \Upsilon(\beta + 2\Gamma\Xi^2(\beta + 1)(1 + 1/\Delta_h))$	$2e^{\delta_h} \Upsilon L\Xi^3(1 + 1/\Delta_h)$

Corollary S1. Consider the definitions and conditions of theorem 3 and theorem 5. Further assume that (i) the maximum per-query semantic dispersion for standard attention is $\delta_s \leq 2\Gamma\Xi^2$, while that of heavy-hitter attention is $\delta_h = c_1\delta_s$, and (ii) the heavy-hitter minimum per-query semantic separation is $\Delta_h = c_2\delta_s$ for some positive constants c_1, c_2 . Then $\lambda_W(\xi_h) < \lambda_W(\xi_s)$ when

$$c_1 + \frac{1}{\delta_s} \log 2 \left(1 + \frac{1}{c_2\delta_s} \right) < 1, \quad (286)$$

and $\lambda_X(\xi_h) < \lambda_X(\xi_s)$ when

$$c_1 + \frac{1}{\delta_s} \log \left(2\Gamma\Xi^2(1 + \beta) \left(1 + \frac{1}{c_2\delta_s} \right) + \beta \right) - \frac{1}{\delta_s} \log(2\Gamma\Xi^2 + 1) < 1. \quad (287)$$

Proof. We arrive at equation (286) by comparing $\lambda_W(\xi_s) = \exp(\delta_s)\Upsilon L\Xi^3$ in remark S1 with $\lambda_W(\xi_h) = 2\exp(\delta_h)\Upsilon L\Xi^3(1 + 1/\Delta_h)$. We arrive at equation (287) by comparing $\lambda_X(\xi_s) = \exp(\delta_s)(2\Gamma\Xi^2 + 1)$ in remark S1 with $\lambda_X(\xi_h)$ defined in equation (285) in remark S4. \square

Based on this result, we want the constant c_1 (corresponding to the semantic dispersion) to be small and the constant c_2 (corresponding to the semantic separation) to be large. However, this condition also depends on the full attention dispersion δ_s . We present this relationship for $\lambda_W(\xi_s)$ vs $\lambda_W(\xi_h)$ in figure 21. For small values of δ_s , c_2 needs to be quite large and c_1 needs to be quite small for $\lambda_W(\xi_h) < \lambda_W(\xi_s)$. However, once δ_s is large enough, the condition in equation (24) holds for almost all values of c_1, c_2 . This indicates that it is relatively easy to satisfy the condition for heavy-hitter sparse attention to have better stability constant $\lambda_W(\xi_h)$ with respect to the learnable attention parameter \mathbf{W} than the $\lambda_W(\xi_s)$ for full attention. However, the conditions for $\lambda_X(\xi_h) < \lambda_X(\xi_s)$ in equation (25) are bit more restrictive as it depends on β which corresponds to the number of query tokens that might attend to the same key – the attention sink ratio. This relationship is visualized in figure 22. While for small values of β (column 1-3) and large enough δ_s , almost all values of c_1, c_2 satisfy equation (25). However, as the value of β increases, the conditions are only satisfied for large values of δ_s and small enough c_1 . We present the distribution of the semantic dispersions, semantic separations and sink ratios different datasets computed over the whole training set with the trained model in table 5. Overall, it shows that the full attention dispersion δ_s is usually significantly larger than the heavy-hitter attention dispersion δ_h . We present different percentiles of the values seen over all queries in all training points across all transformer blocks in the model. Based on these values, we also plug them into the conditions equation (24) and equation (25) in corollary 1 and report the left-hand-side values in the table. We see that, in almost all cases, the left-hand-side values are lower than 1, implying that the heavy-hitter attention has better guarantees, which aligns with the empirical results we see in figure 2. This is especially true when we only consider the values using the 95-th percentile values for semantic dispersions, sink ratios, and the 5-th percentile values for the semantic

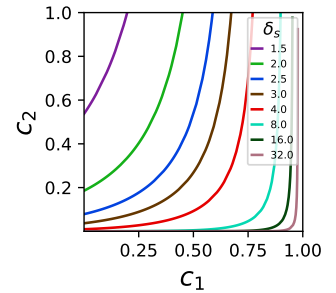


Figure 21: Relationship of c_1, c_2, δ_s in equation (24). For any value of δ_s , the region above the line denotes values of c_1, c_2 for which $\lambda_W(\xi_h) < \lambda_W(\xi_s)$. Note that, once δ_s is large enough, c_2 can be very small, and c_1 can be quite large.

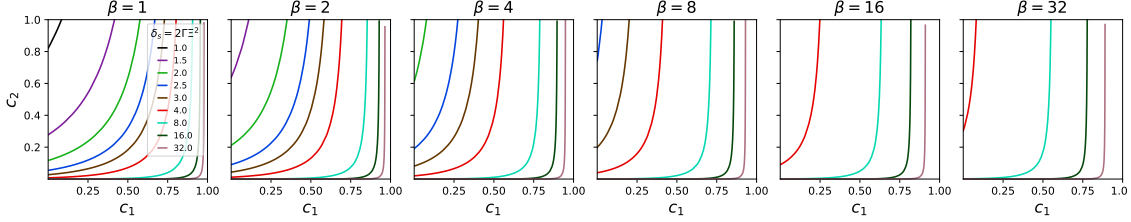


Figure 22: Relationship of $c_1, c_2, \delta_s, \beta$ in equation (25). For any value of δ_s and β , the region above the line denotes values of c_1, c_2 for which $\lambda_X(\xi_h) < \lambda_X(\xi_s)$. In these figures, we assume $\delta_s = 2\Gamma\Xi^2$ so that we just need to vary δ_s without considering different values of Γ and Ξ .

separations, which is the most relevant quantity as we have been studying the worst-case stability constants. There is one case where the values are not less than 1, counter to what we see in the empirical evaluations of figure 2. Note that we are evaluating these conditions at the optimum (the final trained model) instead of over the whole parameter space. For that reason, it is important to look at the whole loss surface which we do in the sequel.

Table 5: Empirical distribution of the semantic dispersions δ_s, δ_h , semantic separations Δ_h and β for different datasets. For each metric, we report the 75-th, 90-th and 95-th percentile (except for Δ_h for which we report the 25-th, 10-th and 5-th percentile as it is a lower bound). The left-hand-side (LHS) of equation (24) and equation (25) are computed using the corresponding percentile values.

Dataset	Full attention dispersion δ_s	HH attention dispersion δ_h	HH separation Δ_h	Sink ratio β
ListOps	[8.61, 18.5, 29.4]	[3.51, 6.74, 9.67]	[0.016, 0.005, 0.002]	[1, 3, 15]
Parity	[8.30, 10.1, 11.2]	[2.31, 3.13, 3.78]	[0.062, 0.022, 0.011]	[8, 13, 16]
Even Pairs	[2.03, 4.73, 9.44]	[1.03, 2.84, 5.50]	[0.009, 0.003, 0.002]	[6, 17, 26]
Missing Dup.	[4.63, 9.25, 17.1]	[2.36, 4.25, 4.88]	[0.018, 0.006, 0.003]	[7, 15, 21]

Dataset	LHS (24)	LHS (25)
ListOps	[0.97, 0.69, 0.56]	[0.96, 0.72, 0.63]
Parity	[0.70, 0.76, 0.80]	[0.87, 0.94, 0.99]
Even Pairs	[3.17, 1.98, 1.31]	[3.59, 2.40, 1.58]
Missing Dup.	[1.53, 1.09, 0.67]	[1.79, 1.30, 0.80]

E.5 Loss Surfaces and Estimated Lipschitz Constants

Beyond understanding the relative behavior of the aforementioned stability (and thus Lipschitz) bounds, we also empirically visualize the training loss landscapes for 4 of the tasks in figure 23. We use the version of transformer block with the ReLU activated MLP (for loss surfaces of transformer blocks with GELU activated MLPs see appendix E.5 in figure 25). We utilize the techniques proposed in Li et al. [2018]. Given the training model parameters Θ , we pick two random directions ϑ_1 and ϑ_2 , and then plot the training loss $\mathcal{L}(\Theta + x\vartheta_1 + y\vartheta_2)$ at the grid point (x, y) , $x, y \in [-1, 1]$.⁵ The grid points are computed as a granularity of $\varepsilon = 0.005$ in both axis, that is, $x, y \in \{-1, -1 + \varepsilon, -1 + 2\varepsilon, \dots, 1 - \varepsilon, 1\}$. We utilize the computed loss at each grid point to generate contour plots (a heatmap visualization of the loss surface is provided in appendix E.5 in figure 24). Note that the grid point $(0, 0)$ corresponds to the loss $\mathcal{L}(\Theta)$ of the trained model. The contours on the loss surfaces of full attention model are somewhat asymmetric – see for example, around the center in figure 23c, figure 23d, and moderately in figure 23a. In contrast, the loss surfaces of the heavy-hitter top- k attention model are quite symmetric, especially around the center.

Beyond visualizing the loss surface in 2-dimensions, we also utilize the loss surface to approximately estimate the Lipschitz constant of the model in the selected random directions $\varepsilon_1, \vartheta_2$. Given the loss values

⁵Note that the random directions are “filterwise normalized”, which means that each matrix of parameters is normalized independently.

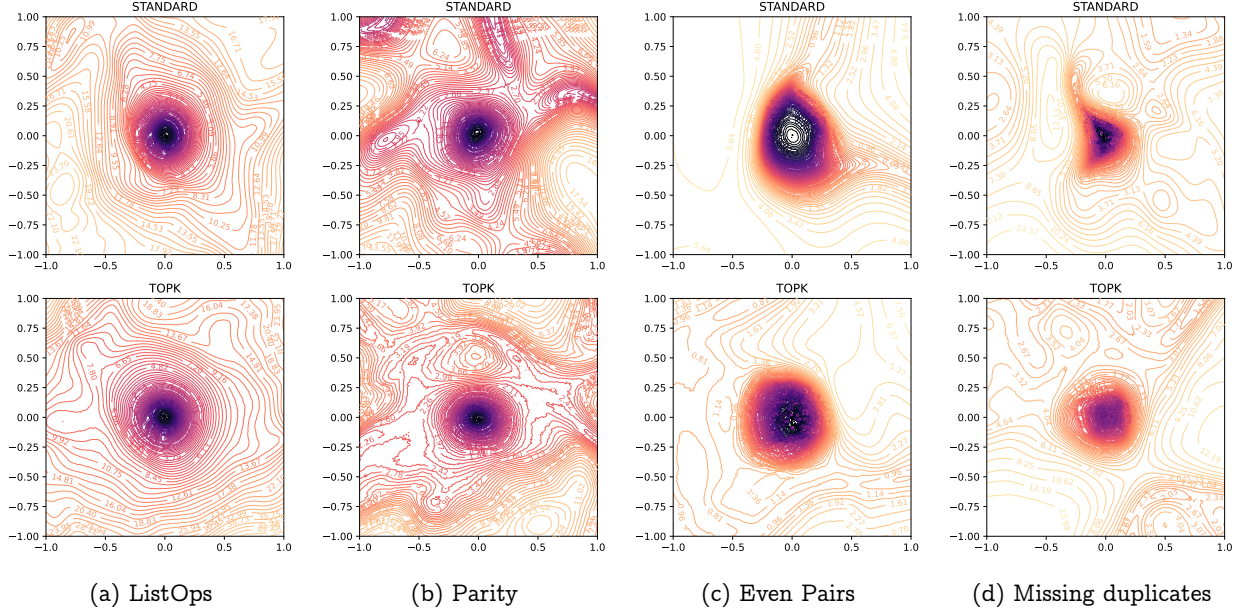


Figure 23: Loss surfaces of the models with full attention (top row) and top- k attention (bottom row) for each of the 4 tasks considered in figure 2 with the corresponding hyperparameters utilizing the filter-normalized version of the loss landscape visualization techniques proposed in Li et al. [2018]. Note that the (0,0) grid point corresponds to the final trained model.

$\mathcal{L}(\theta + x\vartheta_1 + y\vartheta_2)$ at grid points (x, y) , we compute the following ratios at neighboring horizontal and vertical grid points as an estimate of the Lipschitz constant $\lambda_{\mathcal{L}}$ in theorem 2:

$$\frac{|\mathcal{L}(\Theta + x\vartheta_1 + y\vartheta_2) - \mathcal{L}(\Theta + (x + \varepsilon)\vartheta_1 + y\vartheta_2)|}{\varepsilon\|\vartheta_1\|} \quad \text{and} \quad (288)$$

$$\frac{|\mathcal{L}(\Theta + x\vartheta_1 + y\vartheta_2) - \mathcal{L}(\Theta + x\vartheta_1 + (y + \varepsilon)\vartheta_2)|}{\varepsilon\|\vartheta_2\|}.$$

We plot the distribution of these estimates in figure 27 for the loss surfaces in figure 23 of 4 of the tasks for varying grid ranges $r \in (0, 1]$ with $x, y \in [-r, r]$. We plot the 50-th, 75-th, 95-th and 99-th percentile values of these estimates of the full attention model and the heavy-hitter top- k attention model. We see that near the trained model (small values of the grid range r), the distributions of these estimates are close for both the models. However, as we move farther away from the trained model (large values of r in the horizontal axis), the distributions change significantly, and the top- k attention model provides a smaller Lipschitz constant estimate compared to the full attention model across all percentiles. This indicates that, at least empirically, the loss for the top- k attention model has a much more favorable Lipschitz constant compared to that of the full attention model, which in turn implies both faster convergence and better generalization guarantees. Thus, our stability-based theoretical investigation in this section appears to align with our empirical observations in section 4.

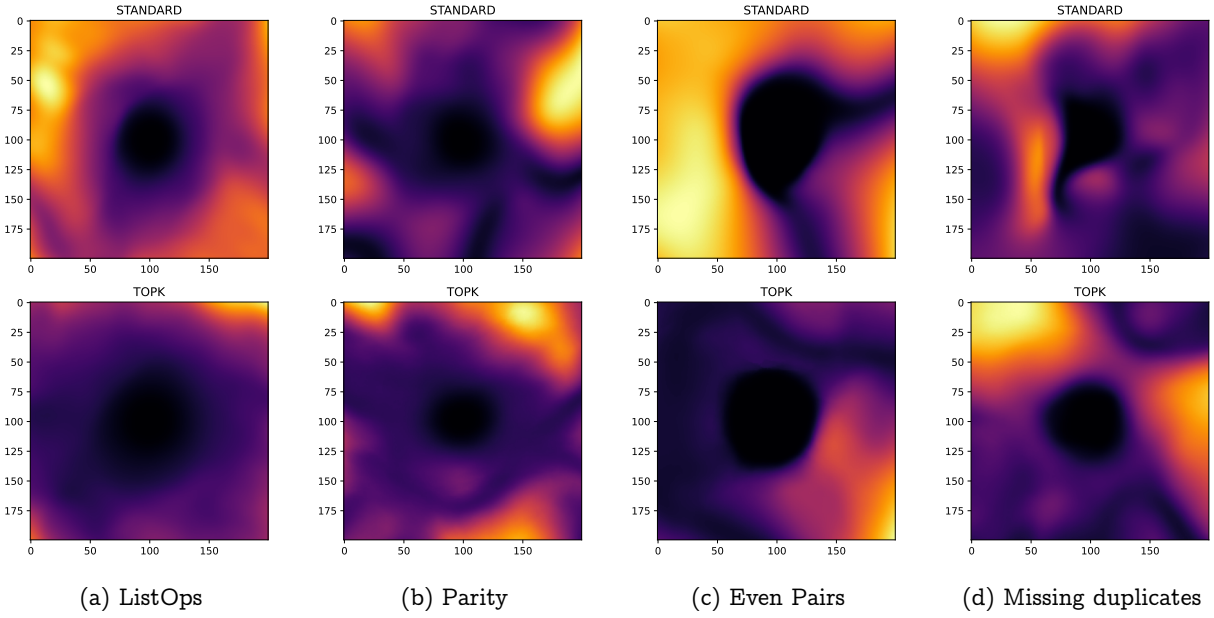


Figure 24: Loss surfaces as in figure 23 but in the form of heatmaps instead of contour plots.

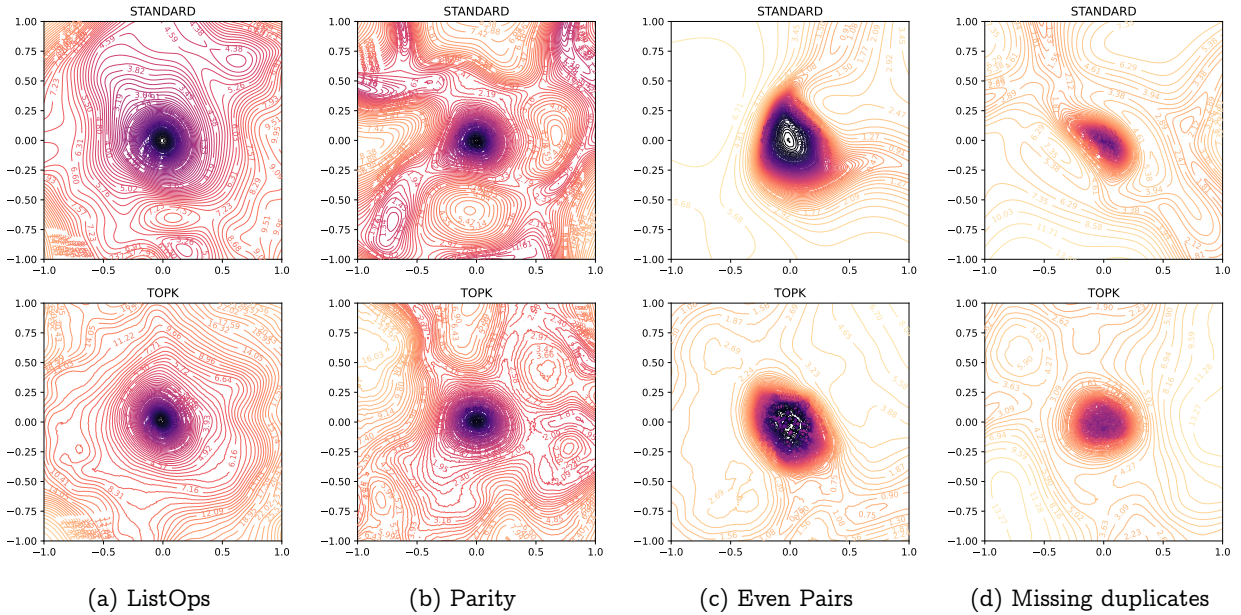


Figure 25: Loss surfaces as in figure 23 of the models with full attention (top row) and top- k attention (bottom row) for each of the 4 tasks considered in figure 2 and table 3. Note that both forms of attention now utilize the MLP with GELU activation for all tasks (as opposed to ReLU activation in figure 23).

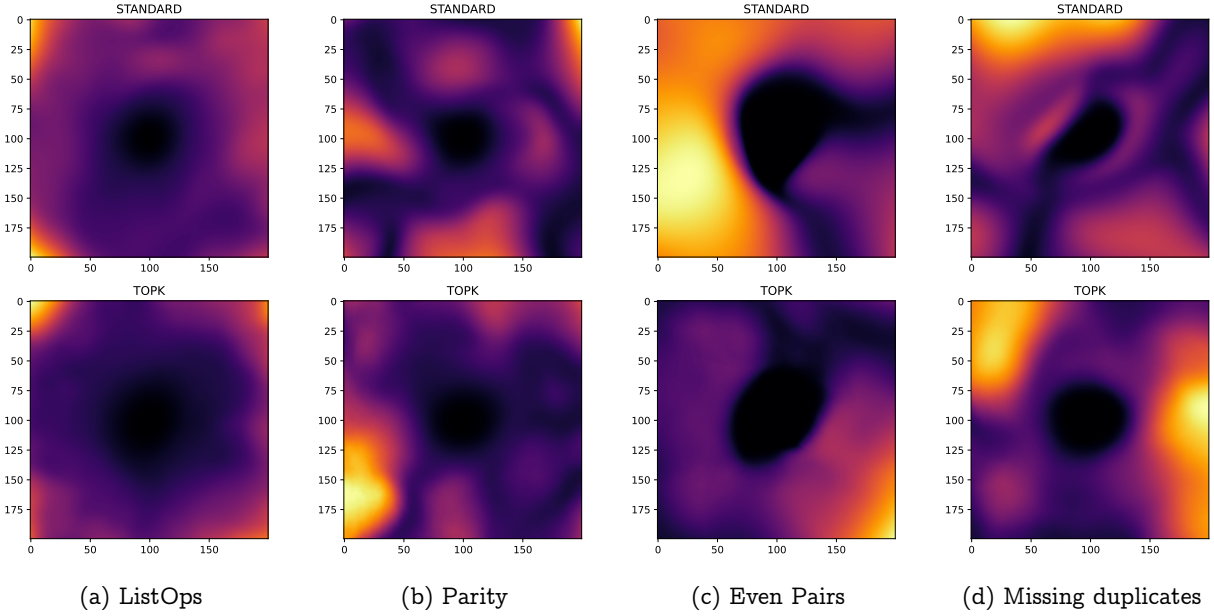


Figure 26: Loss surfaces as in figure 25 but in the form of heatmaps instead of contour plots.

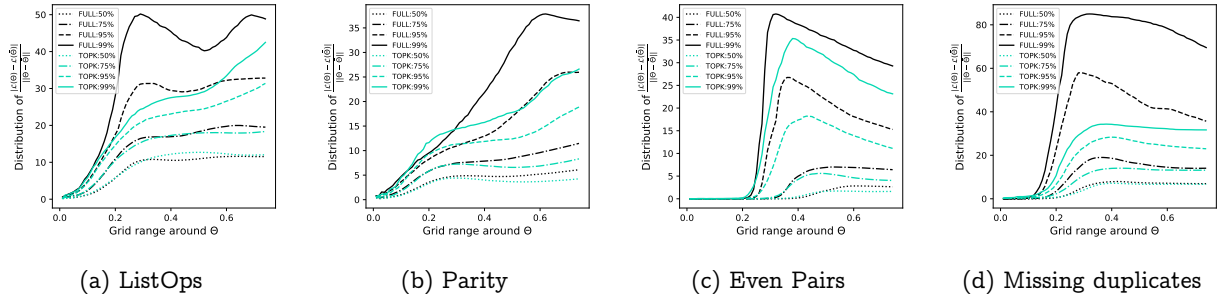


Figure 27: Distribution of the estimated Lipschitz constants computed in the random directions utilized to visualize the loss landscape in figure 23 for full attention and top- k attention each of the 4 tasks considered in figure 2 with the corresponding hyperparameters. We report the distributions of the estimated Lipschitz constants in the vertical axis in terms of the 50-th (dotted), 75-th (dash-dotted), 95-th (dashed) and 99-th (solid) percentiles (lower is better). On the horizontal axis, we denote the radius of the ball around the parameters of the final learned model, and visualize how the distributions vary as the ball radius is increased.